Fall 12-2020

Fungicide Resistance: Surveillance, Risk Assessment and Evolution in Two Soil-Borne Pathogens

Nikita Gambhir
University of Nebraska-Lincoln

FUNGICIDE RESISTANCE: SURVEILLANCE, RISK ASSESSMENT AND EVOLUTION IN TWO SOIL-BORNE PATHOGENS

by

Nikita Gambhir

A DISSERTATION

Presented to the Faculty of

The Graduate College at the University of Nebraska

In Partial Fulfillment of Requirements

For the Degree of Doctor of Philosophy

Major: Agronomy and Horticulture

(Plant Pathology)

Under the Supervision of Professor Sydney E. Everhart

Lincoln, Nebraska

December, 2020

FUNGICIDE RESISTANCE: SURVEILLANCE, RISK ASSESSMENT AND EVOLUTION IN TWO SOIL-BORNE PATHOGENS

Nikita Gambhir, Ph.D.

University of Nebraska, 2020

Advisor: Sydney E. Everhart

Fungicide-resistant pathogens are an increasing threat to fungicide efficacy and plant health. The goal of this dissertation was to advance the foundational knowledge required to prevent and detect fungicide resistance development in the seedling disease pathogen, *Rhizoctonia zeae* and the white-mold pathogen, *Sclerotinia sclerotiorum.* Corn and soybean fields in 12 states (IA, IL, IN, KS, KY, MI, MN, MO, ND, NE, SD, and WI) were surveyed for *R. zeae*. *In vitro* fungicide sensitivity was determined for 91 isolates to fludioxonil, sedaxane, and/or prothioconazole. *Rhizoctonia zeae* was sensitive to all fungicides (EC_{50} < 3 µg/ml) except azoxystrobin (EC_{50} > 100 µg/ml). *In planta* application of azoxystrobin did not significantly change the disease severity or total dry weight of soybean plants ($P > 0.05$), suggesting ineffective control. To understand the intrinsic risk of resistance development in *R. zeae*, the genetic structure of *R. zeae* populations was characterized. Six microsatellite markers were designed for genotyping 200 *R. zeae* isolates. Results showed that the population has a mixed mode of reproduction and is genetically differentiated according to geographic region and year, suggesting limited dispersal and an intermediate risk of resistance development. To prevent fungicide resistance, it is also important to understand the fungicide-risk factors to develop resistance. Sublethal fungicide stress may cause genomic instability in fungal

plant pathogens, which may accelerate the emergence of resistance. Genome-wide mutations were characterized in 55 *S. sclerotiorum* genomes after sublethal fungicide exposure. Results showed that sublethal fungicide exposure increased the frequency of insertions/deletions in one genomic background of *S. sclerotiorum*. The frequency and distribution of mutations varied with genomic background. Understanding factors that increase pathogen mutation rates can inform disease management strategies that delay resistance evolution. On examining the evolutionary role of hypermutators in fungal pathogen populations, the literature reviewed suggested that hypermutators may be a new factor to consider in fungicide resistance development. Overall, this dissertation will advance the knowledge on fungicide- and pathogen-risk factors to develop resistance, which can inform fungicide resistance management.

DEDICATION

I dedicate this dissertation to my family for their unconditional love, support, and faith in me. I couldn't have come this far without all of them by my side.

My mother, Harjot Kaur, without whose vision I wouldn't have embarked this journey. For always inspiring me to pursue my dreams, for having my back, and understanding the unsaid.

My father, Gurprem Singh Gambhir, for sparking my interest in science, for setting an example of a great thinker, and for being my rock.

My husband, Shiv Singla, for his innumerable sacrifices and selfless love. For being my anchor during the ups and downs of this journey and helping me clear my vision when I was swayed with emotions.

My sister, Dhwani Gambhir; my brother, Amitoj Singh Gambhir; my mother-in-law, Asha Rani; my brothers-in-law, Ajay Singla and Arshpreet Singh; and my sister-in-law, Priyanka Singla for always believing in me and being there for me.

My grandparents, Late Gurcharan Singh, Kanta Gambhir, Harbhajan Singh, Daljit Kaur, and Shakuntla Devi, for always motivating me to do my best.

ACKNOWLEDGMENTS

I would like to sincerely thank my advisor, Dr. Sydney E. Everhart for her constant guidance, encouragement, and support throughout this journey. Her amazing mentorship has helped me become a better scientist and human being. I would like to thank my committee members, Drs. Keenan Amundsen, Steven Harris, and Chi Zhang, for being resourceful and supportive throughout the course of my degree. Thanks to my research collaborator, Dr. Anthony Adesemoye, for his help and valuable suggestions on my research projects. Thanks to all the current and former members of the Everhart lab, Asha Mane, Bimal Sajeewa Amaradasa, Edgar Nieto, Julianne Matczyszyn, Karen da Silva, Margarita Marroquin-Guzman, Rebecca Higgins, Sergio Manuel Gabriel Peralta, Srikanth Kodati, Thomas Miorini, and Zhian Kamvar, for cultivating a positive research environment and for always being great teachers and helpful teammates. I would also like to thank the undergraduate students, Anthony Pannullo, Audrey Vega, Cristian Wulkop, Olivia Renelt, and Rachel Persson, who helped me in completing my research projects. I am grateful to my research collaborators, Drs. Olutoyosi Ajayi-Oyetunde, Kaitlyn Bissonnette, Carl Bradley, Martin Chilvers, Ahmad Fakhoury, Tamra Jackson-Ziems, Leonor Leandro, Chris Little, Dean Malvick, Febina Mathew, Berlin Nelson, Gretchen Sassenrath, Damon Smith, Darcy Telenko, Kiersten Wise, Bob Harveson, and Alejandro Rojas, for providing me with the necessary samples to complete my research projects. Thanks to Nicholas Arneson for driving me to soybean fields in Nebraska, thus facilitating sample collection. I am grateful to the staff at the Holland Computing Center, Plant Pathology Greenhouse, and Agronomy and Horticulture Greenhouses for always

helping me in troubleshooting problems. Thanks to all the faculty, staff, and graduate students in the Department of Plant Pathology for inspiring me to strive for excellence and for enriching this journey. I would like to thank all my friends and family, near or far, for being my support system. Finally, I would like to thank the Almighty, without whom nothing would have been possible.

TABLE OF CONTENTS

Page

CHAPTER-1

INTRODUCTION

This dissertation focuses on surveillance, risk assessment and evolution of fungicide resistance in two soil-borne pathogens, *Rhizoctonia zeae* and *Sclerotinia sclerotiorum*. Fungicide sensitivity of *R. zeae* has been characterized in Chapter 2 and its population structure has been characterized in Chapter 3. In Chapter 4, genomic effects of sublethal fungicide exposure have been studied in *S. sclerotiorum* and in Chapter 5, the role of hypermutator fungi in pathogen evolution has been reviewed. Therefore, the current chapter provides an overview of the role of fungicides in crop protection, development of fungicide resistance and its management.

Impact of fungicide resistance on crop protection

Fungicides play a key role in crop protection. Without fungicide application, it is estimated that plant pathogenic fungi would reduce U.S. production of 29 crops by 40% or more (Gianessi and Reigner 2005). Most of the fungicides used today have a single-site mode of action, i.e., these fungicides have one specific target site in a biochemical pathway. For example, Quinone outside Inhibitor (QoI) fungicides inhibit mitochondrial respiration by binding to ubiquinol oxidase (mitochondrial complex III) at Qo site (Fungicide Resistance Action Committee 2020) and Succinate DeHydrogenase Inhibitor (SDHI) fungicides inhibit mitochondrial respiration by binding to succinate dehydrogenase (mitochondrial complex II) at ubiquinone-binding site (Fungicide Resistance Action Committee 2020). The specificity of single-site mode of action fungicides makes them more effective, however, this specificity also increases the risk of

pathogens to develop resistance against these fungicides as little as a single mutation in the fungal DNA can lead to resistance (Fernández-Ortuño et al. 2008).

Fungicide resistance is defined as a stable and heritable trait that confers reduction in sensitivity to a given fungicide. Resistance can be "inherent" or "acquired". For simplicity, the term "resistance" will be used for resistance acquired through exposure to a fungicide under field conditions, while the term "insensitivity" will be used in cases where there is limited evidence of inherent sensitivity. When resistance develops due to a mutation in the gene encoding the fungicide target, it is called qualitative resistance. In this case, the fungicide can no longer bind to its target site and the pathogen becomes completely resistant to the fungicide. When resistance develops due to a mutation that results in a lower fungicide concentration within the fungal cell (e.g., increased activity of efflux pumps or intracellular degradation of fungicide) or an increased expression of the target gene, it is called quantitative resistance. In this case, individuals in the pathogen population can exhibit a range of sensitivity to a given fungicide.

Fungicide resistance is an increasing threat to fungicide efficacy and has already been reported for 203 plant pathogenic fungi (Fungicide Resistance Action Committee 2013). It takes approximately $315 million (adjusted for inflation) and 11 years to discover, develop and register a new fungicide (McDougall 2016), but resistance was reported as early as two years after the launch of some fungicides (Brent and Hollomon 2007). For soybean, fungicide resistant *Cercospora kikuchii* and *C. sojina* were reported (Imazaki et al. 2006; Zhang et al. 2012), and recently, *Rhizoctonia solani* with resistance to QoI fungicides was reported in Louisiana (Olaya et al. 2013). For corn, fungicide resistance has not yet been reported.

Corn and soybean are the most important crops in the U.S. and contribute significantly to the nation's economy with annual sales of $91.52 billion (USDA National Agricultural Statistics Service 2017). Seedling diseases of corn and soybean cause reduced stand establishment and loss in plant vigor, which result in yield loss. Seedling diseases caused by filamentous pathogens have been reported to cause yield losses of 37.3 million bushels in soybean and 23.9 million bushels in corn in the U.S. and Ontario, Canada in 2018 (Crop Protection Network 2020). The major pathogens causing seedling diseases belong to the genera of *Rhizoctonia, Fusarium, Phytophthora, and Pythium.* Fungicide seed treatments are commonly used to manage seedling diseases and include several modes of action, such as QoI, PhenylPyrroles (PP), DeMethylation Inhibitors (DMI), and SDHI. Fungicide-resistant pathogens can lead to monetary losses resulting from disease, repeated applications of ineffective fungicides, and the subsequent need to develop, register and market new fungicides. Management of fungicide resistance is crucial for long-lasting crop protection.

Fungicide resistance management

Prevention and early detection are the pillars of managing fungicide resistance, which are bolstered by the foundational knowledge about factors affecting the risk of resistance development (Fig. 1.1). For prevention of fungicide resistance, proactive measures should be taken like using disease resistant crop varieties, rotating fungicides with different modes of action, and following fungicide label recommendations. To prevent fungicide resistance, it is also important to understand the factors that increase the risk of resistance development. Risk of resistance development depends on both the

pathogen and fungicide in question (Brent and Hollomon 2007). Pathogen risk factors include its generation time, evolutionary potential, dispersal mechanism(s), and reproduction type. Fungicide risk factors include the mode of action, number of applications per season, and dose applied. In addition to prevention, it is important to detect resistance at an early stage to avoid significant crop losses.

Resistance can be detected by monitoring fungicide sensitivity. Determining changes in fungicide sensitivity requires knowledge of existing sensitivity to different classes of fungicides. In the case of the soil-borne pathogen *R. zeae* from Nebraska, fungicide sensitivity has not been characterized previously. Soil-borne pathogens are categorized as low-risk of resistance development (Brent and Hollomon 1998). However, resistance has been reported for some soil-borne pathogens. For example, potato pathogens *Fusarium sambucinum, F. oxysporum,* and *F. coeruleum* were found to be insensitive or resistant to PP fungicides (Gachango et al. 2012; Peters et al. 2008). *Pythium* and *Phytopythium spp.* from soybean have been found to be insensitive to azoxystrobin and trifloxystrobin (Radmer et al. 2017). *Fusarium graminearum* from corn and soybean seedlings has been found to be mostly insensitive to QoI fungicides and occasionally resistant to PP (Broders et al. 2007). QoI resistance has been reported in *Rhizoctonia solani* in Louisiana (Olaya et al. 2013). *Rhizoctonia zeae* has been recently identified as the major *Rhizoctonia* species associated with seedling diseases of corn and soybean in Nebraska (Kodati 2019). This was the first study that showed *R. zeae* to be pathogenic on soybean in the North Central U.S. It is important to know if this less known pathogen of soybean can be effectively controlled by the currently used fungicides in Nebraska.

The risk of resistance development is not known for *R. zeae*. Risk-assessment helps to design pathogen-specific strategies to prevent fungicide resistance. Information on the evolutionary potential, reproductive system, and dispersal modes/mechanisms can be obtained by studying the population structure of the pathogen. The structure of *R. zeae* has not been characterized previously, but its high rDNA-ITS diversity in the Americas (Aydin et al. 2013) suggests that it may have an increased potential to develop fungicide resistance.

To prevent fungicide resistance, factors promoting resistance evolution also need to be understood. Evolution of fungicide resistance within a completely susceptible population begins with resistance emergence and is followed by selection. Few studies have addressed the emergence phase and it is unclear if fungicide dose plays a role in it (Ajouz et al. 2010; Amaradasa and Everhart 2016; Chen et al. 2015; Dowling et al. 2016; Schnabel et al. 2014; Troncoso-Rojas et al. 2013). Extensive studies have been performed in bacteria for understanding similar effects of antibiotics, which show sub-lethal doses increase mutation rates, leading to antibiotic resistance emergence (Blázquez et al. 2012). Since few studies have been performed on fungal plant pathogens, there is a need to characterize the effects of sub-lethal doses using a model system, such as *Sclerotinia sclerotiorum.*

The genomic features of *S. sclerotiorum* make it a suitable model system for conducting a genome-wide mutation assessment study. Due to the small genome size of *S. sclerotiorum* (38.8 Mb), a greater number of strains can be sequenced cost-effectively than would be possible with a fungus with a larger genome. Its high genomic stability (12% transposable element content; Derbyshire et al. 2017) provide less chances of

background mutations as compared to fungal genomes with higher transposable element content. Since the *S. sclerotiorum* genome is optically mapped (assembled to chromosomal level) and annotated (Derbyshire et al. 2017), distribution of mutations can be studied on a per chromosome-basis. The haploid nature of the *S. sclerotiorum* genome can help to elucidate the phenotypic effect of mutations without concern of dominant alleles masking the recessive alleles.

Another factor promoting rapid evolution of fungicide resistance is the mutation rate of pathogen populations. Hypermutator fungal strains have an elevated mutation rate than the wild-type strains owing to a defect in the DNA mismatch repair system (Iyer et al. 2006; Boiteux and Jinks-Robertson 2013). Studies in *Saccharomyces cerevisiae* and human fungal pathogens have shown that hypermutators can expedite stress adaptation and hasten the evolution of antifungal resistance (Healey et al. 2016; Thompson et al. 2006). Knowledge about the biology and dynamics of fungal hypermutators is important to examine the evolutionary role of hypermutators in fungal pathogen populations and project implications of hypermutators in the evolution of fungal plant pathogen populations. Understanding the factors that determine the emergence and evolution of fungal hypermutators can open a novel avenue of managing rapidly evolving fungicide resistance.

For advancing the knowledge on fungicide- and pathogen-risk factors to develop resistance, the objectives of this dissertation were to:

1. Determine sensitivity of *Rhizoctonia zeae* from corn and soybean to four fungicides;

2. Characterize structure and mode of reproduction in *Rhizoctonia zeae* populations from corn and soybean using microsatellite markers;
3. Characterize the effects of long-term exposure of sub-lethal fungicide doses on genomes of *Sclerotinia sclerotiorum*;
4. Review literature on the evolutionary role of hypermutators in fungal pathogen populations and project its implications in plant pathology.

The dissertation will provide knowledge that will inform fungicide resistance management, specifically for soybean and corn. It will also provide new information about the effects of fungicides on the genomes of a fungal pathogen and how information on hypermutators may be a new factor to consider in development of fungicide resistance.

References

Ajayi-Oyetunde, O.O., and Bradley, C.A. 2017. Identification and characterization of *Rhizoctonia* species associated with soybean seedling disease. Plant Dis. 101:520-533.

Ajouz, S., Decognet, V., Nicot, P.C., and Bardin, M. 2010. Microsatellite stability in the plant pathogen *Botrytis cinerea* after exposure to different selective pressures. Fungal Biol. 114:949-954.

Amaradasa, B.S., and Everhart, S.E. 2016. Effects of sublethal fungicides on mutation rates and genomic variation in fungal plant pathogen, *Sclerotinia sclerotiorum*. PLoS One 11:e0168079.

Aydin, E.B., Gurkanli, C.T., Ozkoc, I., Demirci, E., Erper, I., Karaca, G., Hsieh, T.F., Vajna, L. and Poltronieri, L.S. 2013. rDNA-ITS diversity of *Waitea circinata* var. *zeae* (anamorph: *Rhizoctonia zeae*). J. Plant Pathol. 95:587-595.

Blázquez, J., Couce, A., Rodríguez-Beltrán, J., and Rodríguez-Rojas, A. 2012. Antimicrobials as promoters of genetic variation. Curr. Opin. Microbiol. 15:561-569.

Boiteux S, Jinks-Robertson S. DNA repair mechanisms and the bypass of DNA damage in *Saccharomyces cerevisiae*. 2013. Genetics. 193:1025-1064.

Broders, K.D., Lipps, P.E., Paul, P.A., and Dorrance, A.E. 2007. Evaluation of *Fusarium graminearum* associated with corn and soybean seed and seedling disease in Ohio. Plant Dis. 91:1155-1160.

Brent, K.J., and Hollomon, D.W. 1998. Fungicide resistance: the assessment of risk. FRAC Monograph No. 2. Global Crop Protection Federation, Brussels, Belgium.

Brent, K. J., and Hollomon, D. W. 2007. Fungicide resistance in crop pathogens: how can it be managed? FRAC Monograph No. 1 (2nd, rev. ed.). Fungicide Resistance Action Committee, Brussels, Belgium.

Crop Protection Network. 2020. Estimates of corn, soybean, and wheat yield losses due to disease: An online tool. https://loss.cropprotectionnetwork.org/. doi: 10.31274/cpn-20191121-0.

Chen, F., Everhart, S.E., Bryson, P.K., Luo, C., Song, X., Liu, X., and Schnabel, G. 2015. Fungicide-induced transposon movement in *Monilinia fructicola*. Fungal Genet. Biol. 85:38-44.

Derbyshire, M., Denton-Giles, M., Hegedus, D., Seifbarghi, S., Rollins, J., Kan van, J., Seidl, M.F., Faino, L., Mbengue, M., Navaud, O., Raffaele, S., Hammond-Kosack, K., Heard, S., and Oliver, R. 2017. The complete genome sequence of the phytopathogenic fungus *Sclerotinia sclerotiorum* reveals insights into the genome architecture of broad host range pathogens. Genome Biol. Evol. 9:593-618.

Dowling, M.E., Bryson, P.K., Boatwright, H.G., Wilson, J.R., Fan, Z., Everhart, S.E., Brannen, P.M., and Schnabel, G. 2016. Effect of fungicide applications on *Monilinia fructicola* population diversity and transposon movement. Phytopathology 106:1504-1512.

Fernández-Ortuño, D., Torés, J.A., De Vicente, A., and Pérez-García, A. 2008. Mechanisms of resistance to QoI fungicides in phytopathogenic fungi. Int. Microbiol. 11:1-9.

Fungicide Resistance Action Committee. 2013. List of plant pathogenic organisms resistant to disease control agents. CropLife Int., Brussels, Belgium.

Fungicide Resistance Action Committee. 2020. FRAC Code List 2020: Fungal control agents sorted by cross resistance pattern and mode of action (including FRAC Code numbering). CropLife Int., Brussels, Belgium.

Gachango, E., Hanson, L.E., Rojas, A., Hao, J.J., and Kirk, W.W. 2012. *Fusarium spp.* causing dry rot of seed potato tubers in Michigan and their sensitivity to fungicides. Plant Dis. 96:1767-1774.

Gianessi L.P. and Reigner N**.** 2005. The value of fungicides in U.S. crop production. Washington, DC, CropLife Foundation.

Healey, K.R., Zhao, Y., Perez, W.B., Lockhart, S.R., Sobel, J.D., Farmakiotis, D., Kontoyiannis, D.P., Sanglard, D., Taj-Aldeen, S.J., Alexander, B.D. and Jimenez-Ortigosa, C., 2016. Prevalent mutator genotype identified in fungal pathogen *Candida glabrata* promotes multi-drug resistance. Nat Commun. 2016. 7:11128.

Imazaki, I., Ishikawa, K., Yasuda, N., Miyasaka, A., Kawasaki, S., and Koizumi, S. 2006. Incidence of thiophanate-methyl resistance in *Cercospora kikuchii* within a single lineage based on amplified fragment length polymorphisms in Japan. J. Gen. Plant Pathol. 72:77-84.

Iyer, R.R., Pluciennik, A., Burdett, V. and Modrich, P.L., 2006. DNA mismatch repair: Functions and mechanisms. Chem Rev. 106:302-323. doi:10.1002/chin.200620268.

Kodati, S. 2019. Diversity and pathogenicity of *Rhizoctonia* spp. from different plant hosts in Nebraska. Doctoral Dissertation. University of Nebraska, Lincoln.

McDougall P. 2016. The cost of new agrochemical product discovery, development and registration in 1995, 2000, 2005-8 and 2010 to 2014. R and D expenditure in 2014 and expectations for 2019. Consultancy study for CropLife International, CropLife America and the European Crop Protection Association.

Olaya, G., Sarmiento, L., Edlebeck, K., Buitrago, C., Sierotzki, H., Zaunbrecher, J., and Tally, A. 2013. Azoxystrobin (QoI) resistance monitoring of *Rhizoctonia solani* isolates causing rice sheath blight in Louisiana. Phytopathology 103:106-106.

Peters, R.D., Platt, H.W., Drake, K.A., Coffin, R.H., Moorehead, S., Clark, M.M., Al-Mughrabi, K.I. and Howard, R.J. 2008. First report of fludioxonil-resistant isolates of *Fusarium spp.* causing potato seed-piece decay. Plant Dis. 92:172-172.

Radmer, L., Anderson, G., Malvick, D.M., Kurle, J.E., Rendahl, A., and Mallik, A. 2017. *Pythium, Phytophthora, and Phytopythium spp.* associated with soybean in Minnesota, their relative aggressiveness on soybean and corn, and their sensitivity to seed treatment fungicides. Plant Dis. 101:62-72.

Schnabel, G., Chen, F., Everhart, S.E., Bridges, W.C., and Liu, X. 2014. Studies on sensitivity reduction in solo and mixture treatments and fungicide-induced mutagenesis in *Monilinia fructicola*. Modern fungicides and antifungal compounds VII: proceedings of the 17th International Reinhardsbrunn Symposium, April 21-25, 2013, Friedrichroda, Germany.

Thompson, D.A., Desai, M.M. and Murray, A.W., 2006. Ploidy controls the success of mutators and nature of mutations during budding yeast evolution. Curr Biol. 16:1581-1590.

Troncoso-Rojas, R., Báez-Flores, M.E., Pryor, B., García, H.S., and Tiznado-Hernández, M.E. 2013. Inter simple sequence repeat polymorphism in *Alternaria* genomic DNA exposed to lethal concentrations of isothiocyanates. Afr. J. Microbiol. Res. 7:838-852.

USDA National Agricultural Statistics Service. 2017. Census of agriculture. Complete data available at www.nass.usda.gov/AgCensus.

Zhang, G.R., Newman, M.A., and Bradley, C.A. 2012. First report of the soybean frogeye leaf spot fungus (*Cercospora sojina*) resistant to quinone outside inhibitor fungicides in North America. Plant Dis. 96:767-767.

Figure

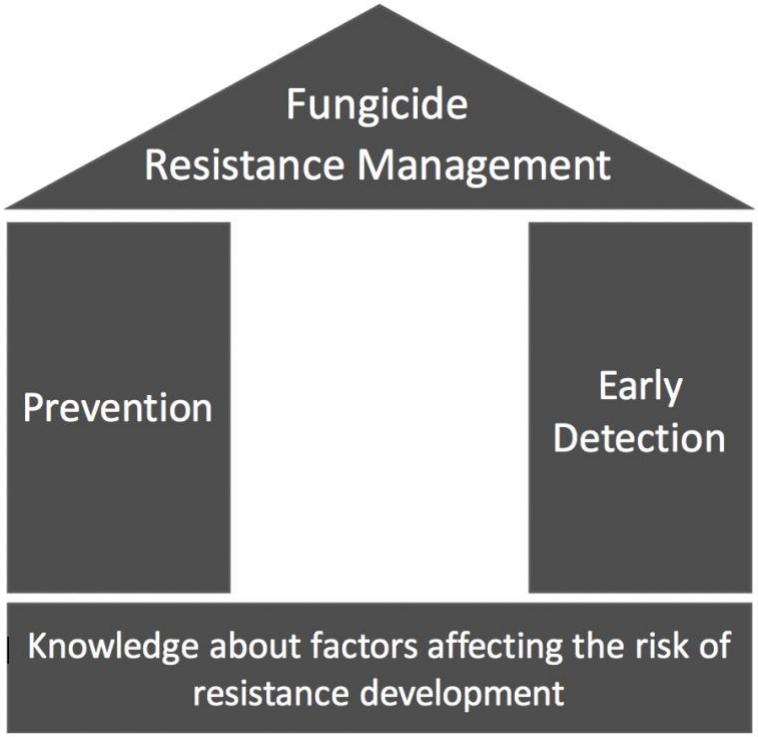

Fig. 1.1. Framework of fungicide resistance management. Prevention and early detection are the pillars of fungicide resistance management. Foundational knowledge of factors affecting the risk of resistance development is required to bolster these pillars. Prevention involves the use of proactive measures to avoid resistance development, early detection includes monitoring of fungicide resistance to prevent significant crop losses due to resistant pathogens, and the factors affecting risk of resistance development comprise of fungicide-risk factors and pathogen-risk factors.

CHAPTER-2

RHIZOCTONIA ZEAE: DISTRIBUTION AND FUNGICIDE SENSITIVITY OF ISOLATES COLLECTED FROM CORN AND SOYBEAN FIELDS IN NEBRASKA

Abstract

Corn and soybean are the major crops in the North Central U.S. *Rhizoctonia zeae* was recently identified as the major *Rhizoctonia* species in corn and soybean fields in Nebraska and was shown to be pathogenic on corn and soybean seedlings. Fungicide seed treatments are commonly used to manage seedling diseases and include several modes of action, such as demethylation inhibitors (DMI), phenylpyrroles (PP), succinate dehydrogenase inhibitors (SDHI), and quinone outside inhibitors (QoI). To establish the current control level provided by fungicides, we isolated *R. zeae* from corn and soybean fields in Nebraska and examined their sensitivity to four different seed treatment fungicides. Relative effective concentration for 50% inhibition (EC_{50}) was estimated for 91 *R. zeae* isolates. Average EC_{50} for prothioconazole (DMI) was 0.219 µg/ml, fludioxonil (PP) was 0.099 µg/ml, sedaxane (SDHI) was 0.078 µg/ml, and azoxystrobin (QoI) was > 100 µg/ml. To validate insensitivity to azoxystrobin, *in planta* assays were performed. Azoxystrobin did not have a significant effect in reducing the disease severity or dry weight of soybean plants ($P > 0.05$). For prothioconazole, fludioxonil, and sedaxane, EC_{50} did not differ significantly among isolates collected from different years (2015-2017; $P > 0.05$). Single discriminatory concentrations were identified as 0.1 µg/ml for each fungicide except azoxystrobin such that sensitivity shifts can be monitored in the future using a single concentration of each fungicide. This is the first study to establish

the current sensitivity of *R. zeae* to commonly used seed treatment fungicides in Nebraska and can be used to monitor sensitivity shifts in future. This information will help to guide strategies for chemical control of *R. zeae* in Nebraska.

Introduction

Corn (*Zea mays* L.) and soybean [*Glycine max* (L.) Merr.] are the major crops grown in the North Central United States and are often grown in rotation. Nebraska ranks third for corn production and fifth for soybean production in the country. Monetary losses due to corn and soybean diseases can considerably affect the state's economy owing to reduced farm income and negative impact on allied industries. Seedling diseases caused by filamentous pathogens have been reported to cause yield losses of 37.3 million bushels in soybean and 23.9 million bushels in corn in the U.S. and Ontario, Canada in 2018 (Crop Protection Network 2020). The major pathogens causing seedling diseases include *Rhizoctonia, Fusarium, Phytophthora, and Pythium.*

The form genus *Rhizoctonia* consists of several phylogenetically distinct species including *Thanatephorus cucumeris (R. solani), Ceratobasidium* spp. (Binucleate Rhizoctonia; BNR), and *Waitea circinata*, which are further classified into Anastomosis Groups (AGs) or varieties. *Rhizoctonia solani* is classified into 14 AGs (Carling 1996; Carling et al. 1999; Ogoshi 1987) and *Waitea circinata* is classified into five varieties: var. *agrostis*, var. *circinata*, var. *oryzae*, var. *prodigus*, and var. *zeae* (Kammerer et al. 2011; Leiner and Carling 1994; Toda et al. 2007). *Rhizoctonia solani* AG-2-2IIIB, AG-4, and *R. zeae* (*W. circinata* var. *zeae*) have been widely associated with corn seedling diseases (Führer Ithurrart et al. 2004; Sumner and Bell 1986), while *R. solani* AG-2-

2IIIB, AG-4 and AG-5 have been associated with soybean seedling diseases (Ajayi-Oyetunde 2017; Bolkan and Ribeiro 1985; Liu and Sinclair 1991; Nelson et al. 1996; Ploetz et al. 1985; Sneh et al. 1991; Zhao et al. 2005). In Nebraska, *Rhizoctonia* spp. from corn and soybean have been recently characterized (Kodati 2019). *Rhizoctonia zeae* was the major species identified and was shown to be pathogenic on both corn and soybean. This was the first study that showed *R. zeae* to be pathogenic on soybean in the North Central U.S. It is important to know if this relatively less studied but important pathogen of soybean can be effectively controlled by the currently used fungicides in Nebraska.

Fungicide seed treatments generally used for control of *Rhizoctonia spp.* include azoxystrobin, sedaxane, fludioxonil, and prothioconazole for soybean (Ajayi-Oyetunde and Bradley 2018) and azoxystrobin and fludioxonil for corn (Specht et al. 2017). These fungicides belong to four Fungicide Resistance Action Committee (FRAC) groups; succinate dehydrogenase inhibitors (SDHI), quinone outside inhibitors (QoI), demethylation inhibitors (DMI), and phenylpyrroles (PP). Fungicide resistance is an acquired and heritable change in the fungal DNA leading to a decrease in fungicide sensitivity. Fungicide-resistant pathogens can lead to monetary losses due to repeated applications of ineffective fungicides, uncontrolled disease, and development, registration and marketing of new fungicides. Apart from developing resistance, failure of fungicide control can also result from the pathogen's inherent ability to be insensitive to the fungicide mode of action.

Risk of resistance development depends on intrinsic factors of the fungicide and the pathogen population. SDHI fungicides bind to succinate dehydrogenase (mitochondrial complex II) at ubiquinone-binding site and inhibit mitochondrial

respiration (Fungicide Resistance Action Committee 2020). These were launched in 1966, but their narrow spectrum of control limited their use. Broad spectrum SDHI fungicides came into the market in 2003 and have been widely used since then. These are medium to high-risk fungicides and field resistance has been reported for 13 pathogens (Sierotzki and Scalliet 2013). QoI fungicides bind to ubiquinol oxidase (mitochondrial complex III) at Qo site and inhibit mitochondrial respiration (Fungicide Resistance Action Committee 2020). These first came into the market in 1996 and are labeled for a broad range of plant pathogens. These are high-risk fungicides and field resistance has been reported for 39 pathogens (Fungicide Resistance Action Committee 2012). DMIs block the substrate binding site of 14-α demethylase. This inhibits biosynthesis of ergosterol, an important component of the fungal membrane, thus disrupting membrane fluidity and permeability (Becher and Wirsel 2012). DMI fungicides first came into the market in 1969 (Russell 2005), are labeled for a broad range of pathogens, and are medium-risk fungicides (Fungicide Resistance Action Committee 2020). The azole group of DMIs is widely used as antifungal drugs and fungicides. Resistance has been reported in four human pathogens and nine plant pathogens (Becher and Wirsel 2012; Mair et al. 2016). PPs are synthetic analogs of pyrrolnitrin, an antifungal compound produced naturally by some bacteria. They bind to the class III hybrid histidine kinase (HHK) and mimic osmotic stress, increasing intracellular turgor and membrane potential. It might affect other enzymes like hexokinases and sugar transporters (Kilani and Fillinger 2016). PPs were introduced into the market in 1988 and are non-systemic fungicides. Although these are low-risk fungicides (Fungicide Resistance Action Committee 2020; Kilani and

Fillinger 2016), occasional resistance has been reported (Broders et al. 2007; Gachango et al. 2012; Peters et al. 2008).

Although soil-borne pathogens have been broadly categorized as at low-risk to develop resistance (Brent and Hollomon 1998), QoI resistance has been reported in *R. solani* AG 1-IA on rice (Lunos 2016) and *R. solani* AG 3 on potato (Djébali et al. 2014). Decreased sensitivity to QoIs has been reported in *R. solani* AG-2-2 on sugar beet (Arabiat and Khan 2016) and *R. zeae* from bermudagrass has been found to be insensitive to QoIs (Kerns et al. 2017). Certain *R. solani* AGs from soybean were recently reported to be moderately to extremely sensitive to SDHI and DMI fungicides in Illinois (Ajayi-Oyetunde et al. 2017). Additionally, high rDNA-ITS diversity of *R. zeae* in the Americas (Aydin et al. 2013) and high genotypic diversity in the closely related *R. circinata* populations (Chen 2011) suggests that *R. zeae* may have high potential to develop fungicide resistance.

Knowledge about the sensitivity profile of *R. zeae*, which is the predominant *Rhizoctonia* species in corn and soybean fields in Nebraska, can help to guide management decisions and enable monitoring of fungicide sensitivity in the future. The objectives of our research were to (i) survey corn and soybean fields in Nebraska to isolate *Rhizoctonia* species; (ii) determine *in vitro* sensitivity of *Rhizoctonia zeae* to azoxystrobin, sedaxane, fludioxonil, and prothioconazole; and (iii) determine *in planta* sensitivity to azoxystrobin.

Materials and methods

Sample Collection. Soil and plant samples were collected from six soybean fields in the year 2015 and nine soybean fields each in years 2016 and 2017 in Nebraska. Additional soil and plant samples collected by Kodati (2019) from 30 corn fields and 27 soybean fields in Nebraska in 2015–2017 were used for this study. Eight *R. zeae* isolates from soybean in 2012 and 2013 were also obtained from Illinois (Ajayi-Oyetunde et al. 2017). Fields were sampled in the month of June when plants were between VE–V2 stage. Soil samples were taken in a 'W' or 'Z' transect and at least six soil samples were collected from each field. A soil probe or shovel was used to dig 15.2 cm deep and collect 700–950 cm^3 of soil in plastic bags (Ziplock, S.C. Johnson and Son, Inc., Racine, WI). To avoid cross-contamination, the probe/shovel was rinsed with distilled water and then sprayed with a solution of 70% ethanol or a chemical disinfectant (Lysol, Reckitt Benckiser LLC, Parsippany, NJ) before collecting the next sample.

For collecting plant samples, the field was scouted to identify and collect plants showing aboveground and/or belowground symptoms of seedling diseases. Aboveground symptoms included: a localized area of the field with stunted plant growth or no seedlings emerged (contiguous plants were collected in this case). Plants were carefully excavated based on aboveground symptoms using a shovel to avoid injury during this process. Belowground symptoms assessed were reddish brown lesions or discoloration on the hypocotyl or roots (Fig. 2.1). From one spot in the field, 2–3 symptomatic plants were collected in one plastic bag and sealed, and these were considered as one plant sample. GPS coordinates were recorded for each field and in certain fields, these were recorded

for each sample. Samples were stored in a cooler with icepacks, transported to the laboratory and stored at 4°C until processed.

Sample Processing. Soil samples were initially processed using four different methods: a seed bait method, a seedling bait method, an organic-debris method, and a modified toothpick method. Preliminary results showed that seedling bait method and organic-debris method were less effective and were not pursued further. For the seed bait method, sugar beet seeds (*Beta vulgaris* L.) were used since these are a known bait for isolating *Rhizoctonia* spp. (Papavizas et al. 1962). Soil samples were air-dried for two days. Cheesecloth sacks (5 cm x 5 cm) were filled with 10 twice-sterilized sugar beet seeds. A sterile conical Falcon® tube (50 ml; GeneMate, USA) was half-filled with the soil sample, topped with one cheesecloth sack and covered with approximately 20 ml additional soil to ensure that seeds were in contact with the soil. Added were 5 ml of sterile distilled water to moisten the sack. The tube was loosely closed and kept in dark for 3 days at 25°C. After 3 days, seeds were removed from soil and surface sterilized. The seeds were washed twice with distilled water for 60 s each, followed by 70% ethanol for 30 s and a final wash with distilled water for 60 s. Seeds were air dried for 2 h and transferred onto semi-selective media. For the modified toothpick method (Kodati 2019; Paulitz and Schroeder 2005), soil samples were put in 10–15 cm diameter sterile clay pots and distilled water was added to 15% wt./wt. Four sterile toothpicks (birch) were placed vertically in each pot with three-quarters of the toothpick inside the soil. The pots were incubated in the greenhouse at 21±2°C for 48 h. Toothpicks were collected using

sterile forceps and placed on semi-selective media. The most effective soil-processing method was found to be the toothpick method and was used for further isolations.

For processing plants, each plant was first washed under tap water to remove the soil sticking to the roots. Symptomatic hypocotyl or roots were cut into pieces and surface sterilized by washing twice in distilled water for 50 s each, followed by washing with 70% ethanol for 30 s and then with distilled water for 60 s. Excess water from the plant pieces was soaked on sterile paper towels and these were transferred to the semi-selective media on Petri plates (100x150 mm).

Isolation and identification of *Rhizoctonia* spp. A pilot study was conducted to evaluate different semi-selective media for isolating *Rhizoctonia* spp. including the modified Ko and Hora medium (Castro et al. 1988; Ko and Hora 1971), TS Medium (Spurlock 2013), and RSM medium (Kodati 2019). The RSM medium showed the best results and was hence used for further isolations. For making 1 L of RSM medium, 18 g of agar was sterilized in 1 L of distilled water at 121°C, 15 psi for 30 minutes. After the media cooled to 55–65°C, 100 mg of streptomycin sulfate, 100 mg of penicillin-G sodium salt, and 800 µl of 1 M sodium hydroxide were added.

The toothpicks or the surface sterilized plant pieces were transferred to RSM plates and stored at 22 ±1°C. After 36–48 h, the plates were examined under a stereomicroscope at 400X magnification for identifying hyphal features of *Rhizoctonia* spp., which includes having straight septate hyphae and right-angled branching. Hyphal tips from the putative *Rhizoctonia* spp. were transferred aseptically to quarter-strength Potato Dextrose Agar (9.75 g/L PDA, 5.25 g/L agar) or PDA amended with 0.01%

tetracycline (PDAt). After 24–36 h, cultures were visually examined for contamination and were serially transferred to new plates (quarter-strength PDA or PDAt) until pure cultures were obtained. For identifying the *Rhizoctonia* species, the ITS region of 122 isolates was sequenced previously (Kodati 2019). The morphology of the sequenced isolates was used as a reference to classify other *Rhizoctonia* spp. used in the study. Morphological differentiation was based on the color of the mycelial colony, size and color of the sclerotia, and development of the sclerotia either on or inside the media (Kodati 2019). *Rhizoctonia zeae* has a white/buff to salmon-colored mycelial colony on PDA and salmon colored sclerotia of up to 1 mm diameter that develop on and inside the media. On maturity, the colony color and sclerotia become orange in color.

For short-term storage, isolates were allowed to produce sclerotia on PDA plates at 22 ±1°C and these were stored at 4°C. For long-term storage, eight mycelial plugs from actively growing margins were excised and stored in 1 ml solution of Potato Dextrose Broth (PDB) and glycerol (30% v/v) at -80°C in 2 ml Nalgene cryogenic vials (Thermo Fisher Scientific, Waltham, MA).

***In vitro* fungicide sensitivity determination.** Ninety-one *R. zeae* isolates were selected for determining *in vitro* sensitivity to four fungicides (Table 2.1). However, due to problems with isolate contamination, not all isolates could be tested for all fungicides. Four recommended fungicide seed treatments with different modes of action selected for this study were: azoxystrobin (QoI), fludioxonil (PP), prothioconazole (DMI), and sedaxane (SDHI). The serial agar dilution method was used to determine the relative Effective Concentration for 50% inhibition (EC_{50}). A pilot study was conducted to find

the appropriate concentrations for each fungicide that could be used in the agar dilution method. For azoxystrobin, the growth of *R. zeae* could not be inhibited up to 50% at the highest soluble concentration of azoxystrobin (100 µg/ml). The addition of alternative oxidase inhibitors, salicylhydroxamic acid (SHAM) and *n*-propyl gallate (PG) at different concentrations was not able to inhibit the growth by more than or equal to 50% and hence azoxystrobin could not be used in the *in vitro* assessment (data not shown).

Rhizoctonia zeae isolates were revived by aseptically transferring sclerotia on 1.5% water agar and incubated at 25°C. After 36–48 h, a 5 mm plug was excised from the actively growing mycelial edge and transferred to PDA and incubated in the dark at 25°C. After 36–48 h, a 5 mm plug was excised from the actively growing mycelial edge and transferred on fungicide amended media. A stock solution of a fungicide was made by dissolving the appropriate weight of the technical grade fungicide (fludioxonil, active ingredient [a.i.] 98%; prothioconazole a.i. 95%; or sedaxane a.i. 98%) in acetone. An appropriate volume of the stock solution was added to the molten PDA when the temperature was between 50–55°C to achieve the final concentrations for fludioxonil: 0.01, 0.05, 0.1, 0.25, 0.5 µg/ml; prothioconazole: 0.05, 0.1, 0.5, 1 µg/ml; and sedaxane: 0.005, 0.01, 0.1, 1 µg/ml. Non-amended PDA served as a control. Three replicates were used for each isolate-fungicide combination and the experiment was repeated. The mycelial growth was marked after 48 h by placing points on the edges of the longest diameter and its perpendicular diameter, which were measured using a digital Vernier caliper. The average of the two diameters was used for determining the growth. The three-parameter log-logistic model (LL.3) was used for fitting the dose-response curve in the *ezec* package (Kamvar 2016), which is a wrapper of the *drc* package (Ritz et al. 2015)

in R version 3.6.2 (R Core Team 2019). EC_{50} data from both experiments were combined as the homogeneity of variance was not significantly different among experiments ($P > 0.05$). Since the data were not normally distributed, the Kruskal Wallis Rank Sum test was performed to test the difference in EC_{50} among years and crop.

Discriminatory concentration selection. One discriminatory concentration was identified for each fungicide such that it could predict the EC_{50} of each isolate, as described by Jo et al. (2006). Briefly, the growth datasets from the two experiments were pooled for each fungicide and the resulting dataset was divided into 7:3 proportions, where 70% of the dataset was used to identify the discriminatory concentration and 30% of the dataset was used to validate the dose. A linear regression model between log EC_{50} and relative growth at each dose of each fungicide was generated. Dose at which the model showed best coefficient of determination (r^2) was chosen as the discriminatory concentration. The model was validated by performing linear regression between the log EC_{50} estimated from the dose-response model and the log EC_{50} predicted from the discriminatory concentration. If the regression obtained predicted and observed log EC_{50} followed a near 1:1 relationship, it was considered valid.

***In planta* fungicide sensitivity assessment.** Since *R. zeae* isolates were not sensitive to azoxystrobin *in vitro*, an *in planta* investigation was carried out to examine if the insensitivity was reliable or an artifact of the unblocked alternative oxidase pathway. Efficacy of the commercial formulation of azoxystrobin in controlling three *R. zeae* isolates (G2421, C2155, 12RS48) was evaluated on soybean plants in a growth chamber.

The parameters tested were soybean stand count, disease severity of root and hypocotyl rot, and plant biomass. The assay was performed as described by Ajayi-Oyetunde et al. (2017), with slight modifications. For inoculum preparation, 170 g of sorghum seed and 125 ml distilled water were mixed in 500 ml Erlenmeyer flasks and autoclaved for 30 min at 121°C and 15 psi. After 24 h, these were autoclaved again, and the last autoclaving was done after 2–3 days to ensure no latent spore germination. After the flasks cooled, 15 plugs (10 mm diameter) were excised from 4-day-old PDA culture of *R. zeae* and added to the sorghum seed. The flasks were then incubated at room temperature for 14 days and shaken every other day. The inoculated seed was air-dried for 3 days and stored in sealed plastic bags at 4°C until used.

Seeds of soybean 'Williams 82' were treated with a commercial formulation of azoxystrobin at the highest label rate (298.9 µl per kg seed). Pots were half-filled with 2:1 steam pasteurized sand:soil mixture, covered with 2g inoculum, and then filled with a 5 cm layer of the sand:soil mixture. Each pot was planted with nine seeds. The experiment was set up as a randomized complete block design with four replications and each bench was considered a block. Each block included two negative controls; the single negative control consisted of untreated soybean seeds and the double-negative control consisted of azoxystrobin treated soybean seeds. The experiment was conducted in a growth chamber at a day/night temperature of 25°C/21°C and a 14h photoperiod with a light intensity of 700 µmol. At 18 days after planting, the plants were evaluated for stand count and hypocotyl or root disease severity. The disease was rated on a scale of 0 to 5, which was modified from Nelson et al. (1996) and Ajayi-Oyetunde et al. (2017) because *R. zeae* did not show much disease symptoms on lateral roots. The disease severity scale used was as

follows: 0 = no lesion on root or hypocotyl; 1 = lesions <2.5 mm on hypocotyl or tap root; 2 = lesions 2.5 to 5 mm on hypocotyl or tap root; 3 = lesions >5 mm on hypocotyl or tap root; 4 = lesions girdling the hypocotyl or covering > 80% tap root; and 5 = plant dead, or no roots. The disease severity index was calculated by using the formula, DSI = Σ (score x number of plants with the disease score) / (5 x Number of plants). After rating the disease severity, the plants were cut into shoots and roots, air-dried at 53±1°C by keeping them in labeled paper envelopes for eight days, after which dry weights of roots and shoots were taken. The experiment was conducted twice.

Data were tested for normality using the Shapiro-Wilk Test and for homogeneity of variance using Levene's test (*car* package; Fox and Weisberg 2019). If data were normal and variance was homogeneous, then data from the two experiments were pooled and Analysis of Variance (ANOVA) was performed for continuous data and a Chi-square test was performed for count data. If the data lacked normality but variance was homogeneous, then data from the two experiments were pooled and a Kruskal-Wallis test was performed. When neither the data were normal, nor the variance was homogeneous, then the permuted version of the Wald-type statistic was calculated using the *GFD* package (Friedrich et al. 2017). All the analysis was performed in R version 3.6.2 (R Core Team 2019).

Results

***Rhizoctonia zeae* collection.** Collectively, 24 counties in Nebraska were sampled over a span of three years (Fig. 2.2). Most of the corn fields sampled were located in the western part of the state, while most of the soybean fields sampled were located in

eastern Nebraska. A total of 187 isolates of *Rhizoctonia* spp. were obtained from plants and soil, out of which 109 isolates were *R. zeae* and were obtained from 19 counties. Fifty-seven of these *R. zeae* isolates were previously identified using ITS sequencing (Kodati 2019). In the current study, we identified 52 additional isolates using the morphological features of *R. zeae* (right-angled hyphal branching, white/buff to salmon-colored mycelial colony on PDA, and salmon colored sclerotia of up to 1 mm diameter that develop on and inside the media). Out of 109 *R. zeae* isolates, 71 isolates were obtained from soybean and 38 isolates were obtained from corn. In 2015, only three *R. zeae* isolates were obtained, while 52 and 54 *R. zeae* isolates were obtained in 2016 and 2017 respectively. Most of the isolates (85%) were obtained from soil and the remaining isolates were obtained from plants. Eight *R. zeae* isolates were provided by collaborators and characterized previously (Ajayi-Oyetunde et al. 2017).

***In vitro* fungicide sensitivity assessment.** *In vitro* sensitivity was assessed for 91 isolates to fludioxonil, prothioconazole, and/or sedaxane. Most *Rhizoctonia zeae* isolates were sensitive ($EC_{50} < 1$ µg/ml) to fludioxonil, prothioconazole, and sedaxane. Average EC_{50} was 0.095 µg/ml fludioxonil (range: 0.07–0.23 µg/ml), 0.19 µg/ml prothioconazole (range: 0.093–2.29 µg/ml), and 0.072 µg/ml sedaxane (range: 0.05–0.22 µg/ml). For prothioconazole, only one isolate was considered moderately sensitive ($1 \leq EC_{50} < 10$ µg/ml). In contrast, 50% inhibition was not achieved at the highest dissolvable concentration of azoxystrobin (100 µg/ml) even on independent addition of SHAM and PG, suggesting that the average EC_{50} was >100 µg/ml azoxystrobin for all the isolates tested.

There was no significant difference in isolate sensitivity (EC_{50}) to fludioxonil or prothioconazole among host crops (Fig. 2.3; $P > 0.05$). There was a significant difference in EC_{50} to sedaxane among host crops ($P \leq 0.05$), which was also observed when data were compared according to geographical location of sampled corn fields in the west and sampled soybean fields in the east. EC_{50} for all fungicides did not differ significantly among years ($P > 0.05$). EC_{50} of isolates for all fungicides varied within and among counties. For sedaxane, the EC_{50} for isolates obtained from Keith, Webster, Scotts Bluff, and Lancaster counties varied from 0.048 µg/ml to 0.075 µg/ml, while the EC_{50} for isolates obtained from Valley county ranged from 0.079 µg/ml to 0.218 µg/ml (Fig. 2.4).

Discriminatory concentration selection. Discriminatory concentrations were identified as 0.1 µg/ml for fludioxonil, prothioconazole, and sedaxane (Fig. 2.5). The regression equation between relative growth at 0.1 µg/ml fludioxonil and log EC_{50} was $y = -3.6 + 0.026x$ ($r^2 = 0.95$; $P < 0.0001$; Fig. 2.5a) and the validation equation was $y = 0.21 + 1.1x$; ($r^2 = 0.86$; $P < 0.0001$; Fig. 2.5b). The regression equation between relative growth at 0.1 µg/ml prothioconazole and log EC_{50} was $y = -3.5 + 0.027x$ ($r^2 = 0.52$; $P < 0.0001$) and the validation equation was $y = 0.62 + 1.3x$; ($r^2 = 0.96$; $P < 0.0001$). The regression equation between relative growth at 0.1 µg/ml fludioxonil and log EC_{50} was $y = -4.7 + 0.053x$ ($r^2 = 0.88$; $P < 0.0001$) and the validation equation was $y = -0.58 + 0.77x$; ($r^2 = 0.89$; $P < 0.0001$). The validation equations for all three fungicides followed a near 1:1 relationship (intercept = 0, slope = 1).

***In planta* fungicide sensitivity assessment.** To evaluate whether insensitivity to azoxystrobin was an artifact of the unblocked alternative oxidase pathway, *in planta* fungicide sensitivity was assessed. Three *R. zeae* isolates evaluated in these experiments

had significantly different DSI than the negative control and the azoxystrobin control ($P \leq 0.05$) suggesting that all isolates were able to cause disease on soybean plants. Additionally, isolates G2421 and 12RS48 significantly reduced the dry weight of the soybean plants ($P \leq 0.05$). Azoxystrobin treatment showed no significant difference in DSI, SC, or total dry weight of the soybean plants compared to the inoculated control (Table 2.2; $P > 0.05$). Interestingly, the azoxystrobin control (no fungal inoculation) showed significantly less shoot dry weight and total dry weight than the negative control ($P \leq 0.05$), however, the DSI were not significantly different.

Discussion

In this study, 91 isolates of *R. zeae* were tested for their sensitivity to fludioxonil, prothioconazole, sedaxane, and/or azoxystrobin. These isolates were obtained from Nebraska in 2015–2017 and from Illinois in 2012–2013. We found that most of the *R. zeae* isolates were sensitive to fludioxonil, prothioconazole, and sedaxane. However, azoxystrobin was ineffective both *in vitro* and *in planta*, suggesting that in field applications would not provide *R. zeae* disease control. The sensitivity of isolates to different fungicides varied among years, host crops, and within and among counties.

Although most of the *R. zeae* isolates were found to be extremely sensitive to fludioxonil, prothioconazole, and sedaxane, few isolates were found to have lower sensitivity, which might represent a slow shift in the sensitivity of the population (Fig. 2.3). The results are similar to sensitivity of *R. solani* AG-2-2 IIIB in Illinois to penflufen, sedaxane, ipconazole, and prothioconazole, where the authors found that *R. solani* isolates were moderately to extremely sensitive to these fungicides (Ajayi-

Oyetunde et al. 2017). In this study, no significant differences were detected in the fungicide sensitivity of isolates compared among years, which may be due to the brief time scale over which isolates were collected and compared, with an absence of historical isolates to compare and identify any shift in sensitivity. However, results from the present study can be used in the future to identify shifts in sensitivity, which can be assessed using the discriminatory concentrations identified.

While determining *in vitro* sensitivity to azoxystrobin, both SHAM and PG were independently added to the media to block the alternative oxidase (AOX) pathway and accurately determine the EC_{50}. Many eukaryotic species have an AOX pathway in their mitochondria, which branches off from the respiratory electron transport chain (ETC). It is mostly induced by inhibition of ETC. The AOX pathway allows electrons from ubiquinol to directly reduce O_2, circumventing the need of complexes III and IV. Non-utilization of these complexes leads to reduced ATP production in the AOX pathway (Wood and Hollomon 2003; McDonald et al. 2009). Hydroxamic acids (e.g., SHAM) and *n*-alkyl-gallates (e.g., PG) inhibit AOX and are often included in *in vitro* QoI fungicide sensitivity assays (Pasche et al. 2004; De Miccolis Angelini et al. 2012). AOX overcomes fungicide toxicity *in vitro* resulting in an increased amount of fungicide required to inhibit pathogens like *Ascochyta rabiei, Fusarium graminearum,* conidia of *Pyricularia grisea,* and mycelia of *Venturia inaequalis* (Wise et al. 2008; Kaneko and Ishii 2009; Kim et al. 2003; Steinfeld et al. 2001). While some pathogens, like *Leptosphaeria maculans* do not use AOX *in vitro* (Fraser et al. 2016), AOX pathway may be constitutive for pathogens like *Botrytis cinerea* and *Fusicladium effusum* (De Miccolis Angelini et al. 2012; Seyran et al. 2010). PG and SHAM show differences in their

inhibitory effects on AOX (Parrish and Leopold 1978; Price III et al. 2015; Umbach and Siedow 2000), which may be due to differences in their binding site on the oxidase (Kay and Palmer 1985). In the current study, both SHAM and PG independently reduced the colony diameter of *R. zeae* compared to the non-amended PDA control, but the addition of these chemicals to azoxystrobin amended media did not reduce its EC_{50} to less than 100 µg/ml. A similar effect on growth was observed previously (Lunos 2016) and insensitivity of *R. zeae* and *R. solani* AG-1 to QoI fungicides, even with the addition of SHAM, was observed by Lee (2004). However, other studies have reported a range of sensitivity to QoI fungicides in *R. zeae* and *R. solani* AG-1-IA, AG-1-IB, and AG-2-2IIIB (Amaradasa et al. 2014; Lunos 2016). In *R. solani*, azoxystrobin and trifloxystrobin have been reported to be less effective *in vitro* than *in planta*, which may be due to an additional mechanism of alternative oxidation that is not inhibited by SHAM (LaMondia 2012; Arabiat and Khan 2016).

In the *in planta* azoxystrobin assays, it was observed that azoxystrobin treatment in the absence of *R. zeae* inoculum reduced the biomass of the soybean plant. This observation can be attributed to the reduced photosynthetic activity of soybean due to azoxystrobin treatment (Nason et al. 2007). In the *in planta* experiments, *R. zeae* isolates reduced the biomass of the plant, however, the stand count was not significantly affected. The effect of *R. zeae* on stand count has not been reported before. The amount of reduction in biomass varied with the aggressiveness of the *R. zeae* isolate under study. This is an important observation since the amount of biomass can partly determine the crop yield (Long et al. 2006).

Rhizoctonia zeae has been found to be virulent on soybean and was found to be the most prevalent *Rhizoctonia* species isolated from corn and soybean fields in Nebraska in the current study, as well as in a recent study (Kodati 2019). Previous studies have documented different *Rhizoctonia* species throughout Nebraska. *Rhizoctonia solani* AG-3 was isolated from potato (Castro et al. 1983), *R. solani* AG-5 from leafy spurge (Yuen and Masters 1995), *R. solani* AG-2-2 and *R. zeae* from sugar beet (during 2006–2009; Webb et al. 2015), and *R. solani* AG-1-ID, AG-2-2 IIIB, AG-2-2-IV, AG-4 (HGs I, II, III), AG-5, and BNR were isolated from dry bean (Venegas 2008). Additionally, *Rhizoctonia zeae* was recently isolated from dry bean and native grasses (Kodati 2019). The widespread distribution of *R. zeae* in Nebraska and its association with different crops (including native grasses) suggests that this pathogen might be native to Nebraska. However, this hypothesis needs to be tested by a population genetics study. The biocontrol activity of *R. zeae* against *R. solani* and certain *Fusarium* and *Pythium* spp. (Webb et al. 2015) could have helped to achieve the widespread distribution of this pathogen. Although *R. zeae* is virulent on soybean (Kodati 2019), its negative impact on yield, if any, remains unknown. Field studies are required to estimate yield losses caused by this pathogen.

The present study establishes the current sensitivity profile of *R. zeae* in Nebraska, which is the predominant *Rhizoctonia* species in corn and soybean fields. Azoxystrobin seed treatment fungicide was not able to control this pathogen, but other seed treatment fungicides, fludioxonil, prothioconaole, and sedaxane, were effective against *R. zeae*. It is important to correctly identify the seedling disease pathogen in a field to apply appropriate fungicide seed treatments. For disease management

recommendations, field studies are required to test the control provided by different fungicides against the diversity of soil-borne pathogens present in Nebraska.

References

Ajayi-Oyetunde, O. O., and Bradley, C. A. 2018. *Rhizoctonia solani*: Taxonomy, population biology, and management of rhizoctonia seedling disease of soybean. Plant Pathol. 67:3–17.

Ajayi-Oyetunde, O. O., Butts-Wilmsmeyer, C. J., and Bradley, C. A. 2017. Sensitivity of *Rhizoctonia solani* to succinate dehydrogenase inhibitor and demethylation inhibitor fungicides. Plant Dis. 101:487–495.

Amaradasa, B. S., Lakshman, D., McCall, D. S., and Horvath, B. J. 2014. *In vitro* fungicide sensitivity of *Rhizoctonia* and *Waitea* isolates collected from turfgrasses. J. Environ. Hortic. 32:126–132.

Arabiat, S., and Khan, M. F. 2016. Sensitivity of *Rhizoctonia solani* AG-2-2 from sugar beet to fungicides. Plant Dis. 100:2427–2433.

Aydin, E.B., Gurkanli, C.T., Ozkoc, I., Demirci, E., Erper, I., Karaca, G., Hsieh, T.F., Vajna, L. and Poltronieri, L.S. 2013. rDNA-ITS diversity of *Waitea circinata* var. *zeae* (anamorph: *Rhizoctonia zeae*). J. Plant Pathol. 95:587–595.

Becher, R., and Wirsel, S. G. 2012. Fungal cytochrome P450 sterol 14α-demethylase (CYP51) and azole resistance in plant and human pathogens. Appl. Microbiol. Biotechnol. 95:825–840.

Bolkan, H. A., and Ribeiro, W. R. C. 1985. Anastomosis groups and pathogenicity of *Rhizoctonia solani* isolates from Brazil. Plant Dis. 69:599–601. https://doi.org/10.1094/PD-69-599

Brent, K. J., and Hollomon, D. W. 1998. Fungicide resistance: the assessment of risk. FRAC Monogr. No. 2. Global Crop Protection Federation, Brussels.

Broders, K. D., Lipps, P. E., Paul, P. A., and Dorrance, A. E. 2007. Evaluation of *Fusarium graminearum* associated with corn and soybean seed and seedling disease in Ohio. *Plant Disease,* 91:1155–1160.

Carling, D. E. 1996. Grouping in *Rhizoctonia solani* by hyphal anastomosis reaction. Pages 37–47 in: *Rhizoctonia* Species: Taxonomy, Molecular Biology, Ecology, Pathology and Disease Control. B. Sneh, S. Jabaji-Hare, S. Neate, and G. Dijst, eds. Kluwer Academic Publishers, Dordrecht, The Netherlands. https://doi.org/10.1007/978-94-017-2901-7_3

Carling, D. E., Pope, E. J., Brainard, K. A., and Carter, D. A. 1999. Characterization of mycorrhizal isolates of *Rhizoctonia solani* from an orchid, including AG-12, a new anastomosis group. Phytopathology 89:942–946.

Castro, C., Davis, J. R., and Wiese, M. V. 1983. Differential medium for identification of *Rhizoctonia solani* AG-3. Plant Dis. 67:1069.

Chen, C. 2011. The geographic distribution, genetic structure and cultural management of *Waitea circinata* var. *circinata*, the causal agent of brown ring patch. Doctoral Dissertation. University of California, Riverside.

Crop Protection Network. 2020. Estimates of corn, soybean, and wheat yield losses due to disease: An online tool. https://loss.cropprotectionnetwork.org/. doi: 10.31274/cpn-20191121-0.

De Miccolis Angelini, R. M., Rotolo, C., Masiello, M., Pollastro, S., Ishii, H., and Faretra, F. 2012. Genetic analysis and molecular characterisation of laboratory and field mutants of *Botryotinia fuckeliana* (*Botrytis cinerea*) resistant to QoI fungicides. Pest Manag. Sci. 68:1231–1240

Djébali, N., Elkahoui, S., Taamalli, W., Hessini, K., Tarhouni, B., and Mrabet, M. 2014. Tunisian *Rhizoctonia solani* AG3 strains affect potato shoot macronutrients content, infect faba bean plants and show *in vitro* resistance to azoxystrobin. Australas. Plant Pathol. 43:347–358.

Fox, J., and Weisberg, S. 2019. An R companion to applied regression (3rd ed.). Thousand Oaks, CA: Sage. Retrieved from https://socialsciences.mcmaster.ca/jfox/Books/Companion/

Fraser, M., Hwang, S. F., Ahmed, H. U., Akhavan, A., Stammler, G., Barton, W., and Strelkov, S. E. 2016. Sensitivity of *Leptosphaeria maculans* to pyraclostrobin in Alberta, Canada. Can. J. Plant Sci. 97:83–91.

Friedrich, S., Konietschke, F., and Pauly, M. 2017. GFD: An R package for the analysis of general factorial designs. J. Stat. Softw. 79:1–18. doi:10.18637/jss.v079.c01

Führer Ithurrart, M. E., Büttner, G., and Petersen, J. 2004. Rhizoctonia root rot in sugar beet (*Beta vulgaris* ssp. *altissima*) - Epidemiological aspects in relation to maize (*Zea mays*) as a host plant. J. Plant Dis. Prot. 111:302–312.

Fungicide Resistance Action Committee. 2020. FRAC Code List 2020: Fungal control agents sorted by cross resistance pattern and mode of action (including FRAC Code numbering). CropLife Int., Brussels, Belgium.

Gachango, E., Hanson, L. E., Rojas, A., Hao, J. J., and Kirk, W. W. 2012. *Fusarium* spp. causing dry rot of seed potato tubers in Michigan and their sensitivity to fungicides. Plant Dis. 96:1767–1774.

Jo, Y. K., Niver, A. L., Rimelspach, J. W., and Boehm, M. J. 2006. Fungicide sensitivity of *Sclerotinia homoeocarpa* from golf courses in Ohio. Plant Dis. 90:807–813.

Kammerer, S.J., Burpee, L.L. and Harmon, P.F. 2011. Identification of a new *Waitea circinata* variety causing basal leaf blight of seashore paspalum. Plant Dis. 95:515–522.

Kamvar, Z.K. 2016. ezec: Easy interface to effective concentration calculations. R package version 1.0.1.

Kaneko, I., and Ishii, H. 2009. Effect of azoxystrobin on activities of antioxidant enzymes and alternative oxidase in wheat head blight pathogens *Fusarium graminearum* and *Microdochium nivale*. J. Gen. Plant Pathol. 75:388–398.

Kay, C. J., and Palmer, J. M. 1985. Solubilization of the alternative oxidase of cuckoo-pint (*Arum maculatum*) mitochondria. Stimulation by high concentrations of ions and effects of specific inhibitors. Biochem. J. 228:309–318.

Kerns, J., Yan, Y., and Butler, E. 2017. Characterization, pathogenicity, and *in vitro* sensitivity of *Rhizoctonia* spp. associated with leaf and sheath spot of bermudagrass putting greens in North Carolina and Alabama. Int. Turfgrass Soc. Res. J. 13:203–212.

Kilani, J., and Fillinger, S. 2016. Phenylpyrroles: 30 years, two molecules and (nearly) no resistance. Front. Microbiol. 7:2014.

Kim, Y. S., Dixon, E. W., Vincelli, P., and Farman, M. L. 2003. Field resistance to strobilurin (QoI) fungicides in *Pyricularia grisea* caused by mutations in the mitochondrial cytochrome b gene. Phytopathology 93:891–900.

Ko, W. H., and Hora, F. K. 1971. A selective medium for the quantitative determination of *Rhizoctonia solani* in soil. Phytopathology, 61:707–710.

Kodati, S. 2019. Diversity and pathogenicity of *Rhizoctonia* spp. from different plant hosts in Nebraska. Doctoral Dissertation. University of Nebraska, Lincoln.

Lee, D. J. 2004. Population Dynamics of *Rhizoctonia* species in tall fescue and creeping bentgrass in response to disease management programs.

Leiner R. H., and Carling D. E., 1994. Characterization of *Waitea circinata* (*Rhizoctonia*) isolated from agricultural soils in Alaska. *Plant Dis.* 78:385–388.

Liu, Z., and Sinclair, J. B. 1991. Isolates of *Rhizoctonia solani* anastomosis group 2-2 pathogenic to soybean. *Plant Dis.* 75:682–687. https://doi.org/10.1094/PD-75-0682.

Long, S. P., Zhu, X. G., Naidu, S. L., and Ort, D. R. 2006. Can improvement in photosynthesis increase crop yields? Plant Cell Environ. 29:315–330.

Lunos, A. G. 2016. Geographic distribution and severity of strobilurin fungicide resistance among *Rhizoctonia solani* on rice in southwestern Louisiana. Master's Thesis. Louisiana State University, Baton Rouge.

Mair, W. J., Deng, W., Mullins, J. G., West, S., Wang, P., Besharat, N., Ellwood, S.R., Oliver, R.P., and Lopez-Ruiz, F. J. 2016. Demethylase inhibitor fungicide

resistance in *Pyrenophora teres* f. sp. *teres* associated with target site modification and inducible overexpression of Cyp51. Front. Microb. 7:1279.

McDonald, A. E., Vanlerberghe, G. C., and Staples, J. F. 2009. Alternative oxidase in animals: unique characteristics and taxonomic distribution. J. Exp. Biol. 212:2627–2634.

Nason, M. A., Farrar, J., and Bartlett, D. 2007. Strobilurin fungicides induce changes in photosynthetic gas exchange that do not improve water use efficiency of plants grown under conditions of water stress. Pest Manag. Sci. 63:1191–1200

Nelson, B., Helms, T., Christianson, T., and Kural, I. 1996. Characterization and pathogenicity of *Rhizoctonia* from soybean. Plant Dis. 80:74–80. https://doi.org/10.1094/PD-80-0074.

Ogoshi, A. 1987. Ecology and pathogenicity of anastomosis and intraspecific groups of *Rhizoctonia solani* Kuhn. Annu. Rev. Phytopathol. 25:125–143.

Papavizas, G. C., and Davey, C. B. 1962. Isolation and pathogenicity of *Rhizoctonia* saprophytically existing in soil. Phytopathology 52:834–840.

Parrish, D. J., and Leopold, A. C. 1978. Confounding of alternate respiration by lipoxygenase activity. Plant Physiol. 62:470–472.

Pasche, J. S., Wharam, C. M., and Gudmestad, N. C. 2004. Shift in sensitivity of *Alternaria solani* in response to QoI fungicides. Plant Dis. 88:181–187.

Paulitz, T. C., and Schroeder, K. L. 2005. A new method for the quantification of *Rhizoctonia solani* and *R. oryzae* from soil. Plant Dis. 89:767–772.

Peters, R. D., Platt, H. W., Drake, K. A., Coffin, R. H., Moorehead, S., Clark, M. M., Al-Mughrabi, K. I. and Howard, R. J. 2008. First report of fludioxonil-resistant isolates of *Fusarium* spp. causing potato seed-piece decay. Plant Dis. 92:172–172.

Ploetz, R. C., Mitchell, D. J., and Gallaher, R. N. 1985. Characterization and pathogenicity of *Rhizoctonia* species from a reduced-tillage experiment multicropped to rye and soybean in Florida. Phytopathology 75:833–839. https://doi.org/10.1094/Phyto-75-833.

Price III, P. P., Purvis, M. A., Cai, G., Padgett, G. B., Robertson, C. L., Schneider, R. W., and Albu, S. 2015. Fungicide resistance in *Cercospora kikuchii*, a soybean pathogen. Plant Dis. 99:1596–1603.

R Core Team. 2019. R: A language and environment for statistical computing. R Foundation for Statistical Computing, Vienna, Austria. URL: https://www.R-project.org/.

Ritz, C., Baty, F., Streibig, J. C., and Gerhard, D. 2015. Dose-response analysis using R. PLoS One 10:e0146021.

Russell, P. E. 2005. A century of fungicide evolution. J. Agric. Sci. 143:11–25.

Seyran, M., Brenneman, T. B., and Stevenson, K. L. 2010. *In vitro* toxicity of alternative oxidase inhibitors salicylhydroxamic acid and propyl gallate on *Fusicladium effusum*. J. Pest Sci. 83:421–427.

Sierotzki, H., and Scalliet, G. 2013. A review of current knowledge of resistance aspects for the next-generation succinate dehydrogenase inhibitor fungicides. Phytopathology 103:880–887

Sneh, B., Burpee, L., and Ogoshi, A. 1991. Identification of *Rhizoctonia* Species. APS Press, St. Paul, MN.

Specht, J., Hoegemeyer, T., Graef, G., Ruff, L., Torrion, J., Grassini, P., Edreira, J., Tenorio, F., Farmaha, B., Miller, J., Shaver, T., Wortman, C., Shapiro, C., Krienke, B., Knezevic, S., Jhala, A., Krueger, G., Werle, R., Procter, C., Blanco, H., Elmore, R., Irmak, S., Wright, R., Hunt, T., Giesler, L., Ziems, T., Shulski, M., Dutcher, A., Cooper, S., Glewen, K., Mueller, N., Rees J., and Thompson, L. 2017. Nebraska soybean and corn pocket field guide. University of Nebraska-Extension.

Spurlock, T. N. 2013. Spatial Distributions of *Rhizoctonia* species in Soybean fields Undergoing Annual Rotations with Rice. Doctoral Dissertation, University of Arkansas, Fayetteville.

Steinfeld, U., Sierotzki, H., Parisi, S., Poirey, S., and Gisi, U. 2001. Sensitivity of mitochondrial respiration to different inhibitors in *Venturia inaequalis*. Pest Manag. Sci. 57:787–796.

Sumner, D. R., and Bell, D. K. 1986. Influence of crop rotation on severity of crown and brace root rot caused in corn by *Rhizoctonia solani*. Phytopathology 76:248–252.

Toda, T., Hayakawa, T., Mghalu, J.M., Yaguchi, S. and Hyakumachi, M. 2007. A new *Rhizoctonia* sp. closely related to *Waitea circinata* causes a new disease of creeping bentgrass. J. of Gen. Plant Pathol. 73:379–387.

Umbach, A. L., and Siedow, J. N. 2000. The cyanide-resistant alternative oxidases from the fungi *Pichia stipitis* and *Neurospora crassa* are monomeric and lack regulatory features of the plant enzyme. Arch. Biochem. Biophys. 378:234–245.

Venegas, J. P., Godoy-Lutz, G., Steadman, J. R., Urrea, C., and Harveson, R. 2008. Morphological and molecular characterization of *Rhizoctonia solani* isolates from western Nebraska dry beans. Annu. Rep. Bean Improv. Coop. 51:86.

Webb, K. M., Harveson, R. M., and West, M. S. 2015. Evaluation of *Rhizoctonia zeae* as a potential biological control option for fungal root diseases of sugar beet. Ann. Appl. Biol. 167:75–89.

Wise, K. A., Bradley, C. A., Pasche, J. S., Gudmestad, N. C., Dugan, F. M., and Chen, W. 2008. Baseline sensitivity of *Ascochyta rabiei* to azoxystrobin, pyraclostrobin, and boscalid. Plant Dis. 92:295–300.

Wood, P. M., and Hollomon, D. W. 2003. A critical evaluation of the role of alternative oxidase in the performance of strobilurin and related fungicides acting at the Qo site of complex III. Pest Manag. Sci. 59:499–511.

Yuen, G. Y., and Masters, R. A. 1995. Moisture requirements and host specificity of *Rhizoctonia solani* from leafy spurge (*Euphorbia esula*) in Nebraska. Weed Technol. 9:44–48.

Zhao, G., Ablett, G. R., Anderson, T. R., Rajcan, I., and Schaafsma, A. W. 2005. Anastomosis groups of *Rhizoctonia solani* associated with soybean root and hypocotyl rot in Ontario and resistance of accession PI 442031 to different anastomosis groups. Can. J. Plant Pathol. 27:108–117.

Tables and Figures

Table 2.1. Isolates used for *in vitro* fungicide sensitivity assay.

Isolate ID	Host	Year	County[a]	Fungicide[b]
G2395	Soybean	2017	Nemaha	F/P/S
G2396	Soybean	2017	Nemaha	F/P/S
G2398	Soybean	2017	Mead	F/P/S
G2399	Soybean	2017	Mead	F/P/S
G2415	Soybean	2017	Valley	F/P/S
G2416	Soybean	2017	Dodge	F/P/S
G2413	Soybean	2017	Valley	F/P/S
G2408	Soybean	2017	Lancaster	F/P/S
G2420	Soybean	2017	Burt	F/P/S
G2421	Soybean	2017	Burt	F/P/S
G2495	Soybean	2016	Merrick	F/P/S
G2497	Soybean	2016	Platte	F/P/S
G2496	Soybean	2016	Merrick	F/P/S
G2411	Soybean	2017	Valley	F/P/S
G2397	Soybean	2017	Mead	F/P/S
G2407	Soybean	2017	Lancaster	F/P/S
G2417	Soybean	2017	Burt	F/P/S
S2174	Soybean	2017	Saunders	F/P
C1901	Corn	2016	Scotts Bluff	F/P/S
S2167	Soybean	2017	Clay	F/P/S
C1895	Corn	2016	Scotts Bluff	F/P/S
C1896	Corn	2016	Scotts Bluff	F/P/S
C1897	Corn	2016	Scotts Bluff	F/P/S
C2155	Corn	2017	Keith	F/P/S
S2346	Soybean	2017	Lincoln	F/P/S
C1889	Corn	2016	Keith	F/P
S2355	Soybean	2017	Clay	F/P/S
C2145	Corn	2017	Scotts Bluff	F/P/S
S2169	Soybean	2017	Clay	F/P
C2158	Corn	2017	Keith	F/P/S
S1837	Soybean	2016	Keith	F/P/S
C2162	Corn	2017	Webster	F/P/S
C1881	Corn	2016	Deuel	F/P
C1882	Corn	2016	Deuel	F/P/S
C1907	Corn	2016	Webster	F/P/S
S2166	Soybean	2017	Clay	F/P/S

S2347	Soybean	2017	Lincoln	F/P/S
S2221	Soybean	2017	Keith	F/S
S2170	Soybean	2017	Clay	F/P/S
C1880	Corn	2016	Deuel	F/P/S
G1723	Soybean	2015	Cuming	F/S
C2156	Corn	2017	Keith	F/P/S
S1916	Soybean	2016	Lincoln	F/P/S
C2048	Corn	2017	Webster	F/P/S
C2049	Corn	2017	Webster	F/P/S
S1915	Soybean	2016	Lincoln	F/P/S
C2160	Corn	2017	Webster	F/P/S
C2165	Corn	2017	Webster	F/P
C1375	Corn	2016	Keith	F/P/S
C2351	Corn	2017	Webster	F/P
C2151	Corn	2017	Keith	F/P/S
G2365	Soybean	2016	Nemaha	F/P/S
G2367	Soybean	2016	Antelope	F/P/S
G2498	Soybean	2016	Platte	F/P/S
G2361	Soybean	2016	Nemaha	F/P/S
G2494	Soybean	2016	Merrick	F/S
G2412	Soybean	2017	Valley	F/P/S
G2493	Soybean	2016	Merrick	F/P/S
G2362	Soybean	2016	Nemaha	F
G2488	Soybean	2016	Nemaha	F
G2363	Soybean	2016	Nemaha	F/S
G1725	Soybean	2015	Mead	F/S
W2_1_12	Soybean	2013	IL*	F
12RS40	Soybean	2012	IL*	F
248_2KH	Soybean	2012	IL*	F/P
12RS48	Soybean	2012	IL*	F/P/S
12RS39	Soybean	2012	IL*	F/P
12RS36	Soybean	2012	IL*	F
248_1a KH	Soybean	2012	IL*	F/P
211	Soybean	2012	IL*	F
G2486	Soybean	2017	Burt	P/S
C2150	Corn	2017	Keith	P/S
C2047	Corn	2017	Webster	P/S
C1898	Corn	2016	Scotts Bluff	P/S
C1894	Corn	2016	Scotts Bluff	P/S
G2508	Soybean	2016	Colfax	P/S

G2503	Soybean	2016	Clay	P/S
G2501	Soybean	2016	Clay	P/S
G2502	Soybean	2016	Clay	P/S
G2490	Soybean	2016	Antelope	P/S
G2491	Soybean	2016	Merrick	P/S
G2504	Soybean	2016	Clay	P/S
G2492	Soybean	2016	Merrick	P/S
G2506	Soybean	2016	Clay	P/S
G2500	Soybean	2016	Seward	P/S
G2499	Soybean	2016	Seward	P/S
G2505	Soybean	2016	Clay	P/S
G2364	Soybean	2016	Nemaha	S
G2368	Soybean	2016	Antelope	S
G2507	Soybean	2016	Colfax	S
G2487	Soybean	2016	Mead	S

[a]County information is available except those collected from Illinois (IL)
[b]Fungicide sensitivity was determined for Fludioxonil (F), Prothioconazole (P), and Sedaxane (S)

Table 2.2. Mean and standard errors of Disease severity index (DSI), stand count, and plant dry weight (shoot, root, and total) measured in the *in planta* azoxystrobin sensitivity experiment for three *Rhizoctonia zeae* isolates.

Isolate	Trt[1]	DSI		SC		Shoot dry wt. (g)		Root dry wt. (g)		Total dry wt. (g)	
		Mean[6]	Std Err	Mean	Std Err	Mean	Std Err	Mean	Std Err	Mean	Std Err
G2421	Ct (+)[2]	0.3646[a]	0.0399	8.0000[a]	0.3273	0.2287[a]	0.0143	0.0602[a]	0.0060	0.2889[a]	0.0196
	Az[3]	0.2691[a]	0.0423	7.7500[a]	0.5901	0.2474[a]	0.0138	0.0715[a]	0.0055	0.3189[a]	0.0189
C2155	Ct (+)	0.2721[a]	0.0410	8.3750[a]	0.2631	0.2456[ab]	0.0134	0.0798[ab]	0.0055	0.3253[ab]	0.0186
	Az	0.2347[a]	0.0380	8.6250[a]	0.1830	0.2493[ab]	0.0109	0.0770[ab]	0.0052	0.3263[ab]	0.0158
12RS48	Ct (+)	0.3637[a]	0.0461	8.1429[a]	0.2608	0.2257[a]	0.0120	0.0667[a]	0.0052	0.2925[a]	0.0168
	Az	0.2965[a]	0.0424	8.1250[a]	0.3981	0.2349[a]	0.0123	0.0715[a]	0.0055	0.3064[a]	0.0174
–	Ct (-)[4]	0.0698[b]	0.0265	8.1250[a]	0.2266	0.2728[b]	0.0138	0.0824[b]	0.0057	0.3552[b]	0.0190
–	Az Ct (-)[5]	0.1045[b]	0.0270	8.7500[a]	0.1637	0.2262[a]	0.0111	0.0682[a]	0.0050	0.2944[a]	0.0157

[1]Treatments (Trt) used in the study were:
[2]Ct (+) is the positive control with corresponding isolate inoculum
[3]Az refers to the *Rhizoctonia zeae* inoculated and azoxystrobin treated soybean (Williams 82) plants
[4]Ct (-) refers to uninoculated and untreated soybean (Williams 82) plants
[5]Az Ct (-) refers to uninoculated azoxystrobin treated soybean plants
[6]The same letter within each column of the mean are not significantly different ($P \leq 0.05$).

Fig. 2.1. Soybean plants showing symptoms of seedling disease. Symptoms included brownish sunken lesions, nibbling on the hypocotyl of the plant, discoloration and/or girdling of the taproot, and/or stunted growth of plants.

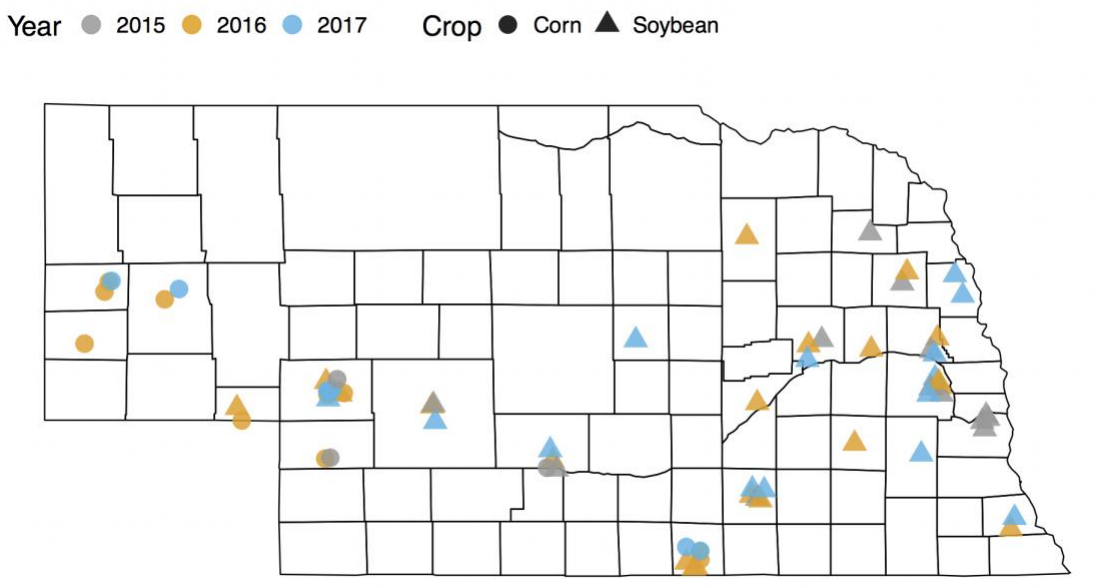

Fig. 2.2. Corn and soybean fields sampled during the years 2015–2017 in Nebraska.

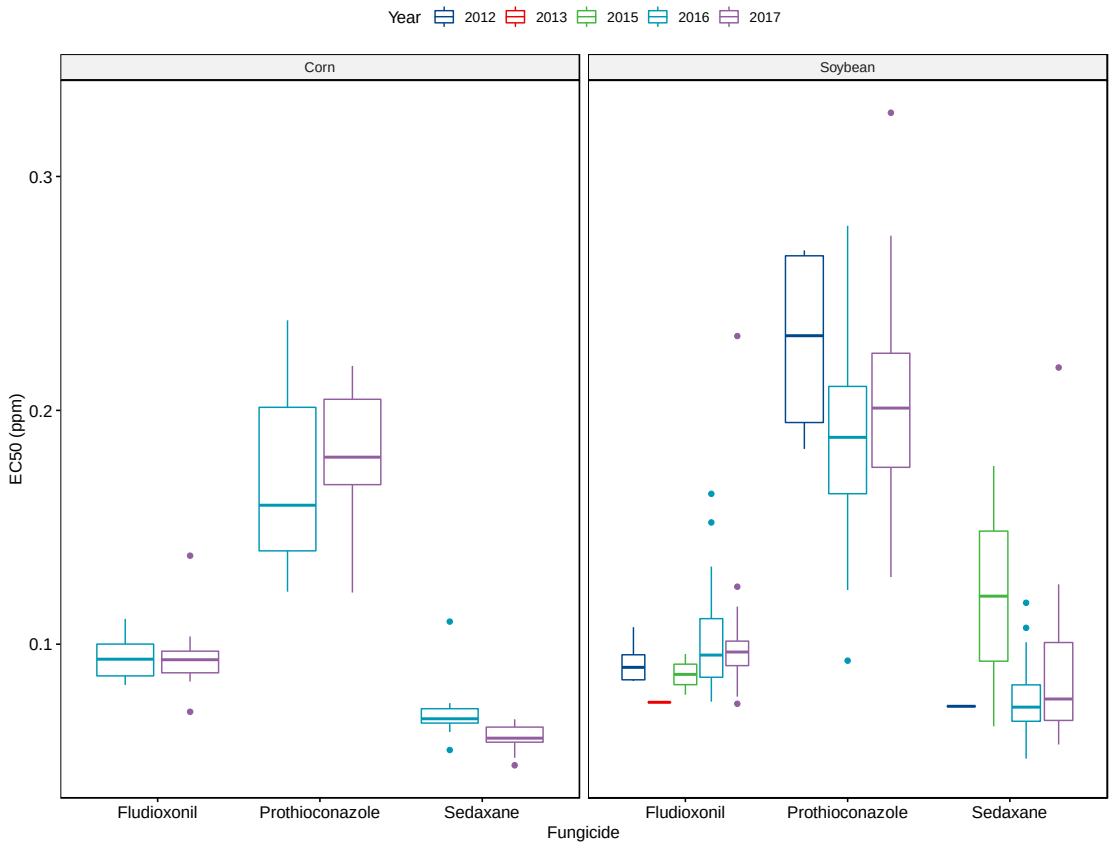

Fig. 2.3. Distribution of EC_{50} to fludioxonil, prothioconazole, and sedaxane for *Rhizoctonia zeae* isolated from a) corn, and b) soybean. Boxes are color-coded according to the year in which fungi were isolated. Isolates collected in 2012 and 2013 were obtained from Illinois, while the remaining isolates were from Nebraska. Data for isolate C2155 is not shown in the boxplot because the EC_{50} to prothioconazole was 2.29 µg/ml, which made it difficult to see the range of other isolates.

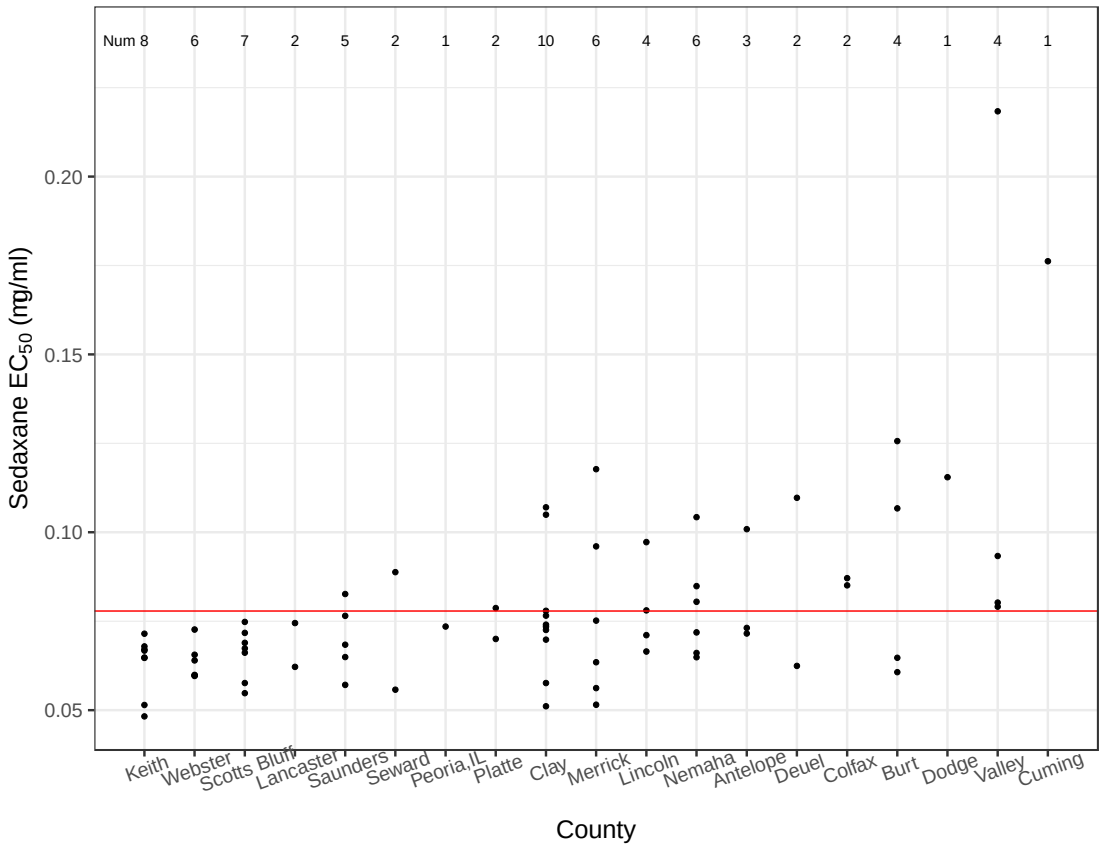

Fig. 2.4. Dot plot of *Rhizoctonia zeae* isolate sensitivity (EC_{50}) to sedaxane fungicide. Isolates were obtained from corn and soybean fields in Nebraska from 2015–2017 and from one soybean field in Illinois. The red horizontal line represents the mean EC_{50} for all the isolates used in the study. The solid dots represent the EC_{50} for each isolate in each county. The numbers on top of the graph represent the number of isolates in each county for which sensitivity was determined to sedaxane.

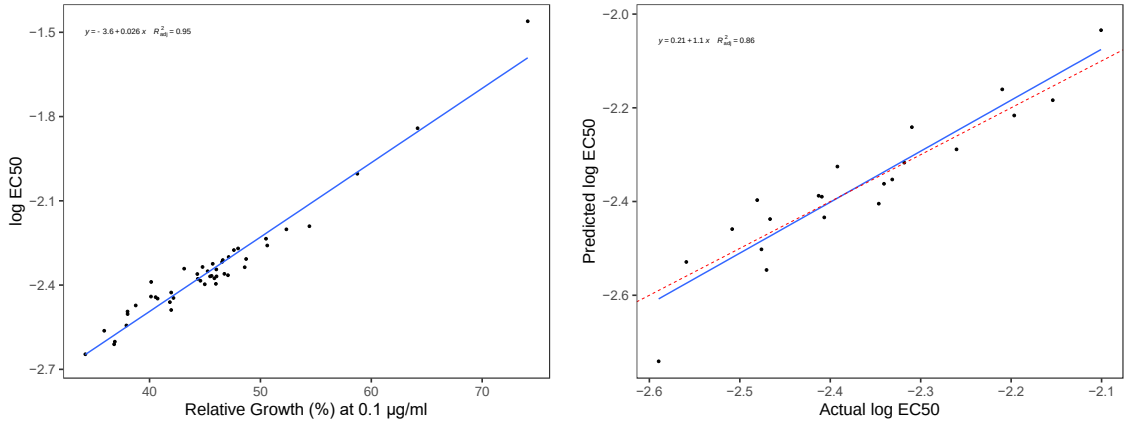

Fig. 2.5. Linear regression model between a) log EC_{50} and relative growth at 0.1 µg/ml of fludioxonil; and b) actual log EC_{50} and predicted log EC_{50} for model validation. Linear regression models between log EC_{50} and relative growth at each dose were generated. The best coefficient of determination (r^2) was generated for the dose 0.1 µg/ml fludioxonil and was hence chosen as the discriminatory concentration. The dose was validated by performing regression between actual log EC_{50} and predicted log EC_{50}, which followed a near 1:1 relationship (shown by red-dashed line).

CHAPTER-3

GENETIC STUCTURE OF *RHIZOCTONIA ZEAE* POPULATIONS FROM SOYBEAN AND CORN IN THE UNITED STATES

Abstract

Rhizoctonia zeae was recently identified as the major *Rhizoctonia* species in soybean and corn fields in Nebraska and was shown to be pathogenic on soybean and corn seedlings. Knowledge of the pathogen population structure is relevant for designing effective disease management strategies. Soil samples were collected in the year 2019 from corn and soybean fields in 12 states (IA, IL, IN, KS, KY, MI, MN, MO, ND, NE, SD, and WI). A total of 165 isolates belonging to different *Rhizoctonia* spp. were isolated from 12 states, of which 68.49% isolates were *R. zeae.* Five *R. zeae* isolates were analyzed by whole genome sequencing and 1,032 candidate microsatellite loci were identified, of which 43 primers were synthesized. Six microsatellite markers showed consistent amplification and polymorphism and were, therefore, used to genotype 200 *R. zeae* isolates obtained mostly from soybean and corn fields in the Northwest Central, Northeast Central, and Southern United States. High genotypic diversity (Simpson's diversity = 0.99) was observed for all the populations. A mixed mode of reproduction was inferred from the linkage disequilibrium analysis. Results from the analysis of molecular variance (AMOVA) suggested that the populations were structured according to geographic region ($P \leq 0.05$) and year of isolation (AMOVA for unfiltered data; $P \leq 0.05$). Collectively, the results suggest that *R. zeae* populations in the U.S. have high

evolutionary potential and this information can be used to devise effective control strategies for this pathogen.

Introduction

A recent survey of *Rhizoctonia* spp. causing soybean seedling diseases in Nebraska showed *R. zeae* (*Waitea circinata* var. *zeae*) was the predominant pathogen (Kodati 2019). Pathogenicity assays showed that it was able to cause disease as severe as that caused by *R. solani* AG 4 HG-II under optimal conditions (Kodati 2019). Characterization of the genetic structure of *R. zeae* populations is important to determine its evolutionary response to different disease management strategies and this insight can be used in managing this pathogen.

Rhizoctonia zeae belongs to the form genus *Rhizoctonia*, which consists of several phylogenetically distinct species including *Thanatephorus cucumeris (R. solani)*, *Waitea circinata*, and *Ceratobasidium* spp. (Binucleate Rhizoctonia; BNR). *Waitea circinata* is classified into five varieties: var. *agrostis*, var. *circinata*, var. *oryzae*, var. *prodigus*, and var. *zeae* (Kammerer et al. 2011; Leiner and Carling 1994; Toda et al. 2007). *Waitea circinata* var. *zeae* (*R. zeae*) has a wide host range. It is known to cause seedling or root diseases of corn (Voorhees 1934; Sumner and Bell 1982), wheat, cotton, and soybean (Tomaso-Peterson and Trevathan 2007), snap bean (Ohkura et al. 2009), Johnsongrass (Demirci and Eken 1999), onion (Erper et al. 2006), sugar beet (Kuznia and Windels 1994), and foliar diseases of corn (Li et al. 1998), creeping bentgrass (Tomaso-Peterson and Trevathan 2007), centipede grass (Haygood and Martin 1990), tall fescue (Martin and Lucas 1984), and bermudagrass (Kerns et al. 2017) among others. Recently, *R. zeae*

was identified to cause seedling disease of soybean in Nebraska and was shown to be the major *Rhizoctonia* species in corn and soybean fields in the state (Kodati 2019).

Previously, in Nebraska, *R. zeae* was isolated from sugar beet seedlings and shown to be a biocontrol agent (Webb et al. 2015). In other states, *R. zeae* has been isolated at lower frequencies from corn or soybean fields. From Arkansas, Illinois, Kansas, Michigan, Minnesota, and Ontario, Canada, 8.8% *Rhizoctonia* spp. from soybean were *R. zeae* (Ajayi-Oyetunde and Bradley 2017). It is currently unknown if *R. zeae* is mostly prevalent in Nebraska, or if it is distributed in other states that are major producers of corn and soybean. It is also important to understand the evolutionary history and evolutionary potential of *R. zeae*, so that this information can be used to inform disease management strategies and circumvent management failures. This information can be gained by determining the genetic diversity, mode of reproduction, and genotype flow between *R. zeae* populations.

A few studies have examined the genetic diversity of *R. zeae* using 18S-28S rDNA-ITS region, 18S rDNA and β-tubulin genes (Aydin et al. 2013; Gürkanli et al. 2016). These studies used a total of 20 isolates from different continents and found that *W. circinata* var. *zeae* had high genetic diversity in the Americas and suggested it as the origin of this pathogen. Another study performed Amplified Fragment Length Polymorphism (AFLP) analysis on 15 *Waitea circinata* var. *zeae* isolates from turfgrass in South Carolina and found high genetic diversity among isolates (El Fiky et al. 2011). No study has examined the genetic structure of *R. zeae* populations. However, high genotypic diversity in the closely related *R. circinata* populations (Chen 2011) suggests

that *R. zeae* may have high evolutionary potential. However, a robust study is required to determine its evolutionary potential.

Studying the genetic structure of pathogen populations can provide information about the genetic diversity, evolutionary potential, and reproductive mode, which can give insight into the risk of fungicide resistance development. Molecular markers that can be used to characterize pathogen population structure include Single Nucleotide Polymorphisms (SNPs), Simple Sequence Repeats (SSRs), Random Amplified Polymorphic DNA (RAPD), Amplified Fragment Length Polymorphism (AFLP), and Restriction Fragment Length Polymorphism (RFLP). SSRs are co-dominant markers and are a powerful tool that is widely used in population genetic studies. Currently, population genetic markers have not been developed to study the genetic structure of *R. zeae* and a reference genome is also not available, using which such markers could be designed. Thus, the aims of our research were to (i) survey corn and soybean fields in the North Central U.S. to isolate *Rhizoctonia* species and obtain additional *R. zeae* isolates from the Southern U.S.; (ii) design SSR primers for *R. zeae*; (iii) determine genetic diversity and mode of reproduction in *R. zeae* populations; and (iv) determine if population is structured by geography, host or year. Knowledge about the evolutionary potential of *R. zeae* in corn and soybean fields in the U.S. can help to guide management decisions in the future.

Materials and methods

Sample Collection. Soil samples were collected from 34 soybean fields and 34 corn fields in the year 2019 from 12 states: IA, IL, IN, KS, KY, MI, MN, MO, ND, NE,

SD, and WI (Table 3.1). An additional 84 isolates were obtained from 51 soybean fields and 30 corn fields that were sampled in 2015–2017 in Nebraska. Eight *R. zeae* isolates were obtained from soybean in 2012 and 2013 from Illinois (Ajayi-Oyetunde et al. 2017). *Rhizoctonia zeae* isolates from corn, soybean, and cotton that had been previously isolated in 2011–2013 were obtained from eight Southern states: AL, AR, GA, LA, MS, NC, TN, TX (Table 3.1). Field cropping history and disease history were noted when information was available. Fields were sampled mostly in the month of June when plants were between VE–V2 stage. Soil samples were taken in a 'W' or 'Z' transect and at least ten soil samples were collected from each field. A soil probe or shovel was used to dig 15.2 cm deep and collect 230–500 cm^3 of soil in plastic bags (Ziplock, S.C. Johnson and Son, Inc., Racine, WI). To avoid cross-contamination, the probe/shovel was rinsed with distilled water and then sprayed with a solution of 70% ethanol or a chemical disinfectant (Lysol, Reckitt Benckiser LLC, Parsippany, NJ) before collecting the next sample.

Sample Processing. Soil samples were processed using the modified toothpick method (Kodati 2019; Paulitz and Schroeder 2005). Soil samples were put in 10 cm diameter sterile clay pots and distilled water was added to 15% wt./wt. Four sterile toothpicks (birch) were placed vertically in each pot with three-quarters of the toothpick inside the soil. The pots were incubated in the greenhouse at 21±2°C for 48 h. Toothpicks were collected using sterile forceps and placed on semi-selective media.

Isolation and identification of *Rhizoctonia* spp. The RSM medium was used for isolating *Rhizoctonia* spp. (Kodati 2019). For making 1 L of RSM medium, 18 g of agar

was sterilized in 1 L of distilled water at 121°C, 15 psi for 30 minutes. After the media cooled to 55–65°C, 100 mg of streptomycin sulfate, 100 mg of penicillin-G sodium salt, and 800 µl of 1 M sodium hydroxide were added.

The toothpicks were transferred to RSM plates and stored at 22 ±1°C. After 36–48 h, the plates were examined under a stereomicroscope at 400X magnification for identifying hyphal features of *Rhizoctonia* spp., which includes having straight septate hyphae and right-angled branching. Hyphal tips from the putative *Rhizoctonia* spp. were transferred aseptically to quarter-strength Potato Dextrose Agar ($1/4^{th}$ PDA) or PDA amended with 0.01% tetracycline (PDAt). After 24–36 h, cultures were visually examined for contamination and were serially transferred to new plates ($1/4^{th}$ PDA or PDAt) until pure cultures were obtained. For identifying the *Rhizoctonia* species, the ITS region of 122 isolates was sequenced previously (Kodati 2019). The morphology of the sequenced isolates was used as a reference to classify other *Rhizoctonia* spp. used in the study. Morphological differentiation was based on the color of the mycelial colony, size and color of the sclerotia, and development of the sclerotia either on or inside the media (Kodati 2019). *Rhizoctonia zeae* has a white/buff to salmon-colored mycelial colony on PDA and salmon colored sclerotia of up to 1 mm diameter that develop on and inside the media. On maturity, the colony color and sclerotia become orange in color. For short-term storage, isolates were allowed to produce sclerotia on PDA plates at 22 ± 1°C and these were stored at 4°C.

Whole Genome Sequencing. DNA was purified from 100 mg of actively growing mycelia of five *R. zeae* isolates (four isolates from different regions in NE and

one isolate from IL) that were scraped from 3 days old cellophane covered Potato Dextrose Agar (PDA) plates. Mycelia were ground with liquid nitrogen in pre-sterilized pestle and mortar. For DNA extraction, DNeasy Plant Mini Kit (Qiagen, Hilden, Germany) was used according to the manufacturer's instructions and DNA was stored at -20°C until further use. DNA concentrations were quantified using Qubit® 3 Fluorometer (Invitrogen, Carlsbad, CA), which ranged from 44–67.6 ng/µL and DNA integrity was evaluated using gel electrophoresis on a 2% agarose gel. On average, 1 µg DNA per sample was shipped on dry ice to Rapid Genomics LLC (Gainesville, FL). High quality DNA from five isolates (and one technical replicate) was subjected to Whole Genome Sequencing (WGS) in one lane of Illumina HiSeq X with 150 paired-end reads and 350 bp insert size.

Data filtering and genome assembly. A total of 60.73 GB of raw data in fastq format were received from the sequencing facility. For each isolate, quality of raw read pairs was assessed using FastQC version 0.11 (Andrews 2010) and sequences below 96.84% accuracy (phred-scaled quality threshold of 15) were trimmed using trimmomatic version 0.38 (Bolger et al. 2014), which were assembled *de novo* using ABySS version 2.1 (Jackman et al. 2017) and a k-mer of size 64 on a high-performance computer cluster provided by the Holland Computing Center at the University of Nebraska-Lincoln.

Designing SSR primers, PCR, and fragment analysis. The unitigs level assembly output from ABySS was used as the input for Msatcommander (Faircloth 2008). Microsatellite loci with perfect repeats of tri-, tetra-, penta-, and hexa-nucleotides

were used to design primers tagged with a CAG tag and pigtailed with GTTT sequence (Rozen and Skaletsky 2000). Forty-three primers were sent for synthesis at Sigma-Aldrich. These primers were selected based on their low pair penalty score and *in silico* polymorphism. Data analyses were performed using the package *dplyr* version 0.8.5 (Wickham 2020) in R version 3.6.2 (R Core Team 2019).

The mean T_m (melting temperature) of all the primers was 59.99°C. To increase the sensitivity and specificity of the Polymerase Chain Reaction (PCR), a touchdown PCR approach was used (Korbie and Mattick 2008). Initial denaturation was carried out at 94°C for 3 min followed by, denaturation at 94°C for 30 s, annealing for 25 s, extension at 72°C for 30 s, and final extension at 72°C for 7 min 30 s. The annealing temperature began with 67°C and was decreased by 1°C after every successive cycle for 11 cycles, after which the annealing temperature of 57°C was used for 24 cycles. Jumpstart hot start Taq polymerase (Sigma) was used to minimize non-specific amplification further. Hi-Di Formamide (Fisher Scientific) and Liz 600 ladder (GeneScan) were added to the PCR products, which were then shipped overnight on dry ice to Ohio State University Comprehensive Cancer Center (OSUCCC) Shared Resources, Ohio for fragment analysis on 3730xl DNA Analyzer (Applied Biosystems, Foster City, CA). The final set of six primers were selected based on their polymorphism and consistency of amplification and 200 individuals were genotyped (Table 3.2).

Data Analyses. Data received were analyzed in GeneMapper version 4.1 (Applied Biosystems, Foster City, CA) to determine allele sizes, following which alleles were binned into their corresponding expected allele size. In the rare instance of

ambiguous allele size, a standardized approach to bin it into smaller of the two sizes was used. Data were organized in an Excel file in the GenAlEx format and imported in R version 3.6.2 (R Core Team 2019) using the package *poppr* version 2.8.1 (Kamvar et al. 2015). The populations were stratified by region, year, and host crop, where the regions consisted of Northeast Central (ENC), Northwest Central (WNC), and Southern (SO) United States.

Four different variations of the datasets were used for analysis: original (uncensored and clone-censored) and Multi Locus Genotype (MLG) contracted data (uncensored and clone-censored). Data were clone-censored such that each MLG was only represented once in a population (Grünwald et al. 2003; Grünwald and Hoheisel 2006; Milgroom 1996). To account for missing data and genotyping errors, MLG contracted data were used. The function 'mlg.filter' from package *poppr* version 2.8.1 (Kamvar et al. 2015) was used for MLG contraction and the distance used for contraction was based on the average neighbor distance.

To test if the six selected loci had the necessary power to discriminate between MLG present in the population, a genotype accumulation curve was generated (Fig .1) and the quality of the loci were checked using locus summary statistics. Individuals with missing data at more than one locus were removed and further analyses were conducted using the remaining 164 individuals.

Genotypic diversity. Genotypic diversity and linkage disequilibrium indices were estimated for each population using the function 'poppr' from package *poppr* version 2.8.1 (Kamvar et al. 2015). Genotypic diversity is a function of genotypic

richness (number of genotypes) and evenness (relative abundance of each genotype). The metrics used to measure genotypic richness included the number of MLGs, and the expected number of Multi Locus Genotypes (eMLGs), which is the rarefied number of MLGs expected at the smallest sample size (Grünwald et al. 2003). Genotypic evenness was measured using the index E_5, which is based on the ratio of the number of abundant genotypes to the number of rare genotypes (Grünwald et al. 2003). Three additional indices were calculated that take both genotypic richness and evenness into account, Stoddart and Taylor's diversity index (*G*), Shannon–Weiner index (*H'*), and Simpson's diversity index (λ).

Linkage disequilibrium, genetic relatedness, and population structure.

Genetic relatedness among MLGs from different regions, hosts, and years was estimated by generating Minimum Spanning Networks (MSN). Bruvo's genetic distance was used to construct the MSN since it is based on the stepwise mutation model, which is appropriate for SSR loci (Bruvo et al. 2004). To assess the type of reproduction in different populations, linkage disequilibrium (LD) among the SSR loci was determined using two indices, the Index of Association (I_A) and the Standardized Index of Association ($\bar{r}_d$). These indices were used to test the null hypothesis of random mating (unlinked loci) using 999 permutations at alpha = 0.05. An analysis of molecular variance (AMOVA) was performed to determine if the populations were genetically differentiated according to region, year, or crop.

Results

***Rhizoctonia zeae* collection.** A total of 165 isolates belonging to different *Rhizoctonia* spp. were isolated from 12 states, out of which 113 isolates (68.49%) were *R. zeae*. The number of isolates obtained from each state ranged from 2 to 20: IA (13), IL (2), IN (9), KS (13), KY (8), MI (8), MN (17), MO (8), ND (11), NE (2), SD (2), and WI (20). Out of the 113 *R. zeae* isolates, 81 isolates were selected for genotyping such that only one isolate was selected from each sample. Additional isolates used for genotyping were obtained from previous studies (Table 3.1).

SSR loci. The unitig-level genome assemblies were used for mining SSR loci. The N50 of the five genome assemblies ranged from 4,776–21,109. Out of the 43 SSR primers pairs designed, six primer pairs showed consistent amplification and polymorphism. Loci with ≥20 alleles were considered hypervariable and hence were not used for further analyses. R19 was the most polymorphic locus with 16 alleles, while R31, R35, and R41 were the least polymorphic loci with 8 alleles (Table 3.2). These loci were perfect trinucleotide repeats. On a scale of 0 to 1, the mean Simpson's gene diversity index and expected heterozygosity (H_{exp}) were 0.75 each and the mean evenness was 0.77. The proximity of these indices to 1 indicated high gene diversity and evenness. The genotype accumulation curve (Fig. 3.1) suggested that these six loci had power to discriminate between different genotypes in the population.

Genotypic diversity. High genotypic richness was observed in all the populations when grouped according to region. A total of 152 MLGs were identified in 165 isolates, which were contracted to 136 MLGs on filtering. In the Northwest Central (WNC)

region, 108 MLGs were found among 112 isolates. In Northeast Central (ENC) region, 32 MLGs were found in 36 individuals and in Southern region (SO), 15 MLGs were found in 17 individuals. The eMLG was the highest for WNC, followed by ENC, and then SO. Two MLGs were shared among the WNC and ENC regions and only one MLG was shared among the ENC and SO regions. Among the different crops, one MLG was shared among soybean, corn, and cotton and two MLGs were shared between soybean and corn. For different years, one MLG was shared between the years 2013 and 2019, one MLG was shared between the years 2011 and 2012, and one MLG was shared among the years 2012, 2016, and 2019. High genotypic diversity was observed when the populations were stratified according to region, crop, and/or year.

After filtering the MLGs to account for genotyping errors and missing data, 98 MLGs were found among 112 isolates in WNC, 30 MLGs in 36 individuals in ENC, and 15 MLGs in 17 individuals in SO region. Four MLGS were shared among the WNC and ENC regions, two MLGs were shared among the WNC and SO regions, two MLGs were shared among the ENC and SO regions, and one MLG was shared among all three regions. Among the different crops, one MLG was shared among soybean, corn, and cotton and seven MLGs were shared between soybean and corn. For different years, one MLG was shared between the years 2013 and 2019, three MLGs were shared between the years 2011 and 2012, one MLG was shared among the years 2012, 2017, and 2019, one MLG was shared among the years 2012, 2016, 2017, 2019, one MLG was shared among 2011 and 2019, 2012 and 2019, 2016 and 2019, 2012 and 2016. High genotypic diversity was observed when the populations were stratified according to region, crop, and/or year.

Overall, the mean E_5 was 0.908 for unfiltered MLGs and 0.839 for filtered MLGs, which indicated high genotypic evenness for all the populations. The Simpson's diversity index (λ) was the highest for WNC population, followed by ENC and then SO for both unfiltered and filtered MLGs.

Reproductive mode, genetic relatedness, and population structure. To infer the mode/type of reproduction in different populations, LD among the SSR loci was estimated. For clone-censored data, populations had evidence for clonal reproduction when stratified for crops, years, and regions ($\bar{r}_d$ = 0.012; $P \leq 0.05$). When populations were subset according to year, the clone-censored data for the years 2016 and 2019 had evidence of sexual reproduction ($\bar{r}_d$ = 0.004; $P > 0.05$). The results were similar for both unfiltered and MLG filtered data.

The topology of the MSN (Fig. 3.2) showed evidence that mixed reproduction has occurred for both original and MLG contracted data. High genotypic diversity and equal representation of most of the MLGs in the MSN suggested sexual recombination, while small distances between certain MLGs indicated clonal reproduction has occurred.

To investigate if clonal reproduction occurred at a finer scale than the state level, MSN was constructed for isolates obtained from each county in Nebraska. A maximum of three samples had the same MLG in a county and isolates from distant counties were connected closely to each other. An MSN was also constructed to see the effect of year in Nebraska (Fig. 3.3). MLGs were not shared among years. AMOVA was performed to determine if the populations were genetically structured according to region, year, crop. Genetic structure was observed for region (Fig. 3.4; $P \leq 0.05$) and year ($P \leq 0.05$), but not

for crop ($P > 0.05$) when MLGs were not contracted and was observed for region only ($P \leq 0.05$) when MLGs were contracted.

Discussion

In this study, 200 isolates of *R. zeae* were genotyped. These isolates were obtained from 20 states in the North Central and Southern U.S. and were isolated in 2009–2019. We inferred that *R. zeae* populations had high genotypic diversity, mixed reproductive mode, and were structured according to region. Populations with low genotype flow and mixed reproductive mode are considered to have intermediate evolutionary potential (McDonald and Linde 2002). Thus, the best way to manage this pathogen would be by using Integrated Pest Management (IPM) strategies and not heavily relying on a single management strategy.

The optimum temperature range for growth and virulence of *R. zeae* is 30–33°C, which is higher than that for *R. solani* (Elliott 1999; Erper et al. 2006; Li et al. 1998; Martin and Lucas 1984; Sumner and Bell 1982; Voorhees 1934). The role of temperature in seedling disease caused by *Rhizoctonia* spp. in field conditions is not completely understood. However, with a rise in global temperatures, the prominence of *R. zeae* might increase, hence it is important to understand its distribution and evolutionary potential.

This is the first study to investigate the distribution of *R. zeae* from corn and soybean fields in the U.S. *Rhizoctonia zeae* was identified as a pathogen of soybean and was found to be the most prevalent *Rhizoctonia* species isolated from corn and soybean fields in Nebraska (Kodati 2019). Previous studies have mostly documented *R. solani* to be associated with soybean and corn fields. *R. solani* AG-2-2 and AG-4 were found to be

primarily associated with soybean seedling diseases in Iowa (Rizvi and Yang 1996). The predominant *Rhizoctonia* spp. associated with soybean seedling diseases was *R. solani* AG-4 in the Red River Valley of Minnesota and North Dakota (Nelson et al. 1996), *R. solani* AG-2-III-B in Ontario, Canada (Zhao et al. 2005), and *R. solani* AG-2-III-B in Arkansas, Illinois, Kansas, Michigan, Minnesota, and Ontario, Canada (Ajayi-Oyetunde and Bradley 2017). From the latter study, only 8.8% *Rhizoctonia* spp. from soybean were *R. zeae*. In the present study, 68.49% of the isolates were *R. zeae.* This can be partly due to the fact that soil was not sampled in previous studies, which were predominantly used in the current study. Although the virulence of *R. zeae* can be similar to *R. solani* AG-4 HG-II on soybean (Kodati 2019), its economic impact on yield is not known. Field studies are required to estimate yield losses caused by this pathogen.

Although comprehensive studies have been performed to study the population structure of *R. solani* (Ajayi-Oyetunde et al. 2019), this is the first study to examine the genetic structure of *R. zeae* at a regional scale. Previous studies on *R. zeae* that examined 18S-28S rDNA-ITS region, 18S rDNA and β-tubulin genes suggested that the Americas might be the origin of this pathogen (Aydin et al. 2013; Gürkanli et al. 2016). High genotypic diversity was observed in all the regions in the present study (Table 3.3) with the highest genotypic diversity found in the WNC region. The WNC region has been covered by native grasslands historically and *R. zeae* has been isolated from native grasslands in Nebraska (Kodati 2019). It is possible that *R. zeae* originated from United States, however, further studies are needed to examine the genotypic diversity of this pathogen from other countries in the Americas. Overall, the reproductive mode was inferred to be clonal. However, sexual reproduction was inferred to have occurred in the

years 2016 and 2019. It is possible that the time of sampling during these years corresponded with favorable conditions for sexual reproduction. Further research is needed to study the disease cycle of this pathogen, so that the critical timing for managing this pathogen can be determined.

The population was inferred to be structured according to region and also showed a signature of structure according to year. Regional structuring can be due to low dispersal of this soil-borne pathogen; however, further studies are required to examine the dispersal mechanism in detail. Finer scale analysis in Nebraska showed that none of the MLGs were shared among years (Fig. 3.3). The differences in MLGs can be because the same field was not always sampled in the subsequent year, and when sampled, the same location in the field might not be sampled. It is possible that certain MLGs, although present in the previous year, were not sampled because of the patchy distribution of the pathogen in the field. One limitation of this study was that within-field populations could not be characterized. Although fine scale sampling was performed, the number of isolates obtained from each field could not be used for within-field comparisons. Future studies can obtain a greater number of samples from each field to characterize within-field populations.

This is the first study to characterize the population structure of *R. zeae* in the U.S. Intermediate evolutionary potential of this pathogen suggests that a combination of management strategies should be used to circumvent failure of a single management strategy.

References

Ajayi-Oyetunde, O.O., and Bradley, C.A. 2017. Identification and characterization of *Rhizoctonia* species associated with soybean seedling disease. Plant Dis. 101:520-533.

Ajayi-Oyetunde, O.O., Everhart, S.E., Brown, P.J., Tenuta, A.U., Dorrance, A.E. and Bradley, C.A., 2019. Genetic structure of *Rhizoctonia solani* AG-2-2IIIB from soybean in Illinois, Ohio, and Ontario. Phytopathology, 109:2132-2141.

Andrews, S. 2010. FastQC: a quality control tool for high throughput sequence data. https://www.bioinformatics.babraham.ac.uk/projects/fastqc/.

Aydin, E.B., Gürkanli, C.T., Ozkoc, I., Demirci, E., Erper, I., Karaca, G., Hsieh, T.F., Vajna, L. and Poltronieri, L.S. 2013. rDNA-ITS diversity of *Waitea circinata* var. *zeae* (anamorph: *Rhizoctonia zeae*). J. Plant Pathol. 587-595.

Bolger, A.M., Usadel, B., and Lohse, M. 2014. Trimmomatic: a flexible trimmer for Illumina sequence data. Bioinformatics 30:2114-2120.

Bruvo, R., Michiels, K.N., D'Souza, T.G. and Schulenburg, H. 2004 A simple method for the calculation of microsatellite genotype distances of ploidy level. Mol. Ecol. 13:2101-2106

Chen, C. 2011. The geographic distribution, genetic structure and cultural management of *Waitea circinata* var. *circinata*, the causal agent of brown ring patch. Doctoral Dissertation. University of California, Riverside.

Demirci, E. and Eken, C. 1999. First report of *Rhizoctonia zeae* in Turkey. Plant Dis. 83:200.

El Fiky, Z., Fouly, H. and Martin, B. 2011. Genetic diversity of *Waitea circinata* var. *zeae* in South Carolina revealed by amplified fragment length polymorphism (AFLP). Egypt. J. Genet. Cytol. 40:145-159.

Elliott, M.L. 1999. Comparison of *Rhizoctonia zeae* isolates from Florida and Ohio turfgrasses. HortScience 34:298-300.

Erper, I., Karaca, G.H., Turkkan, M. and Ozkoc, I., 2006. Characterization and pathogenicity of *Rhizoctonia* spp. from onion in Amasya, Turkey. J. Phytopathol. 154:75-79.

Faircloth, B.C. 2008. MSATCOMMANDER: Detection of microsatellite repeat arrays and automated, locus-specific primer design. Mol. Ecol. Resour. 8:92-94.

Grünwald, N.J., Goodwin, S.B., Milgroom, M.G., and Fry, W. E. 2003. Analysis of genotypic diversity data for populations of microorganisms. Phytopathology 93:738-746.

Grünwald, N.J., and Hoheisel, G-A. 2006. Hierarchical analysis of diversity, selfing, and genetic differentiation in populations of the oomycete *Aphanomyces euteiches*. Phytopathology 96:1134-1141.

Gürkanli, C.T., Aydin, E.B., Demirci, E., Erper, I., Karaca, G., Hsieh, T.F., Poltronieri, L.S. and Özkoç, I. 2016. 18S rDNA and β-tubulin diversity in *Rhizoctonia zeae* Voorhees. Pak. J. Bot. 48:645-651.

Haygood, R.A., and Martin, S.B. 1990. Characterization and pathogenicity of species of *Rhizoctonia* associated with centipede grass and St. Augustine grass in South Carolina. Plant Dis. 74:510-514.

Jackman, S.D., Vandervalk, B.P., Mohamadi, H., Chu, J., Yeo, S., Hammond, S.A., Jahesh, G., Khan, H., Coombe, L., Warren, R.L. and Birol, I. 2017. ABySS 2.0: resource-efficient assembly of large genomes using a Bloom filter. Genome Res. 27:768-777.

Kammerer, S.J., Burpee, L.L. and Harmon, P.F. 2011. Identification of a new *Waitea circinata* variety causing basal leaf blight of seashore paspalum. Plant Dis. 95:515-522.

Kamvar, Z.N., Brooks, J.C., and Grünwald, N.J. 2015. Novel R tools for analysis of genome-wide population genetic data with emphasis on clonality. Front. Genet. 6:208.

Kerns, J., Yan, Y., and Butler, E. 2017. Characterization, pathogenicity, and *in vitro* sensitivity of *Rhizoctonia* spp. associated with leaf and sheath spot of bermudagrass putting greens in North Carolina and Alabama. Int. Turfgrass Soc. Res. J. 13:203-212.

Kodati, S. 2019. Diversity and pathogenicity of *Rhizoctonia* spp. from different plant hosts in Nebraska. Doctoral Dissertation. University of Nebraska, Lincoln.

Korbie, D.J., and J.S. Mattick. 2008. Touchdown PCR for increased specificity and sensitivity in PCR amplification. Nat. Protoc. 3:1452-1456.

Kuznia, R.A. and C.E. Windels. 1994. *Rhizoctonia zeae* pathogenic to spring wheat and sugarbeet seedlings. Phytopathology 84: 1159.

Leiner R.H., and Carling D.E., 1994. Characterization of *Waitea circinata* (*Rhizoctonia*) isolated from agricultural soils in Alaska. *Plant Dis.* 78:385-388.

Li, H.R., Wu, B.C. and Yan, S.Q., 1998. Aetiology of *Rhizoctonia* in sheath blight of maize in Sichuan. Plant Pathol. 47:16-21.

Martin, S.B. and Lucas, L.T. 1984. Characterization and pathogenicity of *Rhizoctonia* spp. and binucleate *Rhizoctonia*-like fungi from turfgrasses in North Carolina. Phytopathology 74:170-175.

McDonald, B.A., and Linde, C. 2002. Pathogen population genetics, evolutionary potential, and durable resistance. Annu. Rev. Phytopathol. 40:349-379.

Milgroom, M.G. 1996. Recombination and the multilocus structure of fungal populations. Annu. Rev. Phytopathol. 34:457-477.

Nelson, B., Helms, T., Christianson, T., and Kural, I. 1996. Characterization and pathogenicity of *Rhizoctonia* from soybean. Plant Dis. 80:74-80.

Ogoshi, A. 1987. Ecology and pathogenicity of anastomosis and intraspecific groups of *Rhizoctonia solani* Kuhn. Annu. Rev. Phytopathol. 25:125-143.

Ohkura, M., Abawi, G.S., Smart, C.D., and Hodge, K.T. 2009. Diversity and aggressiveness of *Rhizoctonia solani* and *Rhizoctonia*-like fungi on vegetables in New York. Plant Dis. 93:615-624.

R Core Team. 2019. R: A language and environment for statistical computing. R Foundation for Statistical Computing, Vienna, Austria. URL: https://www.R-project.org/.

Rizvi, S.S.A., and Yang, X.B. 1996. Fungi associated with soybean seedling disease in Iowa. Plant Dis. 80:57-60.

Rozen, S., and Skaletsky, H.J. 2000. Primer3 on the WWW for general users and for biologist programmers. In: Bioinformatics Methods and Protocols: Methods in Molecular Biology. Krawetz S, Misener S, eds. Humana Press, Totowa, NJ.

Spurlock, T.N. 2013. Spatial distributions of *Rhizoctonia* species in soybean fields undergoing annual rotations with rice. Doctoral Dissertation, University of Arkansas, Fayetteville.

Sumner, D.R. and Bell, D.K. 1982. Root diseases induced in corn by *Rhizoctonia solani* and *Rhizoctonia zeae*. Phytopathology 72:86-91.

Toda, T., Hayakawa, T., Mghalu, J.M., Yaguchi, S. and Hyakumachi, M. 2007. A new *Rhizoctonia* sp. closely related to *Waitea circinata* causes a new disease of creeping bentgrass. J. of Gen. Plant Pathol. 73:379-387.

Tomaso-Peterson, M. and Trevathan, L.E. 2007. Characterization of *Rhizoctonia*-like fungi isolated from agronomic crops and turfgrasses in Mississippi. Plant Dis. 91:260-265.

Voorhees, R.K. 1934. Sclerotial rot of corn caused by *Rhizoctonia zeae*, n. sp. Phytopathology 24:1290-1303.

Webb, K.M., Harveson, R.M., and West, M.S. 2015. Evaluation of *Rhizoctonia zeae* as a potential biological control option for fungal root diseases of sugar beet. Ann. Appl. Biol. 167:75-89.

Wickham, H., François, R., Henry, L., and Müller, K. 2020. dplyr: A grammar of data manipulation. R package version 0.8.5. https://CRAN.R-project.org/package=dplyr

Zhao, G., Ablett, G.R., Anderson, T.R., Rajcan, I., and Schaafsma, A.W. 2005. Anastomosis groups of *Rhizoctonia solani* associated with soybean root and hypocotyl rot in Ontario and resistance of accession PI 442031 to different anastomosis groups. Can. J. Plant Pathol. 27:108-117.

Tables and Figures

Table 3.1. Summary of *Rhizoctonia zeae* isolates from Northwest Central (WNC), Northeast Central (ENC), and Southern (SO) United States that were used for microsatellite genotyping.

Region	Year	Crop	Isolates[a]
ENC (IL, IN, MI, WI)	2012	Soybean	7[b]
	2013	"	1[b]
	2019	Corn	17
	"	Soybean	13
SO (AL, AR, GA, KY, LA, MS, NC, TN, TX)	2011	Corn	11
	"	Cotton	2
	"	Soybean	3
	2012	Corn	2
	"	Peanut	1
	"	Soybean	4
	2019	Corn	2
	"	Soybean	1
WNC (IA, KS, MN, MO, ND, NE, SD)	2009	Sugar beet	2[c]
	2012	Cotton	1
	"	Soybean	1
	2015	"	3
	2016	Corn	13
	"	Soybean	25
	2017	Corn	17
	"	Soybean	28
	2019	Corn	33
	"	Soybean	13

[a]Number of isolates genotyped

[b]Obtained from Ajayi-Oyetunde and Bradley 2017

[c]Obtained from Webb et al. 2015

Table 3.2. Summary statistics for six microsatellite loci designed for characterizing *Rhizoctonia zeae* populations

Locus	Alleles	Size Range (bp)	Repeat Motif	Simpson's Index	H_{exp}[a]	Evenness
R19	16	201–261	ATC	0.83	0.83	0.78
R29	9	361–394	AGG	0.78	0.78	0.87
R31	8	352–370	AAC	0.79	0.79	0.91
R32	14	254–295	AGC	0.65	0.65	0.48
R35	8	231–255	AAG	0.72	0.73	0.82
R41	8	292–331	ACG	0.72	0.72	0.78
Mean	10.5	–	–	0.75	0.75	0.77

[a]Nei's gene diversity

Table 3.3. Indices for genotypic diversity and linkage disequilibrium in *Rhizoctonia zeae* populations from Northwest Central (WNC), Northeast Central (ENC), and Southern (SO) United States.

Indices	WNC	ENC	SO	Total
N	112	35	17	164
MLG[a]	108	32	15	152
eMLG[b]	16.9	16.2	15	16.8
Simpson's diversity				
Original	0.99	0.965	0.927	0.992
MLG contracted	0.988	0.958	0.927	0.99
Evenness (E_5)				
Original	0.969	0.928	0.949	0.909
MLG contracted	0.899	0.866	0.949	0.838
Expected heterozygosity (H_{exp})				
Original	0.741	0.751	0.739	0.75
MLG contracted	0.741	0.751	0.739	0.75
Index of association[c] (I_A)				
Original; Uncensored	0.0638[c]	0.283[c]	0.427[c]	0.0742[c]
MLG contracted; Uncensored	0.0638[c]	0.283[c]	0.427[c]	0.0742[c]
Original; Clone-censored	0.0374[c]	0.134[c]	0.3305[c]	0.03[c]
MLG contracted; Clone-censored	0.0173[c]	0.0529[d]	0.3305[c]	0.0102[c]
Standardized index of association[c] ($\bar{r}_d$)				
Original; Uncensored	0.013[c]	0.0576[c]	0.0866[c]	0.0151[c]
MLG contracted; Uncensored	0.013[c]	0.0576[c]	0.0866[c]	0.0151[c]
Original; Clone-censored	0.00762[c]	0.0273[c]	0.06696[c]	0.00609[c]
MLG contracted; Clone-censored	0.00351[c]	0.01073[d]	0.06696[c]	0.00207[c]

[a]Number of Multi Locus Genotypes
[b]Expected number of Multi Locus Genotypes
[c]P-value ≤ 0.05
[d]P-value > 0.05

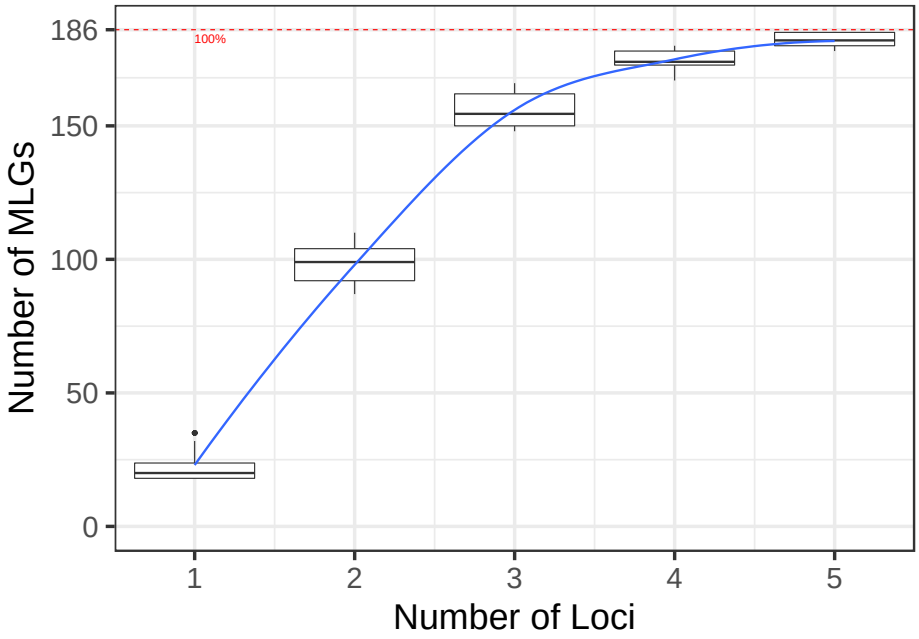

Fig. 3.1. Genotype Accumulation Curve (GAC) showing the discriminatory power of the microsatellite loci used to genotype *Rhizoctonia zeae* populations.

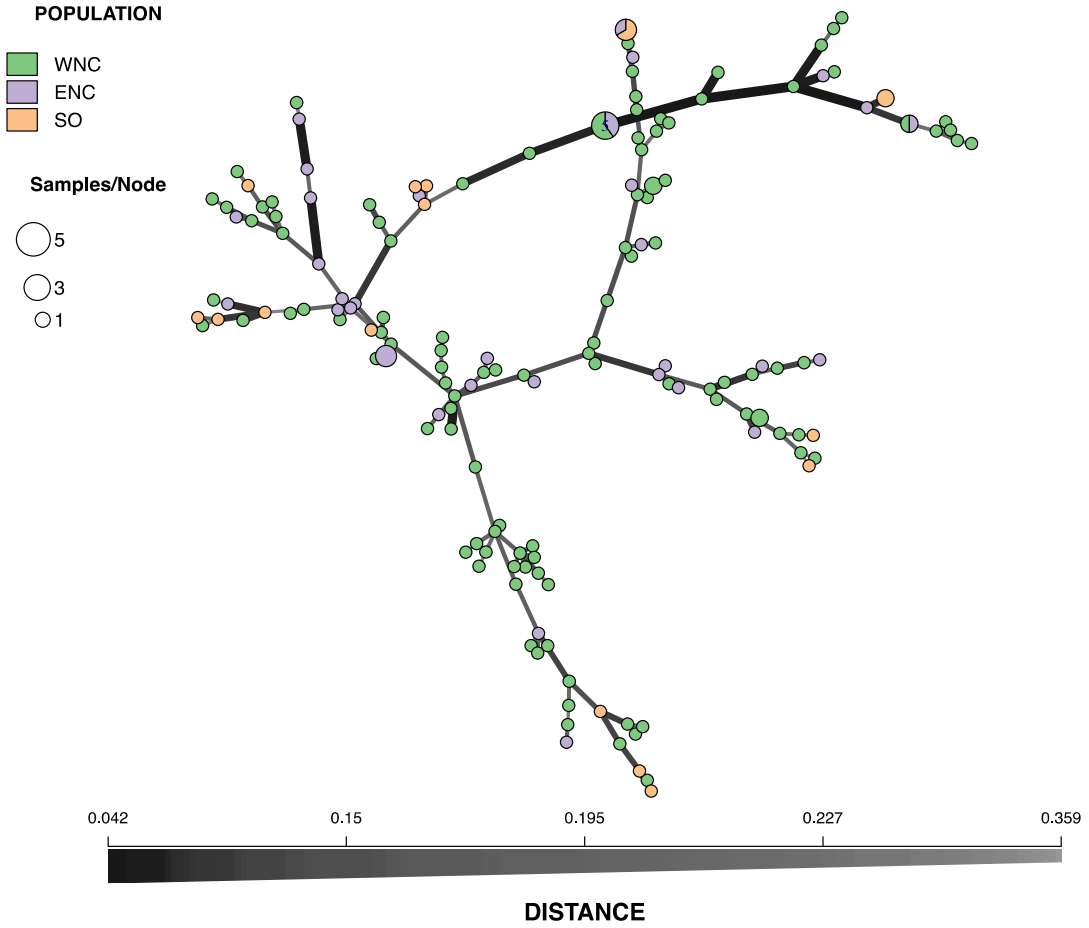

Fig. 3.2. Minimum Spanning Network (MSN) showing the genetic relationship among the Multi Locus Genotypes (MLGs) of *Rhizoctonia zeae* isolated from different regions of the U.S.: Northwest Central (WNC), Northeast Central (ENC), and Southern (SO) U.S. Each node represents a different MLG and the frequency of that MLG is represented by the size of the circle. Node color represents the year in which the isolate was obtained. Thickness and color of the edges are based on Bruvo's genetic distance as shown in the scale bar. The data shown here was neither contracted for MLGs nor clone-censored.

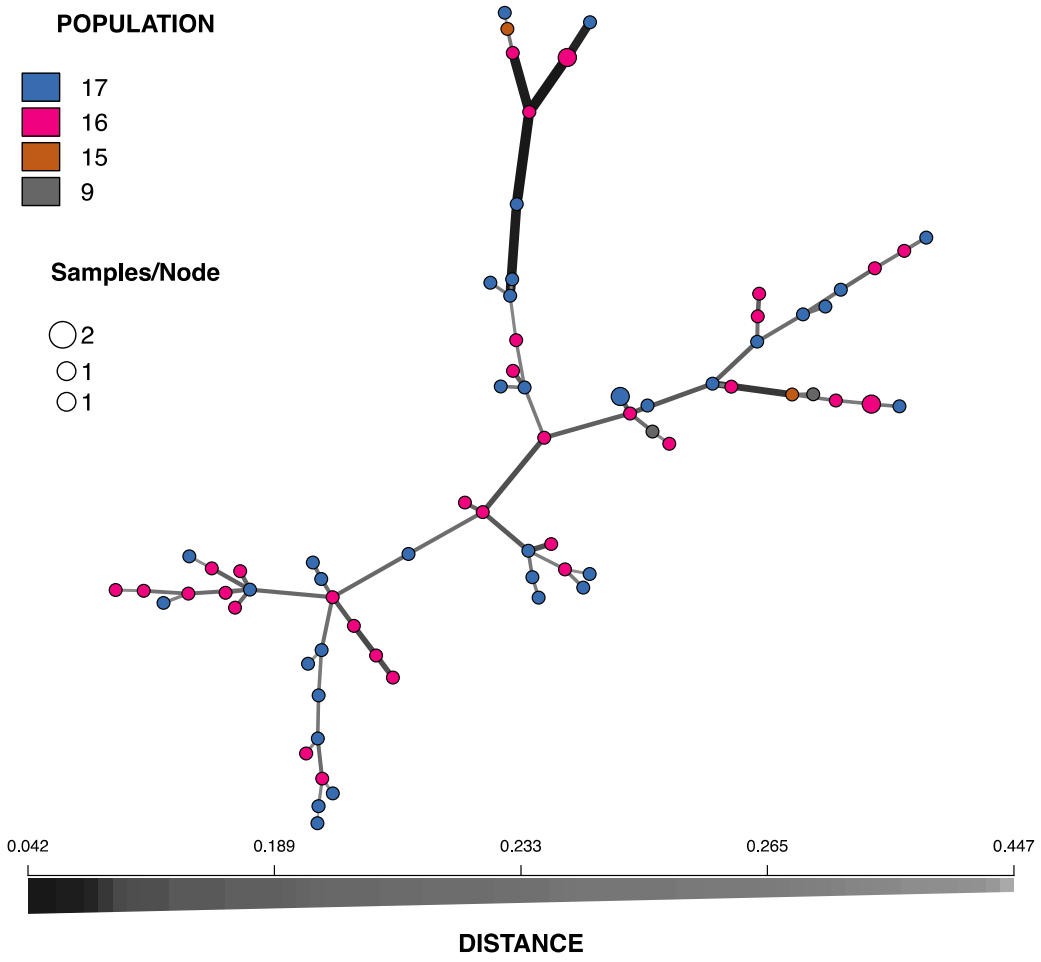

Fig. 3.3. Minimum Spanning Network (MSN) showing the genetic relationship among the Multi Locus Genotypes (MLGs) of *Rhizoctonia zeae* isolated in different years in Nebraska. Each node represents a different MLG and the frequency of that MLG is represented by the size of the circle. Node color represents the year in which the isolate was obtained: 2009 (9), 2015 (15), 2016 (16), and 2017 (17). Thickness and color of the edges are based on Bruvo's genetic distance as shown in the scale bar. The data shown here was neither contracted for MLGs nor clone-censored.

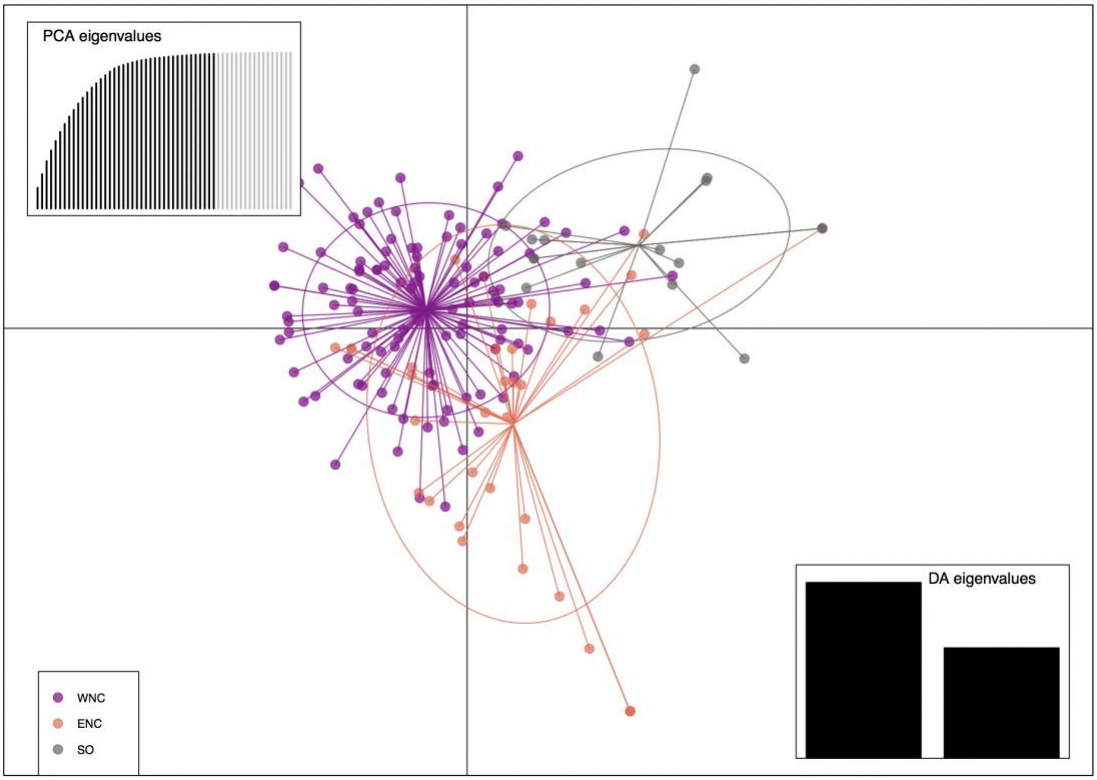

Fig. 3.4. Discriminant Analysis of Principal Components (DAPC) scatter plot showing the first and second principal components discriminating *Rhizoctonia zeae* populations from Northwest Central (WNC), Northeast Central (ENC), and Southern (SO) U.S. Multi Locus Genotypes (MLGs) are represented by dots and are colored according to region. Lines connect the MLGs that are from the same population. The data shown here was neither contracted for MLGs nor clone-censored.

CHAPTER-4

SPONTANEOUS AND FUNGICIDE-INDUCED GENOMIC VARIATION IN *SCLEROTINIA SCLEROTIORUM*

Portions of this material have previously appeared in the following publication: Gambhir, N., Kamvar, Z. N., Higgins, R., Amaradasa, B. S., and Everhart, S. E. 2021. Spontaneous and fungicide-induced genomic variation in Sclerotinia sclerotiorum. Phytopathology doi: 10.1094/phyto-10-20-0471-fi. Used with permission.

Abstract

Stress from exposure to sublethal fungicide doses may cause genomic instability in fungal plant pathogens, which may accelerate the emergence of fungicide resistance or other adaptive traits. In a previous study, five strains of *Sclerotinia sclerotiorum* were exposed to sublethal doses of four fungicides with different modes of action and genotyping showed that such exposure induced mutations. The goal of the present study was to characterize genome-wide mutations in response to sublethal fungicide stress in *S. sclerotiorum* and study the effect of genomic background on the mutational repertoire. The objectives were to determine the effect of sublethal dose exposure and genomic background on mutation frequency/type, distribution of mutations, and fitness costs. Fifty-five *S. sclerotiorum* genomes were sequenced and aligned to the reference genome. Variants were called and quality filtered to obtain high confidence calls for single nucleotide polymorphisms, insertions/deletions (INDELs), copy number variants, and transposable element (TE) insertions. Results suggest that sublethal fungicide exposure

significantly increased the frequency of INDELs in two strains from one genomic background (*P*-value ≤ 0.05), while TE insertions were generally repressed for all genomic backgrounds and under all fungicide exposures. The frequency and/or distribution of SNPs, INDELs, and TE insertions varied with genomic background. A propensity for large duplications on chromosome 7 and aneuploidy of this chromosome were observed in the *S. sclerotiorum* genome. Mutation accumulation did not significantly affect the overall *in planta* strain aggressiveness (*P*-value > 0.05). Understanding factors that affect pathogen mutation rates can inform disease management strategies that delay resistance evolution.

Introduction

Fungicides play a key role in crop protection. Without fungicides, yield of certain crops (e.g. grapes, papaya, and pear) would be reduced by ≥ 95% (Gianessi and Reigner 2005). Most fungicides used today have a single-site mode of action, meaning that they inhibit a particular biochemical pathway by binding to a target site in the fungal cell. This specificity makes them effective but also increases the potential of pathogens evolving resistance to these fungicides. A single mutation in the DNA sequence of the target site may change its binding affinity and render the fungicide ineffective. Fungicide resistance has already been reported for 203 plant pathogenic fungi (Fungicide Resistance Action Committee 2018). It takes approximately $315 million (adjusted for inflation) and 11 years to develop and market a new fungicide (McDougall 2016), but resistance was reported as early as two years after the launch of some fungicides (Brent and Hollomon 2007). In order to delay resistance evolution and prolong the life of currently used

fungicides, it is important to understand the role of different factors in resistance development. Risk of resistance development depends on both the pathogen and fungicide in question (Brent and Hollomon 2007). Pathogen-risk factors include generation time, dispersal mechanism, and reproduction type. Fungicide-risk factors include mode of action, number of applications per season, and dose.

Pathogen populations may be exposed to a range of fungicide doses in the field. Reasons for this include incomplete penetration of fungicides in the plant canopy, drift or run-off of fungicides, and dilution of fungicides inside the plant tissues. Most studies have focused on the role of fungicide dose in selection for resistant alleles (Lucas et al. 2015; van den Bosch et al. 2011). These studies suggest using sublethal fungicide doses to manage resistance because the selection pressure will remain low. Nevertheless, sublethal doses may stress the pathogen and increase its mutation rate, thus accelerating the emergence of mutations conferring resistance (Beckerman et al. 2015; Gressel 2011). Stress can increase mutational frequency by direct and indirect mechanisms (Galhardo et al. 2007; Koshiji et al. 2005; Parker and von Borstel 1987; Shor et al. 2013). For example, osmotic stress can damage DNA by inducing DNA breaks (Parker and von Borstel 1987), while proteotoxic stress can result in reduced expression of the DNA repair pathway genes (Shor et al. 2013). Studies in human fungal pathogens have shown that sublethal antifungal stress increases the rate of point mutations (Avramovska and Hickman 2019), aneuploidy, and chromosomal rearrangements (Avramovska and Hickman 2019; Harrison et al. 2014; Shapiro 2015; Shor and Perlin 2015). But studies on fungal plant pathogens give an unclear picture of the role of sublethal fungicide dose in increasing mutation rate (Ajouz et al. 2010; Amaradasa and Everhart 2016; Chen et al.

2015; Dowling et al. 2016; Schnabel et al. 2014; Troncoso-Rojas et al. 2013). *Botrytis cinerea* strains exposed to iprodione for 20 generations did not show any changes in the allele size at the nine Simple Sequence Repeat (SSR) loci tested (Ajouz et al. 2010). However, isothiocyanate exposure induced random mutations in Inter-Simple Sequence Repeats (ISSR) regions of five *Alternaria alternata* strains with variable mutational frequency among strains (Troncoso-Rojas et al. 2013). In two out of three strains of *Monilinia fructicola*, gain or loss of the transposable element *Mftc1* was observed after *in vitro* exposure to azoxystrobin or a mixture treatment of azoxystrobin and SYP-Z048 (Chen et al. 2015). But field populations of *M. fructicola* neither showed any changes in their SSR profile nor in the translocation of the *Mftc1* transposon after sublethal exposure to azoxystrobin or propiconazole. Collectively, these studies suggest that the effect of fungicide stress on mutational frequency is unclear and the effect varies among strains of the same species (Amaradasa and Everhart 2016; Chen et al. 2015; Troncoso-Rojas et al. 2013) and among exposure to different fungicides (Amaradasa and Everhart 2016; Chen et al. 2015).

One limitation of these studies was the use of genetic markers to determine the effect of fungicide exposure on mutational frequencies, which could only assess the impact of fungicide stress on a small fraction of the genome. Whole Genome Sequencing (WGS) studies show that plant pathogens have extensive genome plasticity (Miller et. al 2018; Moolhuijzen et al. 2018; O'Sullivan et al. 1998) and stresses induce different types of genomic perturbations. Host-induced stress increases chromosomal instability, copper and potassium chlorate stresses affect Transposable Element (TE) movement, while heat stress induces chromosomal instability as well as TE movement in plant pathogens

(Anaya and Roncero 1996; Chadha and Sharma 2014; Kasuga et al. 2016; Kistler et al. 1992; Möller et al. 2018). Fungicide stress-induced genomic instability has not been studied previously in plant pathogens. The complete mutational profile of a fungicide exposed strain may depend on the mode of action of a fungicide, which determines the type of stress it imposes. For example, fungicides that inhibit osmotic signal transduction can cause osmotic stress and induce DNA breaks (Parker and von Borstel 1987). Bias for different types of mutations such as Single Nucleotide Polymorphisms (SNPs), INsertions and DELetions (INDELs), TE movement, and Copy Number Variants (CNVs) are known to vary among stresses (Anaya and Roncero 1996; Chadha and Sharma 2014; Maharjan and Ferenci 2017). WGS can help us to elucidate the effect of fungicides with different modes of action on these different types of genomic variants. Additionally, the interaction effect of genomic background with fungicide stress exposure has been observed (Amaradasa and Everhart 2016; Chen et al. 2015; Troncoso-Rojas et al. 2013), though it has not been formally investigated. Studying fungicide stress on strains with diverse genomic backgrounds can give insight into the population-level dynamics of fungicide stress in *S. sclerotiorum.*

Sclerotinia sclerotiorum is an important pathogen that causes disease on >400 plant species (Boland and Hall 1994) and fungicides are commonly used for disease management. Fungicide resistance in *S. sclerotiorum* has been reported for benomyl, carbendazim, thiophanate-methyl (microtubulin synthesis inhibitors; Attanayake et al. 2013; Gossen et al. 2001; Lehner et al. 2015; Ma et al. 2009; Penaud et al. 2003), azoxystrobin, pyraclostrobin (respiration inhibitors; Tóthová et al. 2019), and iprodione (osmotic signal transduction inhibitor; Molaei et al. 2020). In a previous study, nine *S.*

sclerotiorum strains were exposed to sublethal doses of five fungicides: azoxystrobin, boscalid, iprodione, pyraclostrobin, and thiophanate-methyl for 12 generations with experimental replication (Amaradasa and Everhart 2016). SSR analysis of all the progenitor and fungicide-exposed strains showed that 12 of 85 fungicide-exposed strains were mutated. The goal of the present study was to inspect genome-wide signatures of sublethal fungicide stress in strains of *S. sclerotiorum* with different genomic backgrounds. To accomplish this goal, a subset of strains from the previous study were selected for WGS. To study the effect of genomic background on the mutational repertoire, it was important to sequence multiple progenitor and derived strains.

The genomic features of *S. sclerotiorum* made it a suitable model system for conducting this study. The small genome size of *S. sclerotiorum* (38.8 Mb) enabled us to sequence more strains cost-effectively than would be possible with a fungus with a larger genome. Genome stability (12.96% TE content; Derbyshire et al. 2017) provided less chances of background mutations as compared to fungal genomes with higher TE content. The *S. sclerotiorum* genome is also optically mapped (assembled to chromosomal level) and annotated (Derbyshire et al. 2017), which helped us to make conclusions on a per chromosome-basis. As genomic perturbations can have deleterious effects on strain fitness or aggressiveness (Jeon et al. 2013), investigating the consequences of genomic alterations on phenotype can give an insight into the feasibility of genome plasticity in natural environments. The haploid nature of the *S. sclerotiorum* genome enabled elucidation of the phenotypic effect of mutations on strain aggressiveness without concern of dominant alleles masking the recessive alleles.

To characterize genomic effects of sublethal fungicide stress in *S. sclerotiorum* and study the role of different genomic backgrounds in generating diversity, our objectives were: a) determine mutation frequency in control and fungicide-exposed strains; b) characterize mutations as SNPs, INDELs, CNVs, and TE insertions; c) determine the genomic distribution of mutations; d) elucidate the genetic relationship among progenitor, control, and exposed strains; e) characterize variation among genomic backgrounds; and f) determine the fitness consequences of genome perturbations. We sequenced a subset of *S. sclerotiorum* genomes that were exposed to sublethal fungicide stress previously (Amaradasa and Everhart 2016) and determined the number, type, and distribution of mutations with respect to the progenitor strains. To characterize the variation in the genomic backgrounds of the progenitor strains, genomic variants were determined with respect to the reference genome and effectors were identified from the *de novo* assembly of the five strains. Finally, the phenotypic effect of mutation accumulation on strain aggressiveness was studied to determine the fitness effects of the genome-wide mutations. This is the first study to attempt to characterize genomic signatures of sublethal fungicide stress in a plant pathogen and study the role of within-species diversity on the mutational repertoire produced in response to fungicide stress. Understanding factors that increase the mutation rate and accelerate resistance emergence can help to devise disease management strategies that delay resistance evolution and prolong the life of currently used fungicides.

Materials and methods

Strains and fungicides. Five *S. sclerotiorum* strains (Table 4.1; Strain IDs: 152, 467, 555, 594, 646) were vegetatively cultured under different treatment conditions to obtain 50 experimentally evolved strains as described in Amaradasa and Everhart (2016). In brief, each progenitor strain was subcultured independently on sublethal doses of azoxystrobin, boscalid, iprodione, thiophanate-methyl, and as a negative control to obtain five experimentally evolved strains and the experiment was repeated. Sublethal fungicide exposure was achieved by growing strains on a concentration gradient of fungicide and then collecting mycelia from the sublethal exposure region (50-100% inhibition zone). The amount of collected mycelia was increased by growing it on unamended Potato Dextrose Agar (PDA) so that it could be subjected to another round of sublethal fungicide exposure. The process of sublethal fungicide exposure and inoculum multiplication was repeated a total of 12 times. At the end of the two experiments, ten subcultured strains were derived from each progenitor. The sclerotia of all the strains were stored at 4°C until further use. For the present study, strains were revived from sclerotia by plating them on 1.5% Water Agar (WA) at room temperature. After 5–6 days, a 6 mm plug was excised from the actively growing margin of the mycelial colony and placed upside-down on PDA plates covered with cellophane to facilitate mycelial collection for DNA extraction.

DNA extraction and WGS. DNA was purified from 800–1000 mg of actively growing mycelia of 55 strains that were scraped from 2–3 days old cellophane PDA plates. Mycelia were ground with liquid nitrogen in pre-sterilized pestle and mortar. For DNA extraction, DNeasy Plant Maxi Kit (Qiagen, Hilden, Germany) was used according to the manufacturer's instructions and DNA was stored at -20°C until further use. About

1.3–8.8 µg DNA per sample was shipped on dry ice to the Philadelphia, PA receiving center for Beijing Genomics Institute (BGI, China). The samples were further shipped on dry ice to the BGI laboratory in Hong Kong. Before library preparation, DNA concentration was checked using Qubit® 3 Fluorometer (Invitrogen, Carlsbad, CA), which ranged from 8.4–86.8 ng/µL and DNA integrity was evaluated using gel electrophoresis on a 2% agarose gel. High quality DNA was subjected to WGS in one lane of Illumina HiSeq 4000 with 150 paired-end reads and 350 bp insert size.

Data filtering and variant calling. Sixteen GB of raw data in fastq format with trimmed adapter sequences were received from the sequencing facility. Quality of raw read pairs was assessed using FastQC version 0.11 (Andrews 2010) and sequences below 99.84% accuracy (phred-scaled quality threshold of 28) were trimmed using trimmomatic version 0.36 (Bolger et al. 2014). Fifty-three million reads were aligned to the *S. sclerotiorum* reference genome V1.1 (Derbyshire et al. 2017) using Bowtie version 2.2 (Langmead and Salzberg 2012) and SAMtools version 1.3 (Li et al. 2009) setting the maximum insert size parameter to 800 bp. Optical duplicates were filtered using Picard version 2.9 (Broad Institute 2017). Different variant types were called using different software on networked computers provided by the Holland Computing Center at the University of Nebraska-Lincoln.

SNP and INDEL variants. SNP and INDEL variants were called using HaplotypeCaller and GenotypeGVCFs in GATK version 3.4 (McKenna et al. 2010) and a single Variant Call Format (VCF) file for all the strains was created for further analysis.

All components of the reference guided assembly pipeline and variant calling using GATK were implemented in a makefile available at https://github.com/everhartlab/read-processing. Quality variants were filtered using the package vcfR version 1.7 (Knaus and Grünwald 2017) implemented in R version 3.6.2 (R Core Team 2019). The minimum mapping quality threshold was set to a score of 41 on phred-scale (>99.99% accuracy). To determine the effect of sublethal fungicide exposure in derived strains with respect to each progenitor strain within an experiment, only loci with >5X coverage for all strains in the comparison group were retained. Strain 594 exposed to iprodione in the first experiment appeared to be mislabeled or contaminated based on its pattern of variants and was not included in further analyses. For determining the genomic differences of each progenitor strain with respect to the reference genome, only loci with >5X coverage for at least three out of the five strains were retained. Loci with ≤5X coverage were removed from the analysis.

Variants identified from GATK were characterized as Single Nucleotide Polymorphisms (SNPs) if one nucleotide was substituted and were characterized as INsertions or DELetions (INDELs) if one or more nucleotides were added or deleted as compared to the sequence of the progenitor strain. SNPs were further classified as transitions or transversions. Positions of mutated loci were mapped on chromosomes and their occurrence in coding (exonic) or non-coding (intronic, inter-genic) regions was determined.

To avoid any bias due to regions with high mutation rate, variants in tandem repeats and TEs were identified and discarded. Tandem repeats of more than 50 bp length were identified using MUMmer version 4.0 (Marçais et al. 2018). Consensus sequences

of TEs previously identified in the *S. sclerotiorum* genome were obtained from RepetDB (Amselem et al. 2019) and were BLASTed against the reference genome using BLAST version 2.7 (Altschul et al. 1990) to obtain the respective TE coordinates. A stringent e-value of 1×10^{-30} and 85% identity were chosen as the cut-off. Variants in tandem repeats and TEs were identified and discarded using the packages vcfR version 1.7 (Knaus and Grünwald 2017), dplyr version 0.8.5 (Wickham et al. 2020), and tidyr version 1.1.0 (Wickham and Henrys 2020) in R version 3.6.2 (R Core Team 2019).

Characterization of CNVs. Copy Number Variants (CNVs) i.e. duplications and deletions ≥ 1,500 bp were characterized with CNVnator version 0.4 (Abyzov et al. 2011) using a bin size of 300 bp. Bin sizes of 100–500 bp were tested in 100 bp increments for all progenitor strains and the optimum bin size was selected when the ratio of average read depth to its standard deviation was between 4–5 (as recommended by the software developers). The vcf file generated from CNVnator was imported into R version 3.6.2 (R Core Team 2019) and further analysis was done using vcfR version 1.7 (Knaus and Grünwald 2017) and dplyr version 0.8.5 (Wickham et al. 2020). Quality filtering was done by removing CNVs with e-value (e-val1) ≥ 0.1 and putative repetitive regions (q0 ≥ 0.5; CNVs with ≥ 50% reads mapped with zero mapping quality). For determining the effect of sublethal dose exposure, CNVs in the progenitor strains that overlapped with the corresponding derived strains were removed.

To determine aneuploidy, putative repetitive regions were retained. A strain was said to possess an extra copy of a given chromosome if >85% of the chromosome was

duplicated. If duplications or deletions constituted 40–85% of the chromosome, it was considered as partial gain or loss of the chromosome.

Characterization of TE insertions. Consensus TE fasta sequences (178) from the *S. sclerotiorum* genome (Amselem et al. 2011) were obtained from RepetDB (Amselem et al. 2019). Thirty-six of these TE sequences belonged to Class I transposons, 71 TE sequences belonged to Class II transposons, and 71 TE sequences were unclassified. The consensus sequences were used as an input in RetroSeq (Keane et al. 2013) to detect TE insertion in the progenitor and derived strains. A vcf file of TE insertions were obtained as the output, which were quality filtered according to the number of supporting reads (GQ), confidence on the breakpoint (FL; range from 1–8), and proximity to TEs in the reference genome. TE insertions with FL $\geq$ 6 were kept. Further, if the FL was 6, variants with a minimum GQ of 28 were retained and for higher FL values, variants with a minimum GQ of 20 were retained. The average length of a TE insertion was found to be 225 bp and any TE insertion detected in the 225 bp of an insertion in the control was removed. TE insertions called within 100 bp downstream or upstream of the original TE co-ordinates in the reference genome were filtered out.

Downstream analyses. To study the effect of fungicide exposure on frequency, type, and distribution of mutations, variants that were previously called with respect to the reference genome were filtered such that only those variants were retained that mutated in the derived strains with respect to the progenitor strains. This filtering step was done in R version 3.6.2 (R Core Team 2019) using vcfR version 1.7 (Knaus and

Grünwald 2017) and dplyr version 0.8.5 (Wickham et al. 2020). Statistical difference was tested between the number of mutations in control and fungicide-exposed strains (derived from the same progenitor strain) with respect to genic and intergenic regions, type of mutation (SNP, INDEL, CNV, or TE insertion), type of SNP (transition or transversion), and the chromosome on which the mutations were found. A goodness of fit χ^2-test was performed when the number of observations were more than five and an exact binomial test was performed otherwise at α=0.05 in R (R Core Team 2019).

To identify mutational hotspots, the genome was divided into non-overlapping bins of 500 bp length and the number of mutations in each bin were determined. A bin was considered as a mutational hotspot when the number of mutations in the bin was an outlier as determined by boxplot statistics (more than the 3rd quartile + 1.5 times the interquartile range). A mutational hotspot was considered as a treatment effect when the number of mutations in the corresponding control were <= the 3rd quartile.

Neighbor-joining tree. Effect of sublethal fungicide exposure on the genetic relationship among progenitor, control, and exposed strains was determined by building a Neighbor-Joining (NJ) tree. The NJ tree was built off of Nei's distance with 1000 bootstrap replicates using the packages poppr version 2.8.1 (Kamvar et al. 2015) and ape version 5.2 (Paradis and Schliep 2019) in R version 3.6.2 (R Core Team 2019). Nei's distance was calculated from SNP loci with < 50% missing information. To identify the factors causing variation in the SNP data, Analysis of Molecular Variance (AMOVA) was performed at α=0.05 using the package poppr version 2.8.1 (Kamvar et al. 2015) in R version 3.6.2 (R Core Team 2019).

Change in strain aggressiveness. High number of accumulated mutations resulting from fungicide stress may have a negative effect on the fitness of haploid *S. sclerotiorum* strains. To study the effect of mutation accumulation on strain aggressiveness, straw test was conducted on a moderately resistant dry bean genotype, G122, using the methodology described by Otto-Hanson et al. 2011.

Sclerotia were surface sterilized with a solution of 50% Clorox bleach and 50% dH_2O followed by rinsing twice with dH_2O for three minutes each. Sterile sclerotia were dried on sterile paper towels for 20–30 seconds, plated on 1.5% Water Agar (WA) and stored at room temperature to reactivate the sclerotia. After 5–6 days, a 6 mm plug was taken from the growing mycelial edge and transferred to PDA. Two-day-old PDA cultures were used for inoculating dry bean plants. Sclerotia from two strains could not be revived - iprodione exposed strain 467 in the first experiment and boscalid exposed strain 594 in the second experiment. Aggressiveness assays were performed as two separate experiments set up in completely randomized design with four replications. Dry bean plants were inoculated 21 days after germination using straws with mycelial plugs. Clear drinking straws were cut into pieces of 2.5 cm length each that were sealed at one end. Straw pieces were filled with two mycelial plugs excised from the PDA cultures such that the mycelial surface faced the open end of the straw piece. Stem was cut at 2.5 cm above the fourth node and covered with the straw piece containing inoculum. Plants were incubated at 26 ± 2°C day and 20 ± 2°C night temperatures in the greenhouse for 8 days and were rated using the Modified Petzoldt and Dickson scale ranging from 1–9 (Terán et al. 2006). Data from the two greenhouse experiments were combined.

Statistical analysis of the mean aggressiveness score of progenitor and derived strains was done using Kruskal-Wallis Rank Sum Test at α=0.05 in R version 3.6.2 (R Core Team 2019).

Effector prediction from *de novo* assemblies. To characterize the genomic differences among the five progenitor strains, putative effectors were identified from their respective *de novo* genome assemblies. Raw sequence data were quality corrected using BayesHammer (Nikolenko et al. 2013) and *de novo* assembly was performed using ABySS version 2.1 (Simpson et al. 2009) with k-mers 24, 34, 44, 54, 64, 74, 84, and 94. Quality of the assemblies produced from each of these k-mers was checked using QUAST version 5.0 (Gurevich et al. 2013). The assembly produced from k-mer of 44 had the best assembly statistics and was therefore used for predicting effectors.

First, *de novo* predictions of protein sequences were made from the *de novo* genome assemblies using AUGUSTUS version 3.3 (Stanke and Waack 2003) with the available training parameters from *Botrytis cinerea.* SECRETOOL (http://genomics.cicbiogune.es/SECRETOOL/Secretool.php; Cortázar et al. 2014) was used to identify putatively secreted proteins using the classic secretion pathway with default parameters. Putatively secreted proteins obtained from the SECRETOOL output of each progenitor were used to identify effector candidates. EffectorP version 2.0 (Sperschneider et al. 2018) and manual inspection of conserved domains using the Batch CD-Search tool (Marchler-Bauer et al. 2004, 2011) were used to identify putative effectors. For manual inspection, secreted proteins with domains which are known to be present in effectors in other plant pathogens were identified (Blümke et al. 2014;

Franceschetti et al. 2017; Guyon et al. 2014; Jain et al. 2015; Levin et al. 2017; Pennington et al. 2019). These domains included necrosis inducing proteins, proteases, lipases, peroxidases, glucanases, chitin binding proteins, peptidases, enzyme inhibitors, ribonucleases, and cysteine-rich proteins. Unique effectors from each progenitor strain were identified by BLASTing the effector sequences against effectors from other progenitor strains using BLAST version 2.7 with an e-value cut off of $1x10^{-10}$ and a minimum identity of 85% (Altschul et al. 1990). To identify the similarities between previously identified putative effectors (Derbyshire et al. 2017) and the candidate effectors identified from the five progenitor strains, effector sequences were BLASTed against each other using BLAST version 2.7 with an e-value cut off of $1x10^{-10}$ and a minimum identity of 85% (Altschul et al. 1990).

Results

Genome alignment statistics. We sequenced a total of 55 strains: 5 progenitor, 10 control (unexposed) and 40 fungicide-exposed strains, of which one fungicide-exposed strain was removed from the analysis due to contamination. Read mapping to the reference genome resulted in fair to high read depths and coverage for both nuclear and mitochondrial genomes. The average read depths of nuclear and mitochondrial genomes were 16.47X and 199.64X respectively and the average coverage were 98.5% and 99.6% respectively.

Frequency and characterization of mutations. To investigate the effect of fungicide exposure and genomic background on the rate of spontaneous mutations, the

number of SNPs, INDELs, CNVs, and TE insertions were determined for all the derived strains. The type of point mutation varied according to the genomic background of the strain (Table 4.2). SNPs were more frequent than INDELs in all strains and accounted for 60.74% of point mutations in strain 594 and 84.52% of point mutations in strain 467. Transitions were more frequent than transversions and accounted for 55% of SNPs in strain 467 and 80.94% of SNPs in strain 594.

On average, the frequency of INDELs was higher in fungicide exposed strains than their control (unexposed) counterparts in both experiments (Fig. 4.1). INDEL frequency was significantly higher in strain 555 exposed to azoxystrobin and iprodione in the first experiment (Fig. 4.1; $P \leq 0.05$). The number and type of SNPs (transition or transversion) were not affected by fungicide exposure (Fig. 4.2; $P > 0.05$). G>A (or A>G) transitions were the most common among all strains followed by C>T (or T>C) transitions, but the frequency of different types of transitions and transversions were not significantly affected by fungicide exposure (Fig. 4.3; $P > 0.05$). Collectively, strain 555 independently exposed to iprodione in the first experiment had a significantly higher number of point mutations than the corresponding control (Fig. 4.4; $P \leq 0.05$).

The number of CNVs in derived strains did not show consistent patterns among experiments suggesting that fungicide exposure did not affect CNV frequency and that random CNVs were common in the *S. sclerotiorum* genome (Fig. 4.5). The progenitor strain 152 had aneuploidy of chromosome 7, which was retained partially or completely in 30% of its derived strains. Other progenitor strains did not show aneuploidy but 18% of their derived strains partially or completely gained an extra copy of chromosome 7 (Table 4.3).

Amongst classifiable TE insertions, the greatest number of TE insertions in all genomic backgrounds were Terminal Inverted Repeats (TIR; Fig. 4.6). The number of TE insertions varied according to the fungicide-strain combination (Fig. 4.7). On average, strains 467, 555 and 646 had fewer TE insertions after fungicide exposure compared to the control, except strain 646 exposed to iprodione in the second experiment (Fig. 4.7). Strain 152 had a higher number of TE insertions than the control in azoxystrobin exposed strains, which was significant in the second experiment ($P \leq 0.05$).

To characterize the differences among the genomic backgrounds of the progenitors, point mutations, TE insertions, and CNVs were characterized relative to the reference genome. The progenitor strain 555 had the highest number of point mutations, TE insertions, and CNVs, suggesting that it has maximum divergence from the reference genome (Fig. 4.8). The progenitor strains 152 and 467 did not differ significantly amongst each other in the number of point mutations, TE insertions, and CNVs (Fig. 4.8; $P > 0.05$).

Overall, the genomic background had a prominent effect on the frequency of SNPs, INDELs, and TE insertions, and fungicide exposure affected point mutations and TE insertions in certain fungicide-strain combinations.

Genomic distribution of mutations. Bias in the genomic distribution of point mutations was studied on a per chromosome-basis, in non-overlapping bins of sizes 500 bp and 10,000 bp, and in the coding and non-coding regions. Our results showed that the genomic background affected both the accumulation of mutations on chromosomes (Fig. 4.9), in 10,000 bp bins (Table 4.4), and in coding versus non-coding regions (Table 4.2). Irrespective of fungicide exposure, mutational hotspots were identified on chromosome

15 for strains 152, 467, and 594, chromosome 11 for strains 555, 594, and 646, chromosome 4 for strain 555, chromosome 12 for strain 594, and chromosome 2 for strain 646 (Fig. 4.10). When investigated in 10,000 bp bins, mutational hotspots of size ranging from 1214 bp to 2590 bp were identified that harbored eight genes (Table 4.4). The gene sscle_15g107310 was classified as a heavy metal translocating P-type ATPase, which transports or detoxifies heavy metals and the gene sscle_12g089740 as an MC/SLC25 family protein, which transfers molecules across mitochondrial membranes. The gene sscle_04g033710 had a Protein Kinases (PKc_like super family) conserved domain, while the other genes did not have known conserved domains. The mutational hotspots (Table 4.4) had a total of 76 point mutations, 73 of which were SNPs. Out of 73 SNPs, G>A (or A>G) transitions accounted for 50.68% of SNPs and C>T (or T>C) transitions accounted for 34.24% of SNPs. The mean GC content of these hotspots was 43.9% (range: 38.18% – 45.35%). Genomic background also affected the accumulation of point mutations in coding vs. non-coding regions (Table 4.2). Strain 467 had 83.33% of point mutations in the coding region, while strain 646 only had 27.08% of point mutations in the coding region.

Fungicide exposure affected the genomic distribution of mutations in certain strain-fungicide combinations. Chromosome 11 had a significantly greater number of INDELs in strain 555 exposed to thiophanate-methyl in the first experiment and azoxystrobin in the second experiment than the respective controls ($P \leq 0.05$). On average, the number of point mutations in the non-coding regions of fungicide exposed strain 555 was higher than the control (Fig. 4.11) and iprodione exposure of this strain in the first experiment resulted in a significantly higher mutation frequency ($P \leq 0.05$).

Twenty-one genes only mutated in fungicide-exposed strains (Table 4.5), out of which two genes mutated in more than three fungicide exposed strains. The gene sscle_11g081320 mutated in strain 555 independently exposed to boscalid, iprodione, and thiophanate-methyl in the first experiment and in strain 555 exposed to thiophanate-methyl in the second experiment. The gene sscle_14g101330 mutated in strain 555 independently exposed to azoxystrobin, iprodione, and thiophanate-methyl in the first experiment and in strain 555 independently exposed to iprodione and thiophanate-methyl in the second experiment. The sscle_11g081320 gene is a hypothetical protein with no conserved domains and sscle_14g101330 is a potential nucleoside hydrolase with a bacterial conserved domain of DNA polymerase III subunit gamma/tau.

Overall, the genomic background had a prominent effect on the genomic distribution of point mutations and fungicide exposure affected this distribution in certain strain-fungicide combinations.

Genetic relationships among progenitor and derived strains. A neighbor-joining (NJ) tree was constructed to study the genetic relationship among progenitor, control, and exposed strains. For both the first (Fig. 4.12) and second experiments, strains grouped according to their genomic backgrounds. Strains 152 and 467 were closely related to each other. Most of the genetic variation (46.9%) was due to variation among strains (AMOVA $P \leq 0.05$) and not due to variation among treatments (1.16%; AMOVA $P > 0.05$).

Change in strain aggressiveness. Straw tests were conducted to examine any change in strain aggressiveness due to mutation accumulation. For all progenitor and derived strains, the aggressiveness varied from 3.38 – 6.00 (Table 4.6). Among progenitor strains, the strain 555 was the most aggressive. Strain aggressiveness did not significantly change in control and exposed strains except in iprodione exposed strain 555 in the second experiment ($P \leq 0.05$; Table 4.6). In general, mutation accumulation did not impact strain aggressiveness.

Effector prediction from *de novo* assemblies. On average, 9,613 putative proteins were identified from each of the five *de novo* genome assemblies, out of which an average of 327 proteins were characterized as putative secreted proteins for each progenitor strain. From the secretome, at least 52 effector candidates were identified for each progenitor strain (Table 4.7), out of which one to four effector candidates were unique to a particular progenitor (Table 4.8). Out of the 70 effectors previously identified in the *S. sclerotiorum* genome (Derbyshire et al. 2017), 25 effectors were identified from the five progenitor strains (Table 4.9; e-value $1x10^{-10}$). Some of the newly identified putative effectors have conserved domains that were absent from previously predicted effectors.

Discussion

We found that sublethal fungicide exposure increased the mutation frequency in *S. sclerotiorum* in certain genomic backgrounds. This exposure significantly increased INDEL frequency in one genomic background (Fig. 4.1) and generally suppressed TE

insertions (Fig. 4.7). A pronounced effect of the genomic background was observed on genome instability. In general, strain 555 had more propensity to create genetic variation, which is important for adapting to stressful environments and emergence of fungicide resistance. For possible intervention in resistance evolution, it is important to understand the factors that accelerate adaptation. This study suggests that sublethal fungicide doses can act as a genomic stressor in *S. sclerotiorum* and promote mutagenesis in certain genomic backgrounds, which could accelerate the emergence of alleles conferring fungicide resistance.

Several of the fungicide-exposed strains sequenced in the present study were shown previously to have mutations identified via SSR and AFLP genotyping (Amaradasa and Everhart 2016). Overall, SSR mutations were more frequent for strains exposed to iprodione and azoxystrobin, although strains 152, 467, and 555 only showed changes in AFLP profiles. WGS analysis conducted in the present study showed that the frequency of INDELs increased in almost all genomic backgrounds with a more prominent effect on strain 555 exposed to iprodione and azoxystrobin in the first experiment. Although searches of SSR loci were made using the WGS assemblies, no loci were identified (*data not shown*) and is likely due to the difficulty in assembling repetitive regions (Treangen and Salzberg 2012). Nevertheless, the increased point mutation frequency owing to fungicide stress was congruent with the SSR and AFLP results obtained in the previous study.

The relationship between TE insertion and stress has not been examined in *S. sclerotiorum* before. In other organisms, TEs are known to be activated or suppressed under stress and the consequences can vary with genomic background (Horváth et al.

2017). In the current study, TE insertion was mostly suppressed under sublethal fungicide stress in all genomic backgrounds except in azoxystrobin exposed strain 152 and iprodione exposed strain 646 (Fig. 4.7). Similar to these results, sublethal fungicide stress activated TE movement in a strain by fungicide-dependent manner in *M. fructicola* (Chen et al. 2015).

The effects of fungicide-exposure were evaluated across multiple strains originating from different states in the U.S. (Table 4.1), allowing additional insight into variation by genomic background. The point mutation frequency (Fig. 4.1; Fig. 4.4) and distribution (Fig. 4.9; Fig. 4.10) among strains varied according to the genomic background, which suggests that considerable variation exists in the genome dynamics of *S. sclerotiorum*. Among strains evaluated in the present study, strain 555 had the highest frequency of point mutations in both non-treated controls and in fungicide exposure. This suggests that different strains likely have a different rate of mutation. Such difference may facilitate adaptation of *S. sclerotiorum* to stressful environments, therefore adaptation in the population may be driven by strains that are more prone to mutations. A study conducted in *Candida albicans* also found that the genomic background influences genomic stability and evolution (Gerstein and Berman 2020). Environmental and clinical fungal strains with an increased mutation rate due to faulty DNA repair machinery, called hypermutators, have been shown to adapt more rapidly to antifungal therapy and host stress (Boyce et al. 2017, Healey et al. 2016, dos Reis et al. 2019). Since genes involved in the DNA repair pathway are not fully characterized in most plant pathogens including *S. sclerotiorum*, it is unclear if the higher mutation rate observed in the strain 555 is due to defective DNA repair machinery.

In addition to the genomic plasticity of strain 555, an important difference was observed in the colony morphology of strain 555. Mycelium in the colony was dark gray in color, which is likely due to increased melanin (Butler et al. 2009; Lazarovits et al. 2000). Melanin pigmentation plays diverse roles in fungi. It is a characteristic feature of fungi adapted to extreme heat, cold, pH, oxidative stress, and radiation (Coleine et al. 2020; Gessler et al. 2014; Mironenko et al. 2000). Melanin protects the fungal cell from various stresses and has additional functions that are not fully understood (Eisenman et al. 2020). In the current study, we observed that the genome of the melanized fungal strain produced more mutations in response to fungicide stress, which could facilitate stress adaptation. Further studies are required to explore the relationship, if any, between melanization and stress-induced mutations.

Spontaneous mutations were observed in the control in the present study and similar results were obtained in experimental evolution studies conducted in *Magnaporthe oryzae* and *Zymoseptoria tritici* (Jeon et al. 2013; Möller et al. 2018). After serially transferring *M. oryzae* strains on artificial media up to 10 and 20 times, 200–350 point mutations were observed in the derived strains. Similar to the present study, a mutational bias was observed for SNPs over INDELs, transitions over transversions and a mutational bias was also observed for certain chromosomes. Virulence of *M. oryzae* decreased after 20 generations of serial transfer, however, strain aggressiveness in the present study did not change after mutation accumulation. The decrease in virulence of *M. oryzae* may be due to the deleterious effect of a higher number of mutations accumulated in the genome. The *S. sclerotiorum* haploid genome appears to be tolerant to perturbations, without a fitness cost, suggesting that plasticity may play an important role

in adaptation of *S. sclerotiorum* to stresses like host defenses and unfavorable environmental conditions. The presence of genomic plasticity in this pathogen signifies that even during clonal propagation of *S. sclerotiorum* (Cubeta et al. 1997; Kamvar et al. 2017; Kohli and Kohn 1998), it can use several mechanisms to spontaneously increase genetic diversity.

Antifungal stress posed by azoles and echinocandins in human fungal pathogens is known to increase the rate of point mutations (Avramovska and Hickman 2019) but has a more prominent impact on aneuploidy and chromosomal rearrangements (Avramovska and Hickman 2019; Harrison et al. 2014; Shapiro 2015; Shor and Perlin 2015). A change in aneuploidy or CNVs in response to fungicide stress was not observed in the present study. However, fungicides tested did not belong to azoles and echinocandins, which might explain the difference in the observed genome dynamics. Irrespective of fungicide exposure, a high number of CNVs, especially the propensity for large duplications on chromosome 7 and aneuploidy of this chromosome were observed in the *S. sclerotiorum* genome (Table 4.3). Interestingly, this chromosome harbors regions with high density of repetitive sequences and Repeat Induced Point mutations (RIP), which are associated with clusters of secreted and effector-like proteins (Derbyshire et al. 2017). Rapid gain and loss of the extra copy of this chromosome suggests that this strategy might be frequently used by *S. sclerotiorum* and may be helpful for host stress adaptation. Extensive CNVs were also observed during the vegetative growth of the haploid fungus *Z. tritici* (Möller et al. 2018), suggesting that chromosomal rearrangements might be a common mechanism of generating genetic variation in at least some plant pathogens.

According to the frequency of previous resistance reports in *S. sclerotiorum* (Attanayake et al. 2013; Gossen et al. 2001; Lehner et al. 2015; Ma et al. 2009; Molaei et al. 2020; Penaud et al. 2003; Tóthová et al. 2019), more mutations were expected after thiophanate-methyl exposure. However, out of the four fungicides tested, azoxystrobin and iprodione had more prominent effects on INDELs in strain 555 (Fig. 4.1) and TE insertions in strains 152 and 646 (Fig. 4.7). Although azoxystrobin and iprodione might be more stressful for *S. sclerotiorum*, high field-usage of thiophanate-methyl to control *S. sclerotiorum* may be a more significant driver of fungicide resistance.

A few studies have tested the hypothesis of sublethal fungicide induced mutations in fungal pathogens in the same family as *S. sclerotiorum*. An *in vitro* study in *M. fructicola* showed that 8 of 15 SSR loci mutated in one of the three strains exposed to sublethal doses of azoxystrobin (Schnabel et al. 2014) and the movement of transposable element *Mftc1* was affected by sublethal fungicide dose (Chen et al. 2015). In a follow-up study, field populations of *M. fructicola* were exposed to sublethal doses of azoxystrobin and propiconazole. The sensitivity of field populations did not change significantly, and mutations were not observed in the 7 SSR loci tested (Dowling et al. 2016). This inconsistency may be either due to fungicide degradation and lack of exposure in the field setting or due to genomic changes not captured by the 7 SSR loci. In another study, four *Botrytis cinerea* strains were exposed to iprodione *in vitro*, which did not mutate at any of the nine SSR loci tested (Ajouz et al. 2010). However, such exposure changed the aggressiveness of the strains and led them to develop resistance to iprodione, fludioxonil, and dicloran fungicides. Collectively, these studies suggest that genetic markers may not provide sufficient information to study the effect of sublethal fungicide exposure. This is

the first study to evaluate the role of sublethal fungicide stress in causing mutagenesis at the whole-genome level.

The approach used for sublethal fungicide exposure in the present study was designed such that the effect of fungicide stress on mutation emergence could be examined, while minimizing the effect of selection. To minimize the effect of selection, sublethal fungicide exposed mycelia were collected and multiplied in the absence of fungicide, which was used for subsequent fungicide exposure. Fast-growing mycelial sectors were not used for sub-culturing. These fast-growing sectors might have had alleles conferring resistance or increased tolerance to the fungicide. This speculation is backed by a previous study where fungicide resistance was induced in the laboratory in *S. sclerotiorum* by exposing it to a sublethal fungicide concentration of fludioxonil and transferring the fast-growing sectors to a high fungicide concentration to select for resistance (Kuang et al. 2011). Among the 40 fungicide exposed strains used in the present study, none of them developed fungicide resistance (Amaradasa and Everhart, 2016). However, there was variation in the fungicide sensitivity of fungicide exposed strains (Fig. 4.13). Fungicide sensitivity did not change significantly for 14 strains ($P > 0.05$), decreased significantly for 14 strains, and increased significantly for 12 strains ($P \leq 0.05$; Amaradasa and Everhart, 2016). Such random distribution of the sensitivity corroborates that the selection pressure was minimized during the experiment.

One limitation of the present study was that the genomic variation among the progenitor strains might not be completely represented by alignment to the available reference genome. Genomes of most of the progenitor strains varied considerably among each other and from the reference genome (Fig. 4.8). Strain 152 was derived from the

reference genome strain, *S. sclerotiorum* 1980 UF-70, and hence showed few genomic aberrations than the reference genome. With the sequencing parameters used in the present study, high quality *de novo* assemblies were not achieved. However, the reference guided approach used in the present study yielded high quality variants. Future studies should use *de novo* genome assemblies to examine the novel genomic variation present in populations of *S. sclerotiorum* that may not otherwise be identified using reference-guided assembly alone.

Another limitation of this study was that the identified genomic variants were not validated experimentally. False-positive and false-negative variants can result from sequencing errors, mapping errors, or erroneous detection by variant callers (Hwang et al. 2015). Although variants were quality filtered to obtain high confidence calls, the authors acknowledge that a small percentage of false-positive and false-negative variants may have been retained. Future studies should perform Polymerase Chain Reaction (PCR) or Sanger Sequencing to validate variants of interest before performing further analyses.

Nonetheless, the present study shows that *in vitro* sublethal fungicide exposure can increase the mutation frequency in certain strains of *S. sclerotiorum* and strains with a highly mutable genomic background can generate a bigger allele-pool that may hasten adaptation. A better understanding of the factors that accelerate resistance emergence is important to devise disease management strategies that delay resistance evolution and prolong the life of currently used fungicides.

References

Abyzov, A., Urban, A.E., Snyder, M., and Gerstein, M. 2011. CNVnator: an approach to discover, genotype, and characterize typical and atypical CNVs from family and population genome sequencing. Genome Res. 21:974-984.

Ajouz, S., Decognet, V., Nicot, P.C., and Bardin, M. 2010. Microsatellite stability in the plant pathogen *Botrytis cinerea* after exposure to different selective pressures. Fungal Biol. 114:949-954.

Altschul, S.F., Gish, W., Miller, W., Myers, E.W., and Lipman, D.J. 1990. Basic local alignment search tool. J. Mol. Biol. 215: 403-410.

Amaradasa, B.S., and Everhart, S.E. 2016. Effects of sublethal fungicides on mutation rates and genomic variation in fungal plant pathogen, *Sclerotinia sclerotiorum*. PLoS One 11:e0168079.

Amselem, J., Cornut, G., Choisne, N., Alaux, M., Alfama-Depauw, F., Jamilloux, V., Maumus, F., Letellier, T., Luyten, I., Pommier, C., and Adam-Blondon, A.F. 2019. RepetDB: a unified resource for transposable element references. Mob. DNA, 10**:**6.

Amselem, J., Cuomo, C.A., Van Kan, J.A., Viaud, M., Benito, E.P., Couloux, A., Coutinho, P.M., de Vries, R.P., Dyer, P.S., Fillinger, S., and Fournier, E. 2011. Genomic analysis of the necrotrophic fungal pathogens *Sclerotinia sclerotiorum* and *Botrytis cinerea*. PLoS Genet. 7:e1002230.

Anaya, N., and Roncero, M.I.G. 1996. Stress-induced rearrangement of *Fusarium* retrotransposon sequences. Mol. Gen. Genet. 253:89-94.

Andrews, S. 2010. FastQC: a quality control tool for high throughput sequence data. URL: https://www.bioinformatics.babraham.ac.uk/projects/fastqc/.

Attanayake, R.N., Carter, P.A., Jiang, D., del Río-Mendoza, L., and Chen, W. 2013. *Sclerotinia sclerotiorum* populations infecting canola from China and the United States are genetically and phenotypically distinct. Phytopathology, 103**:**750-761.

Avramovska, O., and Hickman, M.A. 2019. The magnitude of *Candida albicans* stress-induced genome instability results from an interaction between ploidy and antifungal drugs. G3: Genes Genom. Genet. 9:4019-4027.

Beckerman, J.L., Sundin, G.W., and Rosenberger, D.A. 2015. Do some IPM concepts contribute to the development of fungicide resistance? Lessons learned from the apple scab pathosystem in the United States. Pest Manag. Sci. 71:331-342.

Blümke, A., Falter, C., Herrfurth, C., Sode, B., Bode, R., Schäfer, W., Feussner, I., and Voigt, C.A. 2014. Secreted fungal effector lipase releases free fatty acids to inhibit innate immunity-related callose formation during wheat head infection. Plant Physiol. 165:346-358.

Boland, G.J., and Hall, R. 1994. Index of plant hosts of *Sclerotinia sclerotiorum*. Can. J. Plant Pathol. 16:93-108.

Bolger, A.M., Usadel, B., and Lohse, M. 2014. Trimmomatic: a flexible trimmer for Illumina sequence data. Bioinformatics 30:2114-2120.

Boyce, K.J., Wang, Y., Verma, S., Shakya, V.P., Xue, C., and Idnurm, A. 2017. Mismatch repair of DNA replication errors contributes to microevolution in the pathogenic fungus *Cryptococcus neoformans*. mBio 8:e00595-17.

Brent, K.J., and Hollomon, D.W. 2007. Fungicide resistance in crop pathogens: how can it be managed? FRAC Monogr. No. 1, 2nd revised ed. Fungicide Resistance Action Committee, CropLife International, Brussels. Online publication. http://www.frac.info/docs/default-source/publications/monographs/monograph-1.pdf

Broad Institute. 2017. Picard tools. URL: http://broadinstitute.github.io/picard.

Butler, M.J., Gardiner, R.B., and Day, A.W. 2009. Melanin synthesis by *Sclerotinia sclerotiorum*. Mycologia 101:296-304.

Chadha, S., and Sharma, M. 2014. Transposable elements as stress adaptive capacitors induce genomic instability in fungal pathogen *Magnaporthe oryzae*. PLoS One 9:e94415.

Chen, F., Everhart, S.E., Bryson, P.K., Luo, C., Song, X., Liu, X., and Schnabel, G. 2015. Fungicide-induced transposon movement in *Monilinia fructicola*. Fungal Genet. Biol. 85:38-44.

Coleine, C., Masonjones, S., Sterflinger, K., Onofri, S., Selbmann, L., and Stajich, J.E. 2020. Peculiar genomic traits in the stress-adapted cryptoendolithic Antarctic fungus *Friedmanniomyces endolithicus*. Fungal Biol.

Cortázar, A.R., Aransay, A.M., Alfaro, M., Oguiza, J.A., and Lavín, J.L. 2014. SECRETOOL: integrated secretome analysis tool for fungi. Amino Acids 46:471-473.

Cubeta, M.A., Cody, B.R., Kohli, Y., and Kohn, L.M. 1997. Clonality in *Sclerotinia sclerotiorum* on infected cabbage in eastern North Carolina. Phytopathology 87:1000-1004.

Derbyshire, M., Denton-Giles, M., Hegedus, D., Seifbarghi, S., Rollins, J., Kan van, J., Seidl, M.F., Faino, L., Mbengue, M., Navaud, O., Raffaele, S., Hammond-Kosack, K., Heard, S., and Oliver, R. 2017. The complete genome sequence of the phytopathogenic fungus *Sclerotinia sclerotiorum* reveals insights into the genome architecture of broad host range pathogens. Genome Biol. Evol. 9:593-618.

dos Reis T.F., Silva, L.P., de Castro, P.A., do Carmo, R.A., Marini, M.M., da Silveira, J.F., Ferreira, B.H., Rodrigues, F., Lind, A.L., Rokas, A., and Goldman, G.H. 2019. The *Aspergillus fumigatus* mismatch repair MSH2 homolog is important for virulence and azole resistance. mSphere. 4:e00416–19.

Dowling, M.E., Bryson, P.K., Boatwright, H.G., Wilson, J.R., Fan, Z., Everhart, S.E., Brannen, P.M., and Schnabel, G. 2016. Effect of fungicide applications on *Monilinia fructicola* population diversity and transposon movement. Phytopathology 106:1504-1512.

Eisenman, H.C., Greer, E.M., and McGrail, C.W. 2020. The role of melanins in melanotic fungi for pathogenesis and environmental survival. Appl. Microbiol. Biotechnol. 104:4247-4257. doi:10.1007/s00253-020-10532-z

Franceschetti, M., Maqbool, A., Jiménez-Dalmaroni, M.J., Pennington, H.G., Kamoun, S., and Banfield, M.J**.** 2017. Effectors of filamentous plant pathogens: commonalities amid diversity. Microbiol. Mol. Biol. Rev., 81:e00066-16.

Fungicide Resistance Action Committee. 2018. FRAC list of plant pathogenic organisms resistant to disease control agents. URL: http://www.frac.info/docs/default-source/publications/list-of-resistant-plant-pathogens/list-of-resistant-plant-pathogenic-organisms_may-2018.pdf?sfvrsn=a2454b9a_2.

Galhardo, R.S., Hastings, P.J., and Rosenberg, S.M. 2007. Mutation as a stress response and the regulation of evolvability. Crit. Rev. Biochem. Mol. Biol., 42:399-435.

Gerstein, A.C., and Berman, J. 2020. *Candida albicans* genetic background influences mean and heterogeneity of drug responses and genome stability during evolution to fluconazole. bioRxiv, 360347.

Gessler, N.N., Egorova, A.S., and Belozerskaya, T.A. 2014. Melanin pigments of fungi under extreme environmental conditions. Appl. Biochem. Microbiol. 50:105-113.

Gianessi, L.P., and Reigner, N. 2005. The value of fungicides in U.S. crop production. Washington, DCCropLife Foundation.

Gossen, B.D., Rimmer, S.R., and Holley, J.D. 2001. First report of resistance to benomyl fungicide in *Sclerotinia sclerotiorum*. Plant Dis. 85:1206.

Gressel, J. 2011. Low pesticide rates may hasten the evolution of resistance by increasing mutation frequencies. Pest Manag. Sci. 67:253-257.

Gurevich, A., Saveliev, V., Vyahhi, N., and Tesler, G**.** 2013. QUAST: quality assessment tool for genome assemblies. Bioinformatics, 29:1072-1075.

Guyon, K., Balagué, C., Roby, D., and Raffaele, S. 2014. Secretome analysis reveals effector candidates associated with broad host range necrotrophy in the fungal plant pathogen *Sclerotinia sclerotiorum*. BMC Genomics 15:336.

Healey, K.R., Zhao, Y., Perez, W.B., Lockhart, S.R., Sobel, J.D., Farmakiotis, D., Kontoyiannis, D.P., Sanglard, D., Taj-Aldeen, S.J., Alexander, B.D., and Jimenez-Ortigosa, C. 2016. Prevalent mutator genotype identified in fungal pathogen *Candida glabrata* promotes multi-drug resistance. Nat. Commun. 7:11128.

Harrison, B.D., Hashemi, J., Bibi, M., Pulver, R., Bavli, D., Nahmias, Y., Wellington, M., Sapiro, G., and Berman, J. 2014. A tetraploid intermediate precedes aneuploid formation in yeasts exposed to fluconazole. PLoS Biol. 12:e1001815.

Horváth, V., Merenciano, M., and González, J. 2017. Revisiting the relationship between transposable elements and the eukaryotic stress response. Trends Genet. 33:832-841.

Jain, M., Fleites, L.A., and Gabriel, D.W. 2015. Prophage-encoded peroxidase in '*Candidatus* Liberibacter asiaticus' is a secreted effector that suppresses plant defenses. Mol. Plant Microbe In. 28:1330-1337.

Jeon, J., Choi, J., Lee, G.W., Dean, R.A., and Lee, Y.H. 2013. Experimental evolution reveals genome-wide spectrum and dynamics of mutations in the rice blast fungus, *Magnaporthe oryzae*. PLoS One, 8:e65416.

Kamvar, Z.N., Amaradasa, B.S., Jhala, R., McCoy, S., Steadman, J.R., and Everhart, S.E. 2017. Population structure and phenotypic variation of *Sclerotinia sclerotiorum* from dry bean (*Phaseolus vulgaris*) in the United States. PeerJ 5:e4152.

Kamvar, Z.N., Brooks, J.C., and Grünwald, N.J. 2015. Novel R tools for analysis of genome-wide population genetic data with emphasis on clonality. Front. Genet. 6:208.

Kasuga, T., Bui, M., Bernhardt, E., Swiecki, T., Aram, K., Cano, L.M., Webber, J., Brasier, C., Press, C., Grünwald, N.J., and Rizzo, D.M. 2016. Host-induced aneuploidy and phenotypic diversification in the sudden oak death pathogen *Phytophthora ramorum*. BMC Genomics 17:385.

Keane, T.M., Wong, K., and Adams, D.J. 2013. RetroSeq: transposable element discovery from next-generation sequencing data. Bioinformatics, 29:389-390.

Kistler, H.C., and Miao, V.P., 1992. New modes of genetic change in filamentous fungi. Annu. Rev. Phytopathol. 30:131-153.

Knaus, B.J., and Grünwald, N.J. 2017. vcfR: a package to manipulate and visualize variant call format data in R. Mol. Ecol. Resour. 17:44-53.

Kohli, Y., and Kohn, L.M. 1998. Random association among alleles in clonal populations of *Sclerotinia sclerotiorum*. Fungal Genet. Biol. 23:139-149.

Koshiji, M., To, K.K.W., Hammer, S., Kumamoto, K., Harris, A.L., Modrich, P., and Huang, L.E. 2005. HIF-1α induces genetic instability by transcriptionally downregulating MutSα expression. Mol. Cell, 17:793-803.

Kuang, J., Hou, Y.P., Wang, J.X., and Zhou, M.G. 2011. Sensitivity of *Sclerotinia sclerotiorum* to fludioxonil: in vitro determination of baseline sensitivity and resistance risk. Crop Prot. 30:876-882.

Langmead, B., and Salzberg, S.L. 2012. Fast gapped-read alignment with Bowtie 2. Nat. Methods 9:357.

Lazarovits, G., Starratt, A.N., and Huang, H.C., 2000. The effect of tricyclazole and culture medium on production of the melanin precursor 1, 8-dihydroxynaphthalene by *Sclerotinia sclerotiorum* isolate SS7. Pestic. Biochem. Phys. 67:54-62.

Lehner, M.S., Paula Júnior, T.J., Silva, R.A., Vieira, R.F., Carneiro, J.E.S., Schnabel, G., and Mizubuti, E.S.G., 2015. Fungicide sensitivity of *Sclerotinia sclerotiorum*: A thorough assessment using discriminatory concentration, EC_{50}, high-resolution melting analysis, and description of new point mutation associated with thiophanate-methyl resistance. Plant Dis. 99:1537-1543.

Levin, E., Ballester, A.R., Raphael, G., Feigenberg, O., Liu, Y., Norelli, J., Gonzalez-Candelas, L., Ma, J., Dardick, C., Wisniewski, M., and Droby, S. 2017. Identification and characterization of LysM effectors in *Penicillium expansum*. PloS One, 12:e0186023.

Li, H., Handsaker, B., Wysoker, A., Fennell, T., Ruan, J., Homer, N., Marth, G., Abecasis, G., Durbin, R., and 1000 Genome Project Data Processing Subgroup. 2009. The Sequence Alignment Map format and SAMtools. Bioinformatics 25:2078-2079.

Lucas, J.A., Hawkins, N.J., and Fraaije, B.A. 2015. The evolution of fungicide resistance. In: Advances in applied microbiology. United States: Academic Press, 29-92.

Ma, H.X., Chen, Y., Wang, J.X., Yu, W.Y., Tang, Z.H., Chen, C.J., and Zhou, M.G. 2009. Activity of carbendazim, dimethachlon, iprodione, procymidone and boscalid against Sclerotinia stem rot in Jiangsu Province of China. Phytoparasitica 37:421.

Maharjan, R.P., and Ferenci, T. 2017. A shifting mutational landscape in 6 nutritional states: Stress-induced mutagenesis as a series of distinct stress input–mutation output relationships. PLoS Biol. 15:e2001477.

Marçais, G., Delcher, A.L., Phillippy, A.M., Coston, R., Salzberg, S.L., and Zimin, A. 2018. MUMmer4: a fast and versatile genome alignment system. PLoS Comput. Biol., 14:e1005944.

Marchler-Bauer, A., and Bryant, S.H. 2004. CD-Search: protein domain annotations on the fly. Nucleic Acids Res. 32(Web Server issue):W327-31.

Marchler-Bauer, A., Lu, S., Anderson, J.B., Chitsaz, F., Derbyshire, M.K., Deweese-Scott, C., Fong J.H., Geer, L.Y., Geer, R.C., Gonzales, N.R., Gwadz, M., Hurwitz, D.I., Jackson, J.D., Ke, Z., Lanczycki, C.J., Lu, F., Marchler, G.H., Mullokandov, M., Omelchenko, M.V., Robertson, C.L., Song, J.S., Thanki, N., Yamashita, R.A., Zhang, D., Zhang, N., Zheng, C., and Bryant S.H. 2011. CDD: a Conserved Domain Database for the functional annotation of proteins. Nucleic Acids Res. 39(Database issue):D225-9. doi: 10.1093/nar/gkq1189.

McDougall P. 2016. The cost of new agrochemical product discovery, development and registration in 1995, 2000, 2005-8 and 2010 to 2014. R and D expenditure in 2014 and expectations for 2019. Consultancy study for CropLife International, CropLife America and the European Crop Protection Association.

McKenna, A., Hanna, M., Banks, E., Sivachenko, A., Cibulskis, K., Kernytsky, A., Garimella, K., Altshuler, D., Gabriel, S., Daly, M., and DePristo, M.A. 2010. The Genome Analysis Toolkit: a MapReduce framework for analyzing next-generation DNA sequencing data. Genome Res. 20:1297-1303.

Miller, M.E., Zhang, Y., Omidvar, V., Sperschneider, J., Schwessinger, B., Raley, C., Palmer, J.M., Garnica, D., Upadhyaya, N., Rathjen, J., and Taylor, J.M. 2018. *De novo* assembly and phasing of dikaryotic genomes from two isolates of *Puccinia coronata* f. sp. *avenae*, the causal agent of oat crown rust. MBio. 9.

Mironenko, N.V., Alekhina, I.A., Zhdanova, N.N., and Bulat, S.A. 2000. Intraspecific variation in gamma-radiation resistance and genomic structure in the filamentous fungus *Alternaria alternata*: a case study of strains inhabiting Chernobyl reactor no. 4. Ecotoxicol. Environ. Saf. 45:177-187.

Molaei, H., Abrinbana, M., and Ghosta, Y. 2020. Baseline sensitivities to azoxystrobin and tebuconazole in *Sclerotinia sclerotiorum* isolates from sunflower in Iran related to sensitivities to carbendazim and iprodione. J. Phytopathol. 168**:**353-362.

Möller, M., Habig, M., Freitag, M., and Stukenbrock, E.H. 2018. Extraordinary genome instability and widespread chromosome rearrangements during vegetative growth. Genetics 210:517-529.

Moolhuijzen, P., See, P.T., Hane, J.K., Shi, G., Liu, Z., Oliver, R.P. and Moffat, C.S., 2018. Comparative genomics of the wheat fungal pathogen *Pyrenophora tritici-repentis* reveals chromosomal variations and genome plasticity. BMC Genomics 19:279.

Nikolenko, S. I., Korobeynikov, A. I., and Alekseyev, M. A. 2013. BayesHammer: Bayesian clustering for error correction in single-cell sequencing. BMC Genomics 14**:**S7.

O'Sullivan, D., Tosi, P., Creusot, F., Cooke, B.M., Phan, T.H., Dron, M., and Langin, T. 1998. Variation in genome organization of the plant pathogenic fungus *Colletotrichum lindemuthianum*. Curr. Genet. 33:291-298.

Otto-Hanson, L., Steadman, J.R., Higgins, R., and Eskridge, K.M. 2011. Variation in *Sclerotinia sclerotiorum* bean isolates from multisite resistance screening locations. Plant Dis. 95:1370-1377.

Paradis, E. and Schliep, K. 2019. ape 5.0: an environment for modern phylogenetics and evolutionary analyses in R. Bioinformatics 35:526-528.

Parker, K.R., and von Borstel, R.C. 1987. Base-substitution and frameshift mutagenesis by sodium chloride and potassium chloride in *Saccharomyces cerevisiae*. Mutat. Res., 189:11-14.

Penaud, A., Huguet, B., Wilson, V., and Leroux, P. 2003, July. Fungicide resistance of *Sclerotinia sclerotiorum* in French oilseed rape crops. In: Proceedings of 11th International Rapeseed Congress. 6-10 July, Copenhagen. 4:1097-1098.

Pennington, H.G., Jones, R., Kwon, S., Bonciani, G., Thieron, H., Chandler, T., Luong, P., Morgan, S.N., Przydacz, M., Bozkurt, T., and Bowden, S. 2019. The fungal ribonuclease-like effector protein CSEP0064/BEC1054 represses plant immunity and interferes with degradation of host ribosomal RNA. PLoS Pathog. 15:e1007620.

Petzoldt, R., and Dickson, M.H. 1996. Straw test for resistance to white mold in beans. Annu. Rep. Bean Improv. Coop. 39:142-143.

R Core Team. 2019. R: A language and environment for statistical computing. R Foundation for Statistical Computing, Vienna, Austria. URL: https://www.R-project.org/.

Schnabel, G., Chen, F., Everhart, S.E., Bridges, W.C., and Liu, X. 2014. Studies on sensitivity reduction in solo and mixture treatments and fungicide-induced mutagenesis in *Monilinia fructicola*. Modern fungicides and antifungal compounds VII: proceedings of the 17th International Reinhardsbrunn Symposium, April 21-25, 2013, Friedrichroda, Germany.

Shapiro, R.S. 2015. Antimicrobial-induced DNA damage and genomic instability in microbial pathogens. PLoS Pathog. 11:e1004678.

Shor, E., Fox, C.A., and Broach, J.R. 2013. The yeast environmental stress response regulates mutagenesis induced by proteotoxic stress. PLoS Genet. 9**:**e1003680.

Shor, E., and Perlin, D.S. 2015. Coping with stress and the emergence of multidrug resistance in fungi. PLoS Pathog. 11:e1004668.

Simpson, J.T., Wong, K., Jackman, S.D., Schein, J.E., Jones, S.J., and Birol, I. 2009. ABySS: a parallel assembler for short read sequence data. Genome Res. 19:1117-1123.

Sperschneider, J., Dodds, P.N., Gardiner, D.M., Singh, K.B., and Taylor, J.M. 2018. Improved prediction of fungal effector proteins from secretomes with EffectorP 2.0. Mol. Plant Pathol. 19:2094-2110.

Stanke, M., and Waack, S. 2003 Gene prediction with a hidden Markov model and new intron submodel. Bioinformatics, 19(Suppl 2):ii215 –ii225

Terán, H., Lema, M., Schwartz, H.F., Duncan, R., Gilbertson, R., and Singh, S.P. 2006. Modified Petzoldt and Dickson scale for white mold rating of common bean. Annu. Rep. Bean Improv. Coop. 49:115.

Tóthová, M., Hudec, K., and Tóth, P. 2019. Sensitivity of *Sclerotinia sclerotiorum* to strobilurin fungicides in Slovakia. Plant Protect. Sci. 56:13-17.

Treangen, T.J., and Salzberg, S.L. 2012. Repetitive DNA and next-generation sequencing: computational challenges and solutions. Nat. Rev. Genet. 13:36-46.

Troncoso-Rojas, R., Báez-Flores, M.E., Pryor, B., García, H.S., and Tiznado-Hernández, M.E. 2013. Inter simple sequence repeat polymorphism in *Alternaria* genomic DNA exposed to lethal concentrations of isothiocyanates. Afr. J. Microbiol. Res. 7:838-852.

van den Bosch, F., Paveley, N., Shaw, M., Hobbelen, P., Oliver, R. 2011. The dose rate debate: does the risk of fungicide resistance increase or decrease with dose? Plant Pathol. 60:597-606.

Wickham, H., François, R., Henry, L., and Müller, K. 2020. dplyr: A grammar of data manipulation. R package version 0.8.5. https://CRAN.R-project.org/package=dplyr

Wickham, H. and Henry, L. 2020. tidyr: Tidy messy data. R package version 1.1.0. https://CRAN.R-project.org/package=tidyr

Tables and figures

Table 4.1. *Sclerotinia sclerotiorum* strains used in the current study.

Strain	Origin	Year	Aggressiveness[a]	MCG[b]	Host cultivar[c]
152	Nebraska	1980	3.9	4	Great Northern
467	Colorado	1996	4.6	45	Pinto
555	Minnesota	2004	6.4	44	Bunsi
594	California	2004	4.6	21	Bunsi
646	Washington	2005	5.4	60	Bunsi

[a]Aggressiveness was rated on the Modified Petzoldt and Dickson scale of 1–9 (Terán et al. 2006). A moderately resistant dry bean cultivar, G122, was used for evaluation.

[b] MCG: Mycelial Compatibility Group.

[c] Host cultivar of common bean (*Phaseolus vulgaris*) from which these strains were collected.

Table 4.2. Percentage (mean and standard errors) of point mutations (SNPs[a] and INDELs[b]) accumulated across control strains in two experiments.

Strain	Coding region (%)	SNP[a] (%)	Transition (%)
152	63.89 ± 13.89	80.56 ± 2.78	75.71 ± 4.29
467	83.33 ± 16.67	84.52 ± 1.19	55.0 ± 5.00
555	38.83 ± 0.19	76.69 ± 6.24	78.42 ± 1.00
594	34.44 ± 12.22	60.74 ± 12.6	80.94 ± 0.67
646	27.08 ± 2.08	62.5 ± 4.17	74.11 ± 11.61

[a]SNP: Single Nucleotide Polymorphisms.
[b]INDEL: INsertions/DELetions.

Table 4.3. Complete or partial aneuploidy of chromosome 7 in progenitor and derived (control and fungicide exposed) strains.

Strain	Treatment	Experiment	Duplication of chromosome 7	Aneuploidy of chromosome 7
152	Progenitor	-	95.80%	Complete
	Control	2	48%	Partial
	Azoxystrobin	2	96.27%	Complete
	Boscalid	2	95.96%	Complete
467	Azoxystrobin	2	98.24%	Complete
	Thiophanate-methyl	2	97.17%	Complete
555	Control	2	59.60%	Partial
	Iprodione	2	59.13%	Partial
	Thiophanate-methyl	2	71.60%	Partial
594	Control	2	91.79%	Complete
	Thiophanate-methyl	2	92.24%	Complete

Table 4.4. Mutational hotspots identified in genomic backgrounds of five different *S. sclerotiorum* strains after repeated subculturing on Potato Dextrose Agar for 12 generations.

Strain(s)	Chrom-osome	Genome Co-ordinates		Hotspot Size (bp)	Gene(s) in Hotspot	No. of mutations
		Start	End			
152	15	1757488	1759192	1704	sscle_15g107310	10
467						9
555	4	540247	542175	1928	sscle_04g033580; sscle_04g033590	10
		565606	566820	1214	sscle_04g033700; sscle_04g033710	9
555	11	140120	141807	1687	sscle_11g081330	7
		238200	239741	1541	sscle_11g081640	4
555	11	396918	399508	2590	–	9
594						6
646						8
594	12	1076943	1078608	1665	sscle_12g089740	10

Table 4.5. Conserved domains in genes that mutated in fungicide exposed strains in two experiments.

Chromosome	Gene	Strain	Fungicide	Experiment	Conserved Domains in Gene		
					Accession	Short Name	Superfamily
1	sscle_01g001300	594	Thiophanate-methyl	2	cd08249	enoyl_reductase_like	cl16912
	sscle_01g010430	152	Boscalid	1	–	–	–
	sscle_01g010540	594	Boscalid	1	–	–	–
			Thiophanate-methyl	1			
	sscle_01g010950	467	Azoxystrobin	1	COG0659; cd00038	SUL1; CAP_ED	cl33996; cl00047
2	sscle_02g013430	646	Azoxystrobin	2	cl14782; cl06662	RNase_H_like superfamily; RVT_2 superfamily	-
	sscle_02g016630	594	Iprodione	2	cl33182	PTZ00424 superfamily	-
			Thiophanate-methyl	2			
	sscle_02g017910	594	Thiophanate-methyl	2	pfam02668	TauD	cl00184
		646	Azoxystrobin	2			
	sscle_02g021470	594	Boscalid	1	cd04813; cd16454; cl34953	PA_1; RING-H2_PA-TM-RING; HRD1 superfamily	cl28883; cl17238; -
			Thiophanate-methyl	1			

7	sscle_07g061360	555	Thiophanate-methyl	1	cl29593	WD40 superfamily	-
8	sscle_08g062700	555	Thiophanate-methyl	1	–	–	–
			Boscalid	2			
			Iprodione	2			
	sscle_08g068510	555	Azoxystrobin	2	cl21454	NADB_Rossmann superfamily	-
9	sscle_09g074430	555	Iprodione	2	–	–	–
11	sscle_11g081320	555	Boscalid	1	–	–	–
			Iprodione	1			
			Thiophanate-methyl	1			
			Thiophanate-methyl	2			
	sscle_11g084630	594	Boscalid	2	pfam11754	Velvet	cl13238
	sscle_11g086560	555	Iprodione	1	cl38111; cl33183	Atrophin-1 superfamily; PTZ00436 superfamily	-
12	sscle_12g088520	467	Azoxystrobin	1	–	–	–
	sscle_12g090170	555	Iprodione	1	–	–	–

	sscle_12g091290	646	Thiophanate-methyl	2	smart00516; smart01100	SEC14; CRAL_TRIO_N	cl15787; cl16919
13	sscle_13g095720	646	Azoxystrobin	2	pfam12340; pfam12359	DUF3638; DUF3645	cl13737; cl13755
14	sscle_14g101330	555	Iprodione	1	pfam05887; cl36455	Trypan_PARP; PRK14971 superfamily (DNA polymerase III subunit gamma/tau)	cl29137; -
			Thiophanate-methyl	1			
			Azoxystrobin	1			
			Iprodione	2			
			Thiophanate-methyl	2			
15	sscle_15g105730	152	Iprodione	1	cd01650; cd09276	RT_nLTR_like; Rnase_HI_RT_non_LTR	cl02808; cl14782

Table 4.6. Aggressiveness score (mean and standard errors) of control and fungicide exposed strains in two experiments.

Strain	Treatment	Experiment	Aggressiveness Score[a] (Mean and Standard Error)
152	Progenitor	-	4.25 ± 0.16
	Control	1	4.88 ± 0.35
		2	4.38 ± 0.32
	Azoxystrobin	1	4.57 ± 0.30
		2	5.00 ± 0.33
	Boscalid	1	4.50 ± 0.53
		2	4.88 ± 0.30
	Iprodione	1	4.86 ± 0.40
		2	4.63 ± 0.38
	Thiophanate-methyl	1	4.57 ± 0.37
		2	4.38 ± 0.38
467	Progenitor	-	4.63 ± 0.26
	Control	1	5.25 ± 0.31
		2	4.88 ± 0.30
	Azoxystrobin	1	5.13 ± 0.40
		2	4.75 ± 0.49
	Boscalid	1	5.13 ± 0.40
		2	4.50 ± 0.33
	Iprodione	2	5.00 ± 0.44
	Thiophanate-methyl	1	5.13 ± 0.30
		2	4.75 ± 0.37
555	Progenitor	-	5.38 ± 0.26
	Control	1	4.63 ± 0.26
		2	4.75 ± 0.37
	Azoxystrobin	1	5.50 ± 0.19
		2	6.00 ± 0.50
	Boscalid	1	5.13 ± 0.61
		2	6.00 ± 0.19
	Iprodione	1	5.43 ± 0.30
		2	3.38* ± 0.56
	Thiophanate-methyl	1	5.88 ± 0.35
		2	4.75 ± 0.25
594	Progenitor	-	4.57 ± 0.30
	Control	1	4.75 ± 0.41
		2	4.38 ± 0.32
	Azoxystrobin	1	5.13 ± 0.23

		2	5.00 ± 0.38
	Boscalid	1	4.57 ± 0.43
	Iprodione	1	5.75 ± 0.56
		2	5.00 ± 0.38
	Thiophanate-methyl	1	4.50 ± 0.33
		2	4.38 ± 0.38
646	Progenitor	-	4.63 ± 0.53
	Control	1	5.25 ± 0.41
		2	5.43 ± 0.72
	Azoxystrobin	1	5.00 ± 0.22
		2	5.29 ± 0.29
	Boscalid	1	5.71 ± 0.36
		2	5.13 ± 0.30
	Iprodione	1	5.50 ± 0.19
		2	5.63 ± 0.32
	Thiophanate-methyl	1	4.63 ± 0.38
		2	4.88 ± 0.30

[a]Aggressiveness was rated on the Modified Petzoldt and Dickson scale of 1–9 (Terán et al. 2006). A moderately resistant dry bean cultivar, G122, was used for evaluation.
* $P \leq 0.05$ compared to progenitor.

Table 4.7. Predicted effectors from *de novo* assembly of genomes of progenitor strains.

ID	Query	Hit Type	E-Value	Accession	Short Name	Characterization Method
152	>g1628.t1	superfamily	0.00012121	cl06331	Cerato-platanin superfamily	EffectorP
	>g2071.t1	specific	1.17E-52	pfam06172	Cupin_5	EffectorP
	>g2071.t1	specific	2.77E-48	cd06121	cupin_YML079wp	EffectorP
	>g2071.t1	specific	8.53E-42	COG3542	CFF1	EffectorP
	>g3221.t1	specific	1.68E-10	COG0724	RRM	EffectorP
	>g3221.t1	specific	1.23E-08	smart00360	RRM	EffectorP
	>g3221.t1	specific	4.19E-06	pfam00076	RRM_1	EffectorP
	>g4133.t1	superfamily	0.0006351	cl07470	CVNH superfamily	EffectorP
	>g5086.t1	specific	1.03E-46	cd00917	PG-PI_TP	EffectorP
	>g5086.t1	specific	3.52E-27	pfam02221	E1_DerP2_DerF2	EffectorP
	>g5086.t1	specific	8.63E-19	smart00737	ML	EffectorP
	>g6515.t1	specific	1.12E-07	pfam03330	DPBB_1	EffectorP
	>g6571.t1	specific	1.73E-88	pfam05630	NPP1	EffectorP
	>g8007.t1	specific	1.73E-59	pfam01105	EMP24_GP25L	EffectorP
	>g9228.t1	superfamily	3.21E-91	cl08270	Peptidase_S10 superfamily	Manual
	>g9296.t1	specific	3.10E-09	pfam05730	CFEM	Manual
	>g9478.t1	superfamily	2.43E-72	cl08270	Peptidase_S10 superfamily	Manual
	>g93.t1	specific	4.22E-66	cd01061	RNase_T2_euk	Manual
	>g93.t1	specific	4.03E-59	pfam00445	Ribonuclease_T2	Manual
	>g471.t1	specific	3.61E-157	cd02181	GH16_fungal_Lam16A_glucanase	Manual
	>g2032.t1	specific	4.94E-62	pfam00326	Peptidase_S9	Manual
	>g2085.t1	specific	1.30E-80	pfam05630	NPP1	Manual
	>g2124.t1	superfamily	6.06E-108	cl08270	Peptidase_S10 superfamily	Manual
	>g2182.t1	specific	5.39E-05	pfam00187	Chitin_bind_1	Manual
	>g3271.t1	specific	4.23E-33	cd01831	Endoglucanase_E_like	Manual
	>g3271.t1	specific	1.01E-09	pfam13472	Lipase_GDSL_2	Manual

>g3339.t1	specific	8.12E-07	pfam00657	Lipase_GDSL	Manual
>g3477.t1	specific	6.55E-09	pfam05730	CFEM	Manual
>g3523.t1	specific	4.64E-47	pfam01328	Peroxidase_2	Manual
>g3636.t1	specific	2.03E-47	pfam00445	Ribonuclease_T2	Manual
>g3636.t1	specific	2.37E-47	cd01061	RNase_T2_euk	Manual
>g3693.t1	specific	1.20E-14	pfam00187	Chitin_bind_1	Manual
>g3693.t1	specific	0.00253248	pfam00187	Chitin_bind_1	Manual
>g3694.t1	specific	6.54E-05	cd00118	LysM	Manual
>g3694.t1	specific	0.00011021	cd00118	LysM	Manual
>g3694.t1	specific	0.00466543	smart00257	LysM	Manual
>g3816.t1	specific	1.41E-118	cd02181	GH16_fungal_Lam16A_glucanase	Manual
>g4105.t1	specific	7.16E-127	cd04056	Peptidases_S53	Manual
>g4105.t1	specific	1.80E-37	cd11377	Pro-peptidase_S53	Manual
>g4417.t1	specific	1.32E-117	cd04077	Peptidases_S8_PCSK9_ProteinaseK_like	Manual
>g4417.t1	specific	2.77E-38	pfam00082	Peptidase_S8	Manual
>g4417.t1	specific	2.42E-06	pfam05922	Inhibitor_I9	Manual
>g5051.t1	specific	0.00223629	smart00257	LysM	Manual
>g5051.t1	specific	0.00948703	cd00118	LysM	Manual
>g5445.t1	specific	1.38E-150	cd02181	GH16_fungal_Lam16A_glucanase	Manual
>g6183.t1	superfamily	3.06E-19	cl10459	Peptidases_S8_S53 superfamily	Manual
>g6376.t1	specific	1.42E-162	cd02181	GH16_fungal_Lam16A_glucanase	Manual
>g6870.t1	specific	1.47E-11	pfam05730	CFEM	Manual
>g7062.t1	specific	1.11E-06	pfam05730	CFEM	Manual
>g7338.t1	specific	0.00145407	pfam00187	Chitin_bind_1	Manual
>g7338.t1	specific	0.00240685	pfam00187	Chitin_bind_1	Manual
>g7338.t1	specific	0.00895404	pfam00187	Chitin_bind_1	Manual
>g7428.t1	specific	1.48E-11	pfam13472	Lipase_GDSL_2	Manual
>g8017.t1	specific	4.02E-32	cd05380	CAP_euk	Manual
>g9097.t1	none	NA	NA	NA	EffectorP

	>g9135.t1	none	NA	NA	NA	EffectorP
	>g55.t1	none	NA	NA	NA	EffectorP
	>g596.t1	none	NA	NA	NA	EffectorP
	>g632.t1	none	NA	NA	NA	EffectorP
	>g1270.t1	none	NA	NA	NA	EffectorP
	>g1333.t1	none	NA	NA	NA	EffectorP
	>g1342.t1	none	NA	NA	NA	EffectorP
	>g1658.t1	none	NA	NA	NA	EffectorP
	>g3177.t1	none	NA	NA	NA	EffectorP
	>g3602.t1	none	NA	NA	NA	EffectorP
	>g3656.t1	none	NA	NA	NA	EffectorP
	>g4117.t1	none	NA	NA	NA	EffectorP
	>g5769.t1	none	NA	NA	NA	EffectorP
	>g6911.t1	none	NA	NA	NA	EffectorP
	>g6912.t1	none	NA	NA	NA	EffectorP
	>g7186.t1	none	NA	NA	NA	EffectorP
	>g7910.t1	none	NA	NA	NA	EffectorP
	>g8047.t1	none	NA	NA	NA	EffectorP
467	>g7744.t1	specific	6.53E-103	cd06903	lectin_EMP46_EMP47	EffectorP
	>g9012.t1	specific	4.02E-32	cd05380	CAP_euk	Manual
	>g9260.t1	superfamily	3.21E-91	cl08270	Peptidase_S10 superfamily	Manual
	>g9487.t1	specific	0.00115774	pfam00187	Chitin_bind_1	Manual
	>g9487.t1	specific	0.00191619	pfam00187	Chitin_bind_1	Manual
	>g9487.t1	specific	0.00734129	pfam00187	Chitin_bind_1	Manual
	>g79.t1	specific	1.30E-80	pfam05630	NPP1	Manual
	>g210.t1	specific	1.32E-117	cd04077	Peptidases_S8_PCSK9_ProteinaseK_like	Manual
	>g210.t1	specific	2.42E-06	pfam05922	Inhibitor_I9	Manual
	>g435.t1	specific	7.16E-127	cd04056	Peptidases_S53	Manual
	>g507.t1	superfamily	2.43E-72	cl08270	Peptidase_S10 superfamily	Manual

>g1137.t1	specific	1.38E-150	cd02181	GH16_fungal_Lam16A_glucanase	Manual
>g1309.t1	specific	4.22E-66	cd01061	RNase_T2_euk	Manual
>g1924.t1	specific	3.61E-157	cd02181	GH16_fungal_Lam16A_glucanase	Manual
>g2222.t1	superfamily	6.06E-108	cl08270	Peptidase_S10 superfamily	Manual
>g3350.t1	specific	6.55E-09	pfam05730	CFEM	Manual
>g3380.t1	specific	4.64E-47	pfam01328	Peroxidase_2	Manual
>g3558.t1	specific	1.20E-14	pfam00187	Chitin_bind_1	Manual
>g3559.t1	specific	6.54E-05	cd00118	LysM	Manual
>g3559.t1	specific	0.00011021	cd00118	LysM	Manual
>g3822.t1	specific	0.00223629	smart00257	LysM	Manual
>g3823.t1	specific	1.18E-09	pfam00187	Chitin_bind_1	Manual
>g4417.t1	specific	1.41E-118	cd02181	GH16_fungal_Lam16A_glucanase	Manual
>g4478.t1	specific	1.42E-162	cd02181	GH16_fungal_Lam16A_glucanase	Manual
>g5480.t1	specific	3.10E-09	pfam05730	CFEM	Manual
>g6413.t1	superfamily	3.06E-19	cl10459	Peptidases_S8_S53 superfamily	Manual
>g7321.t1	specific	2.03E-47	pfam00445	Ribonuclease_T2	Manual
>g7822.t1	specific	4.23E-33	cd01831	Endoglucanase_E_like	Manual
>g8523.t1	specific	1.47E-11	pfam05730	CFEM	Manual
>g8840.t1	specific	1.11E-06	pfam05730	CFEM	Manual
>g9022.t1	none	NA	NA	NA	EffectorP
>g9395.t1	none	NA	NA	NA	EffectorP
>g9396.t1	none	NA	NA	NA	EffectorP
>g668.t1	none	NA	NA	NA	EffectorP
>g1400.t1	none	NA	NA	NA	EffectorP
>g2162.t1	none	NA	NA	NA	EffectorP
>g2694.t1	none	NA	NA	NA	EffectorP
>g2835.t1	none	NA	NA	NA	EffectorP
>g2844.t1	none	NA	NA	NA	EffectorP
>g3131.t1	none	NA	NA	NA	EffectorP

	>g3802.t1	none	NA	NA	NA	EffectorP
	>g3962.t1	none	NA	NA	NA	EffectorP
	>g4060.t1	none	NA	NA	NA	EffectorP
	>g4084.t1	none	NA	NA	NA	EffectorP
	>g4223.t1	none	NA	NA	NA	EffectorP
	>g4381.t1	none	NA	NA	NA	EffectorP
	>g5307.t1	none	NA	NA	NA	EffectorP
	>g5576.t1	none	NA	NA	NA	EffectorP
	>g5736.t1	none	NA	NA	NA	EffectorP
	>g5981.t1	none	NA	NA	NA	EffectorP
	>g6317.t1	none	NA	NA	NA	EffectorP
	>g6382.t1	none	NA	NA	NA	EffectorP
	>g6468.t1	none	NA	NA	NA	EffectorP
	>g6530.t1	none	NA	NA	NA	EffectorP
	>g6741.t1	none	NA	NA	NA	EffectorP
	>g7945.t1	none	NA	NA	NA	EffectorP
	>g8057.t1	none	NA	NA	NA	EffectorP
555	>g9080.t1	specific	4.22E-66	cd01061	RNase_T2_euk	Manual
	>g751.t1	superfamily	1.38E-107	cl08270	Peptidase_S10 superfamily	Manual
	>g1374.t1	specific	1.38E-150	cd02181	GH16_fungal_Lam16A_glucanase	Manual
	>g1927.t1	specific	4.23E-33	cd01831	Endoglucanase_E_like	Manual
	>g2534.t1	specific	4.64E-47	pfam01328	Peroxidase_2	Manual
	>g2590.t1	specific	1.47E-11	pfam05730	CFEM	Manual
	>g3674.t1	specific	3.10E-09	pfam05730	CFEM	Manual
	>g4397.t1	specific	6.61E-05	cd00118	LysM	Manual
	>g4397.t1	specific	0.00011021	cd00118	LysM	Manual
	>g4398.t1	specific	1.22E-14	pfam00187	Chitin_bind_1	Manual
	>g4577.t1	specific	4.34E-157	cd02181	GH16_fungal_Lam16A_glucanase	Manual
	>g5577.t1	superfamily	3.21E-91	cl08270	Peptidase_S10 superfamily	Manual

>g5991.t1	specific	4.04E-06	pfam05922	Inhibitor_I9	Manual
>g6050.t1	specific	1.57E-116	cd04056	Peptidases_S53	Manual
>g6485.t1	specific	0.00223629	smart00257	LysM	Manual
>g7318.t1	specific	1.22E-79	pfam05630	NPP1	Manual
>g7478.t1	specific	1.42E-162	cd02181	GH16_fungal_Lam16A_glucanase	Manual
>g7774.t1	specific	1.41E-118	cd02181	GH16_fungal_Lam16A_glucanase	Manual
>g8054.t1	specific	6.55E-09	pfam05730	CFEM	Manual
>g8187.t1	superfamily	2.51E-72	cl08270	Peptidase_S10 superfamily	Manual
>g8201.t1	specific	4.02E-32	cd05380	CAP_euk	Manual
>g8261.t1	specific	5.06E-46	pfam00445	Ribonuclease_T2	Manual
>g8405.t1	specific	1.11E-06	pfam05730	CFEM	Manual
>g8990.t1	specific	0.00115774	pfam00187	Chitin_bind_1	Manual
>g8990.t1	specific	0.00191619	pfam00187	Chitin_bind_1	Manual
>g8990.t1	specific	0.00734129	pfam00187	Chitin_bind_1	Manual
>g9433.t1	none	NA	NA	NA	EffectorP
>g162.t1	none	NA	NA	NA	EffectorP
>g329.t1	none	NA	NA	NA	EffectorP
>g842.t1	none	NA	NA	NA	EffectorP
>g856.t1	none	NA	NA	NA	EffectorP
>g1023.t1	none	NA	NA	NA	EffectorP
>g1684.t1	none	NA	NA	NA	EffectorP
>g1714.t1	none	NA	NA	NA	EffectorP
>g1742.t1	none	NA	NA	NA	EffectorP
>g1821.t1	none	NA	NA	NA	EffectorP
>g2158.t1	none	NA	NA	NA	EffectorP
>g3335.t1	none	NA	NA	NA	EffectorP
>g3935.t1	none	NA	NA	NA	EffectorP
>g4507.t1	none	NA	NA	NA	EffectorP
>g4570.t1	none	NA	NA	NA	EffectorP

	>g4862.t1	none	NA	NA	NA	EffectorP
	>g4863.t1	none	NA	NA	NA	EffectorP
	>g5115.t1	none	NA	NA	NA	EffectorP
	>g5228.t1	none	NA	NA	NA	EffectorP
	>g5629.t1	none	NA	NA	NA	EffectorP
	>g5769.t1	none	NA	NA	NA	EffectorP
	>g5936.t1	none	NA	NA	NA	EffectorP
	>g6647.t1	none	NA	NA	NA	EffectorP
	>g6994.t1	none	NA	NA	NA	EffectorP
	>g7013.t1	none	NA	NA	NA	EffectorP
	>g7292.t1	none	NA	NA	NA	EffectorP
	>g8191.t1	none	NA	NA	NA	EffectorP
594	>g9427.t1	specific	1.11E-06	pfam05730	CFEM	Manual
	>g9561.t1	specific	3.07E-09	pfam05730	CFEM	Manual
	>g294.t1	specific	4.22E-66	cd01061	RNase_T2_euk	Manual
	>g1366.t1	specific	1.18E-156	cd02181	GH16_fungal_Lam16A_glucanase	Manual
	>g2474.t1	specific	1.93E-161	cd02181	GH16_fungal_Lam16A_glucanase	Manual
	>g2520.t1	specific	1.38E-150	cd02181	GH16_fungal_Lam16A_glucanase	Manual
	>g2528.t1	superfamily	1.38E-107	cl08270	Peptidase_S10 superfamily	Manual
	>g2642.t1	specific	6.55E-09	pfam05730	CFEM	Manual
	>g3294.t1	specific	4.23E-33	cd01831	Endoglucanase_E_like	Manual
	>g3449.t1	specific	1.30E-80	pfam05630	NPP1	Manual
	>g3844.t1	specific	1.32E-117	cd04077	Peptidases_S8_PCSK9_ProteinaseK_like	Manual
	>g3844.t1	specific	2.42E-06	pfam05922	Inhibitor_I9	Manual
	>g4019.t1	specific	4.64E-47	pfam01328	Peroxidase_2	Manual
	>g4267.t1	specific	1.24E-14	pfam00187	Chitin_bind_1	Manual
	>g4268.t1	specific	6.61E-05	cd00118	LysM	Manual
	>g4268.t1	specific	7.97E-05	cd00118	LysM	Manual
	>g5368.t1	superfamily	3.21E-91	cl08270	Peptidase_S10 superfamily	Manual

>g7234.t1	specific	1.41E-118	cd02181	GH16_fungal_Lam16A_glucanase	Manual
>g7282.t1	superfamily	2.43E-72	cl08270	Peptidase_S10 superfamily	Manual
>g7439.t1	specific	1.42E-47	pfam00445	Ribonuclease_T2	Manual
>g7707.t1	specific	0.00223629	smart00257	LysM	Manual
>g8069.t1	specific	1.13E-11	pfam05730	CFEM	Manual
>g8306.t1	specific	4.02E-32	cd05380	CAP_euk	Manual
>g9508.t1	none	NA	NA	NA	EffectorP
>g391.t1	none	NA	NA	NA	EffectorP
>g634.t1	none	NA	NA	NA	EffectorP
>g745.t1	none	NA	NA	NA	EffectorP
>g859.t1	none	NA	NA	NA	EffectorP
>g1048.t1	none	NA	NA	NA	EffectorP
>g1325.t1	none	NA	NA	NA	EffectorP
>g1535.t1	none	NA	NA	NA	EffectorP
>g1876.t1	none	NA	NA	NA	EffectorP
>g1920.t1	none	NA	NA	NA	EffectorP
>g2101.t1	none	NA	NA	NA	EffectorP
>g2309.t1	none	NA	NA	NA	EffectorP
>g2423.t1	none	NA	NA	NA	EffectorP
>g2893.t1	none	NA	NA	NA	EffectorP
>g3168.t1	none	NA	NA	NA	EffectorP
>g3663.t1	none	NA	NA	NA	EffectorP
>g4125.t1	none	NA	NA	NA	EffectorP
>g4399.t1	none	NA	NA	NA	EffectorP
>g4400.t1	none	NA	NA	NA	EffectorP
>g4513.t1	none	NA	NA	NA	EffectorP
>g6604.t1	none	NA	NA	NA	EffectorP
>g6732.t1	none	NA	NA	NA	EffectorP
>g7057.t1	none	NA	NA	NA	EffectorP

	>g7177.t1	none	NA	NA	NA	EffectorP
	>g7293.t1	none	NA	NA	NA	EffectorP
	>g7353.t1	none	NA	NA	NA	EffectorP
	>g7479.t1	none	NA	NA	NA	EffectorP
	>g8296.t1	none	NA	NA	NA	EffectorP
	>g8440.t1	none	NA	NA	NA	EffectorP
646	>g9212.t1	specific	1.62E-06	pfam05730	CFEM	Manual
	>g289.t1	specific	0.00223629	smart00257	LysM	Manual
	>g290.t1	specific	1.24E-09	pfam00187	Chitin_bind_1	Manual
	>g1160.t1	specific	1.13E-162	cd02181	GH16_fungal_Lam16A_glucanase	Manual
	>g2521.t1	specific	7.16E-127	cd04056	Peptidases_S53	Manual
	>g2539.t1	specific	4.22E-66	cd01061	RNase_T2_euk	Manual
	>g2991.t1	specific	3.61E-157	cd02181	GH16_fungal_Lam16A_glucanase	Manual
	>g3054.t1	superfamily	1.38E-107	cl08270	Peptidase_S10 superfamily	Manual
	>g3929.t1	superfamily	2.43E-72	cl08270	Peptidase_S10 superfamily	Manual
	>g4036.t1	specific	1.41E-118	cd02181	GH16_fungal_Lam16A_glucanase	Manual
	>g4050.t1	specific	4.64E-47	pfam01328	Peroxidase_2	Manual
	>g4476.t1	superfamily	3.21E-91	cl08270	Peptidase_S10 superfamily	Manual
	>g4739.t1	specific	1.47E-11	pfam05730	CFEM	Manual
	>g5269.t1	specific	3.10E-09	pfam05730	CFEM	Manual
	>g5286.t1	specific	6.55E-09	pfam05730	CFEM	Manual
	>g6085.t1	specific	4.02E-32	cd05380	CAP_euk	Manual
	>g6760.t1	specific	6.34E-05	cd00118	LysM	Manual
	>g6760.t1	specific	0.00010564	cd00118	LysM	Manual
	>g6761.t1	specific	1.20E-14	pfam00187	Chitin_bind_1	Manual
	>g7465.t1	specific	1.38E-150	cd02181	GH16_fungal_Lam16A_glucanase	Manual
	>g8015.t1	specific	0.00115774	pfam00187	Chitin_bind_1	Manual
	>g8015.t1	specific	0.00191619	pfam00187	Chitin_bind_1	Manual
	>g8015.t1	specific	0.00734129	pfam00187	Chitin_bind_1	Manual

>g8221.t1	specific	4.23E-33	cd01831	Endoglucanase_E_like	Manual
>g8754.t1	specific	1.32E-117	cd04077	Peptidases_S8_PCSK9_ProteinaseK_like	Manual
>g8754.t1	specific	2.42E-06	pfam05922	Inhibitor_I9	Manual
>g8855.t1	specific	1.30E-80	pfam05630	NPP1	Manual
>g9038.t1	none	NA	NA	NA	EffectorP
>g261.t1	none	NA	NA	NA	EffectorP
>g1051.t1	none	NA	NA	NA	EffectorP
>g1653.t1	none	NA	NA	NA	EffectorP
>g1832.t1	none	NA	NA	NA	EffectorP
>g2563.t1	none	NA	NA	NA	EffectorP
>g2650.t1	none	NA	NA	NA	EffectorP
>g2679.t1	none	NA	NA	NA	EffectorP
>g2733.t1	none	NA	NA	NA	EffectorP
>g3699.t1	none	NA	NA	NA	EffectorP
>g4294.t1	none	NA	NA	NA	EffectorP
>g4335.t1	none	NA	NA	NA	EffectorP
>g4532.t1	none	NA	NA	NA	EffectorP
>g4544.t1	none	NA	NA	NA	EffectorP
>g4853.t1	none	NA	NA	NA	EffectorP
>g5208.t1	none	NA	NA	NA	EffectorP
>g5347.t1	none	NA	NA	NA	EffectorP
>g5641.t1	none	NA	NA	NA	EffectorP
>g6130.t1	none	NA	NA	NA	EffectorP
>g6801.t1	none	NA	NA	NA	EffectorP
>g6815.t1	none	NA	NA	NA	EffectorP
>g7221.t1	none	NA	NA	NA	EffectorP
>g7324.t1	none	NA	NA	NA	EffectorP
>g7813.t1	none	NA	NA	NA	EffectorP
>g7933.t1	none	NA	NA	NA	EffectorP

>g7979.t1	none	NA	NA	NA	EffectorP
>g8962.t1	none	NA	NA	NA	EffectorP
>g8963.t1	none	NA	NA	NA	EffectorP

Table 4.8. Putative effectors from the five progenitor strains that were unique to each strain.

Strain	Query	Hit.type	E.Value	Accession	CDD short name	Method
152	g2032.t1	specific	4.94E-62	pfam00326	Peptidase_S9	Manual
	g2182.t1	specific	5.39E-05	pfam00187	Chitin_bind_1	Manual
	g3339.t1	specific	8.12E-07	pfam00657	Lipase_GDSL	Manual
	g7428.t1	specific	1.48E-11	pfam13472	Lipase_GDSL_2	Manual
467	g2694.t1	none	NA	NA	NA	EffectorP
555	g6050.t1	specific	1.57E-116	cd04056	Peptidases_S53	Manual
	g9433.t1	none	NA	NA	NA	EffectorP
	g2158.t1	none	NA	NA	NA	EffectorP
594	g9508.t1	none	NA	NA	NA	EffectorP
	g3663.t1	none	NA	NA	NA	EffectorP
	g7293.t1	none	NA	NA	NA	EffectorP
646	g7221.t1	none	NA	NA	NA	EffectorP

Table 4.9. Effector candidates from the reference genome that matched the putative effectors from other progenitors at E-value < 1 x 10^{-10} and percent identity >=85%

Reference Genome	ID 152	ID 467	ID 555	ID 594	ID 646
sscle_01g000660	g3177.t1	g4223.t1	g4570.t1	g7353.t1	g7324.t1
sscle_01g006330	g3221.t1	g3131.t1	g7013.t1	g859.t1	g1051.t1
sscle_01g008940	g6912.t1	g9395.t1	g4862.t1	g4399.t1	g8963.t1
sscle_01g008950	g6911.t1	g9396.t1	g4863.t1	g4400.t1	g8962.t1
sscle_04g035160	g1270.t1	g3962.t1	g5115.t1	g2893.t1	g4853.t1
sscle_04g039420	g6571.t1	g6741.t1	g4507.t1	g7177.t1	g9038.t1
sscle_06g050820	g1342.t1	g1400.t1	g1742.t1	g1535.t1	g1832.t1
sscle_06g055280	g5769.t1	g5981.t1	NA	NA	g7933.t1
sscle_07g061960	g5769.t1	g5981.t1	NA	NA	g7933.t1
sscle_08g064180	g1658.t1	g2835.t1	g5629.t1	g391.t1	g2650.t1
sscle_08g067710	g9135.t1	g6530.t1	g329.t1	g6604.t1	g4532.t1
sscle_08g068200	g7338.t1	g9487.t1	g8990.t1	g7479.t1	g8015.t1
sscle_11g084720	g5086.t1	g4381.t1	g1023.t1	g4125.t1	g6801.t1
sscle_12g087960	g8047.t1	g4060.t1	g3935.t1	g1048.t1	g1653.t1
sscle_13g094920	g8007.t1	g9022.t1	g8191.t1	g8296.t1	g6815.t1
sscle_13g097000	g5769.t1	g5981.t1	NA	NA	g7933.t1
sscle_14g098920	g6515.t1	g2844.t1	g7292.t1	g7057.t1	g6130.t1
sscle_14g100310	g1333.t1	g6317.t1	g1684.t1	g745.t1	g5641.t1
sscle_16g111300	g5769.t1	g5981.t1	NA	NA	g7933.t1
sscle_07g057000	NA	g2694.t1	NA	NA	NA
sscle_07g057000	NA	g2694.t1	NA	NA	NA
sscle_03g031910	NA	NA	g9433.t1	NA	NA
sscle_09g074030	NA	NA	g9433.t1	NA	NA
sscle_16g107730	NA	NA	g9433.t1	NA	NA
sscle_10g075140	NA	NA	NA	g9508.t1	NA

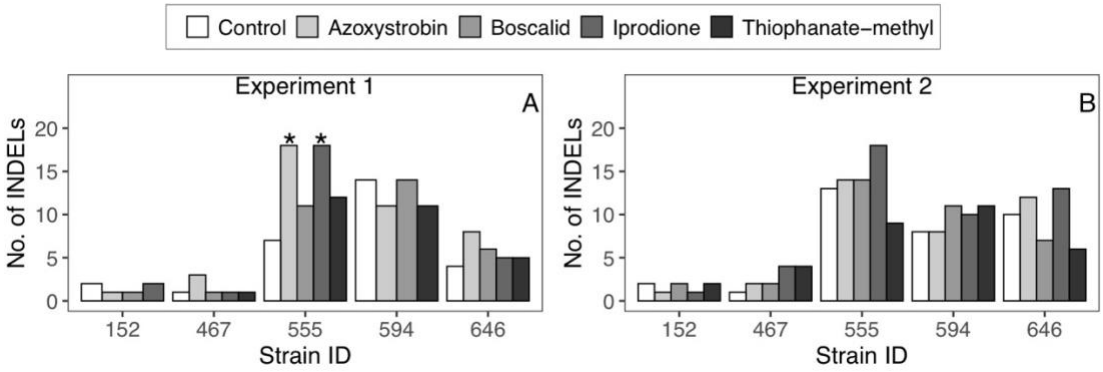

Fig. 4.1. INsertions/DELetions (INDELs) in control and fungicide exposed strains in **A**, first experiment and **B**, second experiment. Bars with asterisks are significantly different ($P \leq 0.05$) compared to the respective control within the strain and experiment. Strain 594 exposed to Iprodione in the first experiment was removed from the analysis because it was contaminated.

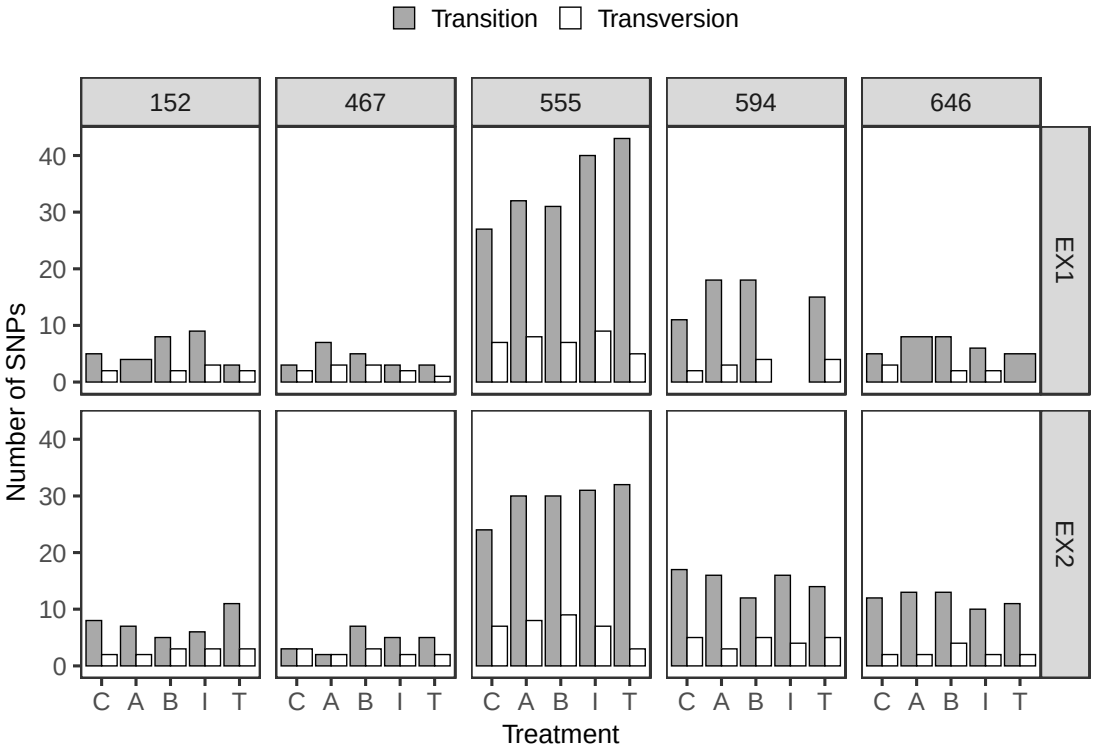

Fig. 4.2. Number of transitions and transversions in the control and fungicide exposed strains in two experiments. Treatment has Control (C), Azoxystrobin (A), Boscalid (B), Iprodione (I), Thiophanate-methyl (T).

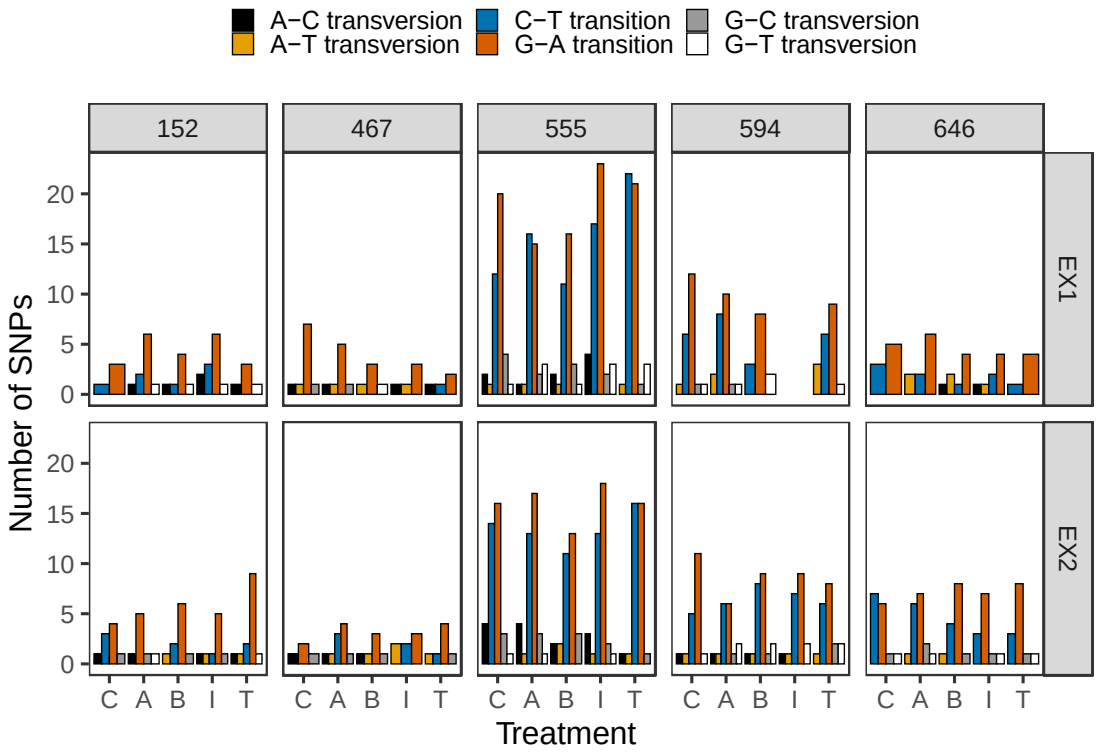

Fig. 4.3. Number of transition and transversion types in the control and fungicide exposed strains in two experiments. Treatment has Control (C), Azoxystrobin (A), Boscalid (B), Iprodione (I), Thiophanate-methyl (T).

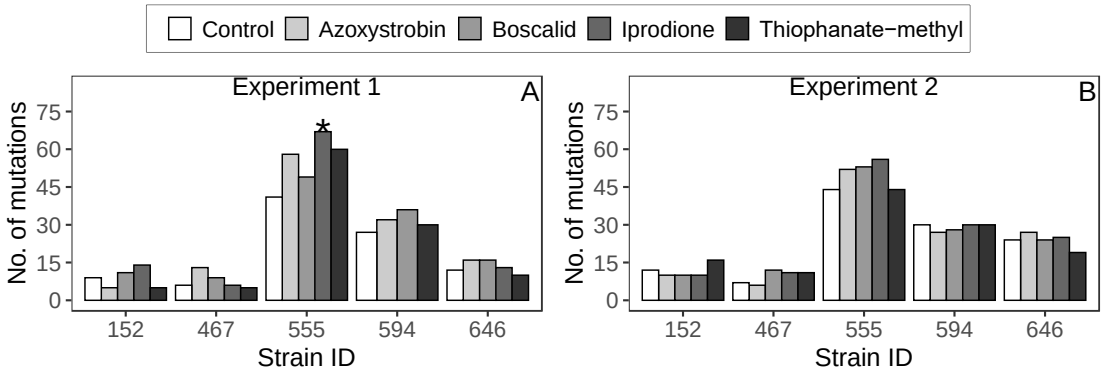

Fig. 4.4. Point mutations in control and fungicide exposed strains in **A**, first experiment and **B**, second experiment. Mutations shown here consist of Single Nucleotide Polymorphisms (SNPs) and INsertions/DELetions (INDELs). Bars with asterisks are significantly different ($P \leq 0.05$ Chi-square test) compared to the respective control within the strain and experiment. Strain 594 exposed to Iprodione in the first experiment was removed from the analysis because it was contaminated.

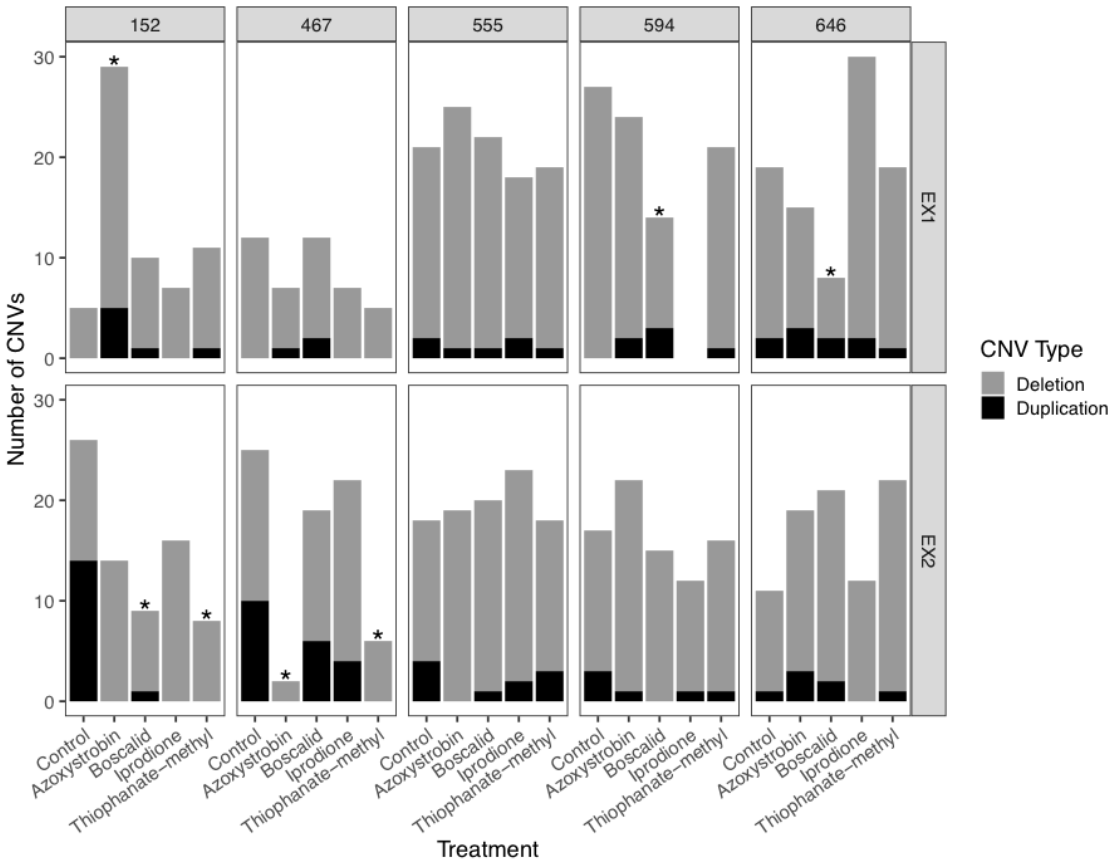

Fig. 4.5. Number of Copy Number Variants (CNVs) in control and fungicide exposed strains in two experiments. Since chromosome 7 had high propensity for duplications and aneuploidy, it was removed from the analysis. The asterisks represent a significant difference in the number of CNVs than the control ($P \leq 0.05$).

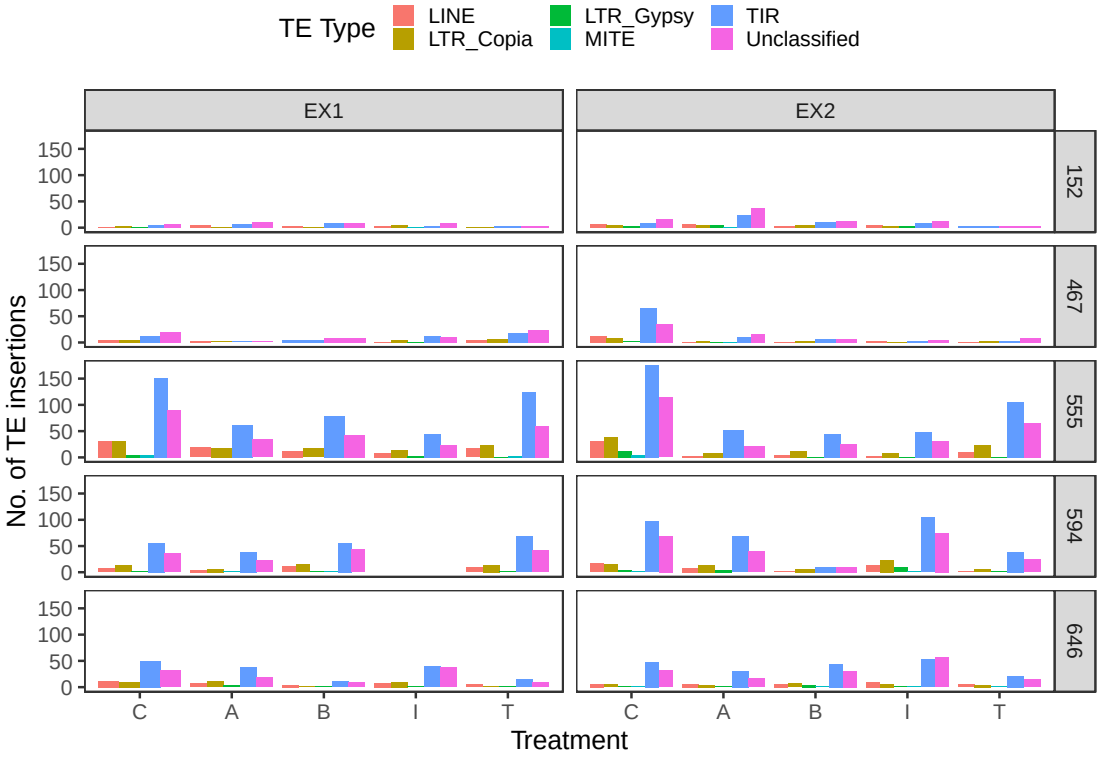

Fig. 4.6. Number of Transposable Element (TE) insertion types in the control and fungicide exposed strains in two experiments. TE insertions were classified as Long Interspersed Nuclear Element (LINE), Long Terminal Repeat (LTR: Copia and Gypsy), Miniature Inverted-repeat Transposable Element (MITE), Terminal Inverted Repeat (TIR) or were not clearly classified (Unclassified). Treatment has Control (C), Azoxystrobin (A), Boscalid (B), Iprodione (I), and Thiophanate-methyl (T).

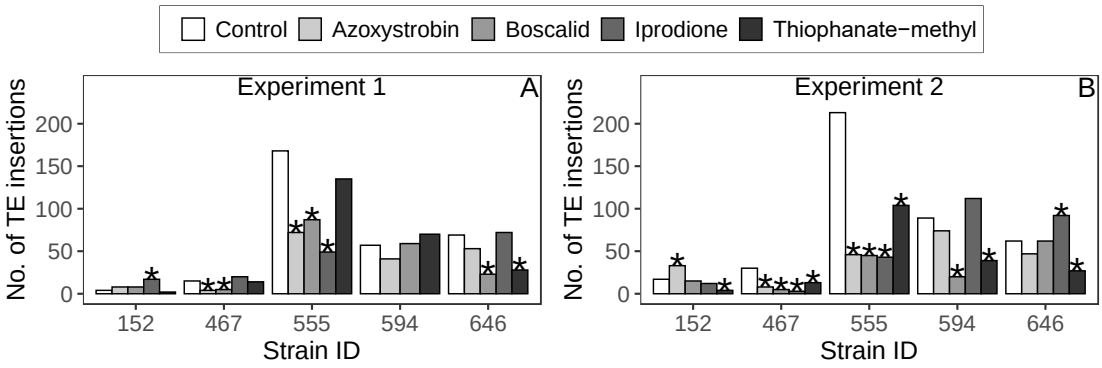

Fig. 4.7. Transposable Element (TE) insertions in control and fungicide exposed strains in **A,** first experiment and **B,** second experiment. Bars with asterisks are significantly different ($P \leq 0.05$ χ^2-test) compared to the respective control within the strain and experiment. Strain 594 exposed to Iprodione in the first experiment was removed from the analysis because it was contaminated.

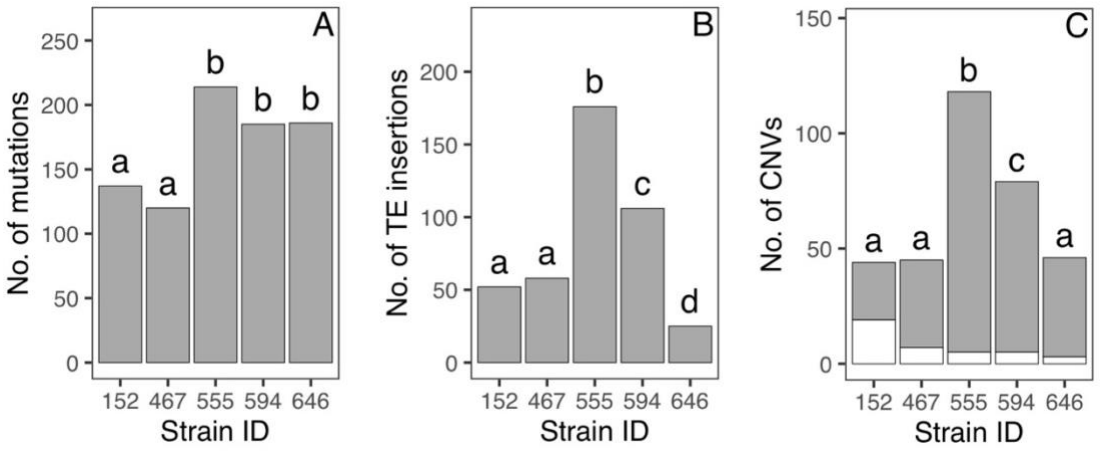

Fig. 4.8. Differences in the genomic background of progenitors as compared to the reference genome as characterized by **A,** Number of mutations, **B,** Number of Transposable Element (TE) insertions and **C,** Number of Copy Number Variants (CNVs). Mutations consist of Single Nucleotide Polymorphisms (SNPs) and INsertions/DELetions

(INDELs). The letter on top of each bar shows significant difference among strains ($P \leq 0.05$).

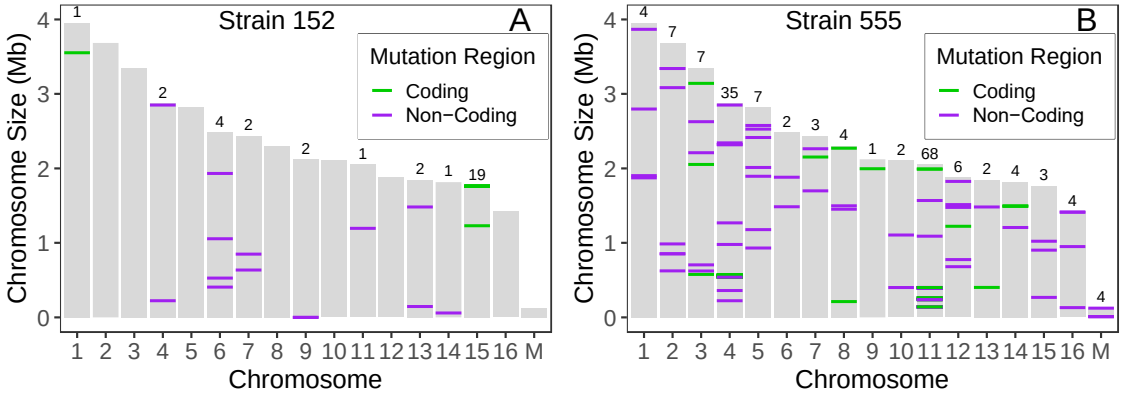

Fig. 4.9. Positions of loci with point mutations from all treatments and experiments represented along the length of 16 chromosomes of *S. sclerotiorum* and the mitochondrial genome represented by 'M' in **A,** strain 152 and **B,** strain 555. Mutated loci in coding (green) and non-coding (purple) regions are depicted as colored bands. To facilitate counting the overlapping loci, total number of mutated loci are given on top of each chromosome.

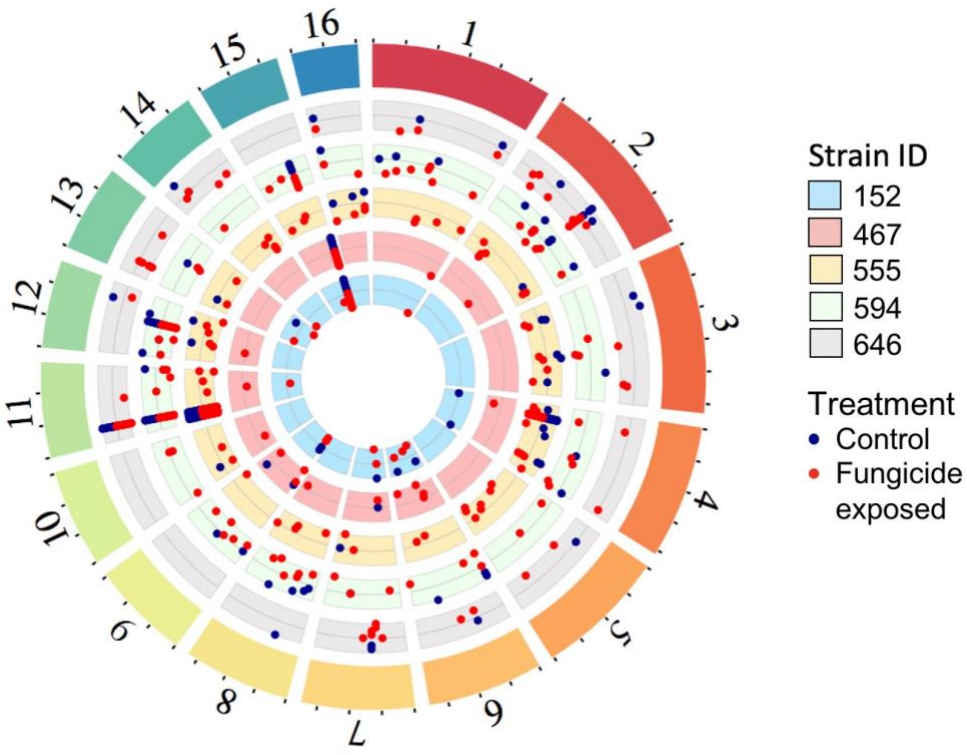

Fig. 4.10. Genomic distribution of point mutations in the control (dark blue) and the fungicide exposed strains (red) on the 16 chromosomes of *Sclerotinia sclerotiorum*. Starting from the innermost circular track, the five genomic backgrounds are represented by differently colored tracks; strain 152 (blue), 467 (pink), 555 (yellow), 594 (green), 646 (gray). For each genomic background, point mutations in two control strains and eight fungicide exposed strains are represented except for the genomic background of strain 594 where point mutations from seven fungicide exposed strains are represented.

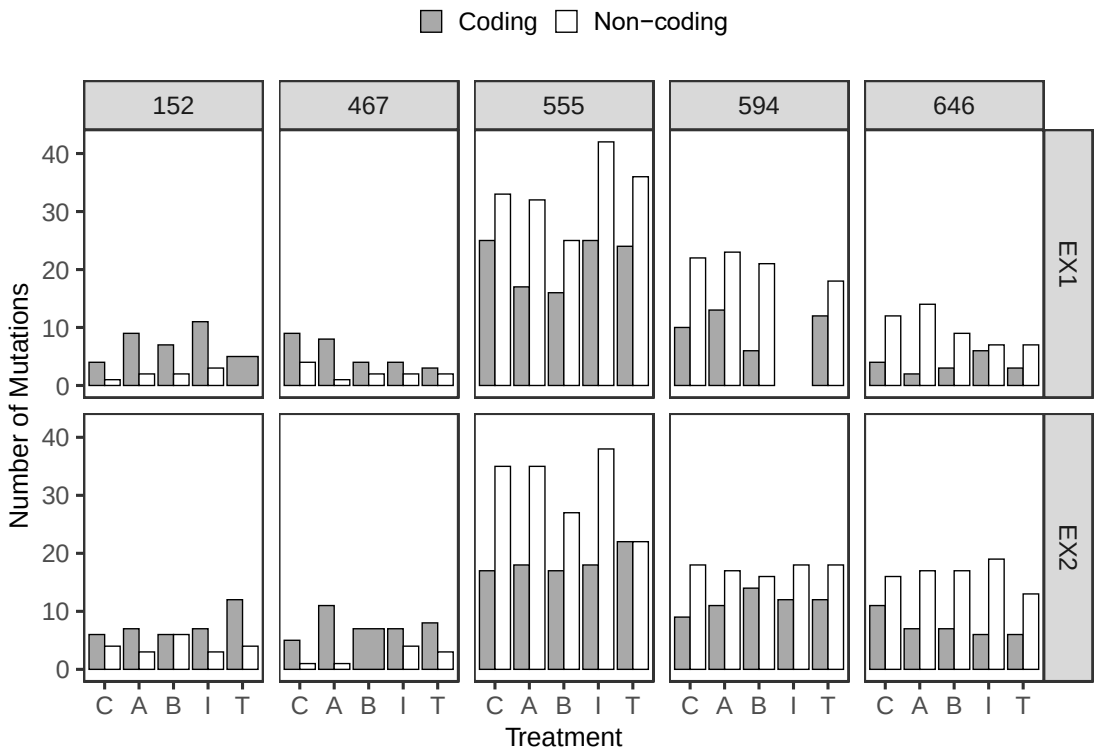

Fig. 4.11. Number of point mutations (SNPs and INDELs) in coding (genic) and non-coding (intergenic) regions of the control and fungicide exposed strains in two experiments. The number of mutations in the non-coding regions of strain 555 exposed to Iprodione in the first experiment were significantly higher than the control ($P \leq 0.05$). Treatment has Control (C), Azoxystrobin (A), Boscalid (B), Iprodione (I), Thiophanate-methyl (T).

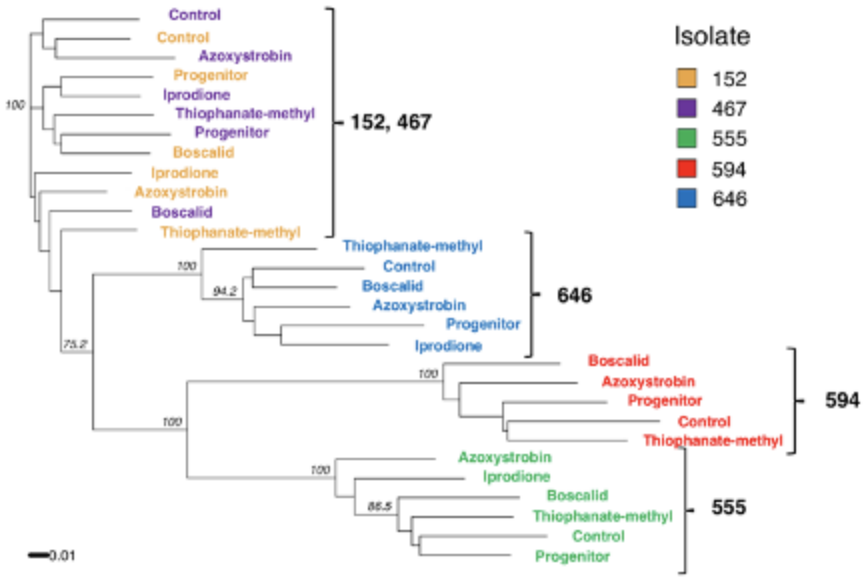

Fig. 4.12. Neighbor-joining tree of control and exposed individuals from the first experiment. The tree was built using Nei's genetic distance, which was calculated from SNP loci with < 50% missing information. Bootstrap support of >75% (1000 replicates) is shown at the nodes. Scale is shown on the bottom-left corner.

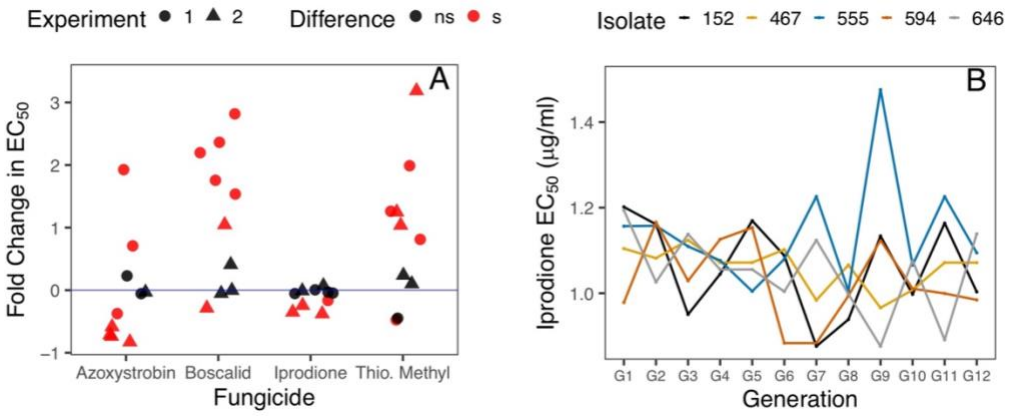

Fig. 4.13. Change in Effective Concentration of 50% inhibition (EC_{50}) of *Sclerotinia sclerotiorum* strains after independent exposure to sublethal doses of four fungicides for 12 generations. **A,** Fold change in EC_{50} after 12 generations of fungicide exposure.

Isolates in red (s) had significantly different EC_{50} ($P \leq 0.05$) than their relative control counterparts and blue horizontal line represents zero-fold difference in EC_{50} and **B,** Change in EC_{50} of Iprodione over the course of fungicide exposure. Fungicide sensitivity of progenitor was determined from results of G1 exposure.

CHAPTER-5

EVOLUTIONARY SIGNIFICANCE OF FUNGAL HYPERMUTATORS: LESSONS LEARNED FROM CLINICAL STRAINS AND IMPLICATIONS FOR FUNGAL PLANT PATHOGENS

Abstract

Rapid evolution of fungal pathogens poses a serious threat to medicine and agriculture. Mutation rate determines the pace of evolution of a fungal pathogen. Hypermutator fungal strains have an elevated mutation rate owing to a defect in the DNA mismatch repair system. Studies in *Saccharomyces cerevisiae* show that hypermutators expedite evolution by generating beneficial alleles at a faster pace than the wild-type strains. However, an accumulation of deleterious alleles in a hypermutator may reduce its fitness. The balance between fitness-cost and mutation-benefit determines the prevalence of hypermutators in a population. This balance is affected by a complex interaction of ploidy, mode of reproduction, population size, and the recent population history. Studies in human fungal pathogens like *Aspergillus fumigatus, Candida albicans, Candida glabrata, Cryptococcus deuterogattii,* and *Cryptococcus neoformans* have highlighted the importance of hypermutators in host adaptation and development of antifungal resistance. However, a critical examination of hypermutator biology, experimental evolution studies, and epidemiological studies suggests that hypermutators may impact evolutionary investigations. This review aims to integrate the knowledge about biology, experimental evolution, and dynamics of fungal hypermutators to critically examine the evolutionary role of hypermutators in fungal pathogen populations and project implications of hypermutators in the evolution of fungal plant pathogen populations. Understanding the

factors determining the emergence and evolution of fungal hypermutators can open a novel avenue of managing rapidly evolving fungal pathogens in medicine and agriculture.

Introduction

Mutations can be produced either due to errors in DNA replication or DNA damage by environmental or intrinsic factors. Since most of the non-synonymous mutations are likely to be deleterious, organisms have evolved two mutation avoidance mechanisms, proofreading by DNA polymerase and the mismatch repair (MMR) system. Errors generated during DNA replication are first rectified by the proofreading activity of DNA polymerase, which decreases the mutation rate of the organism by 10–100 fold [1]. The errors that escape proofreading are subjected to MMR, which further reduces the mutation rate by 50–1000 fold [2]. Some of the mutations resulting from DNA damage and recombination are also rectified by MMR. But what if these mutation avoidance mechanisms become defective? Studies in bacteria, fungi, and mammalian cancer cells have found that MMR defects confer a hypermutator phenotype with an elevated mutation rate [3–5]. Although this phenotype leads to cancer in mammals, it can expedite the evolution of pathogen populations by generating a plethora of mutations for selection to act upon. However, an accumulation of deleterious mutations may reduce its fitness and render this phenotype advantageous for short-term adaptation [6].

Bacterial hypermutators are recognized to hasten the evolution of antibiotic resistance, virulence acquisition, host adaptation, and disease transmissibility [3,7]. The role of hypermutators in fungal pathogen evolution has only gained medical attention in the last decade, while scant attention has been paid to agricultural implications. Studies in

laboratory strains of *Saccharomyces cerevisiae* and human pathogenic fungi have shown that hypermutators can expedite stress adaptation and mediate antifungal resistance and host adaptation [8–10]. Given the importance of hypermutators, this review will critically examine the studies on biology, experimental evolution, and population dynamics of hypermutator *S. cerevisiae* and human fungal pathogens to gain a better understanding of the factors shaping the evolutionary trajectories of hypermutators, how hypermutator biology may impact evolutionary investigations, and the agricultural implications of hypermutators. For the sake of brevity, hypermutators arising from MMR defects will be the focus of this review.

Genetic basis of hypermutator emergence and variation in mutation rate

Hypermutators can arise from non-synonymous mutations in one or more genes involved in the MMR pathway. In *Escherichia coli,* the MMR system consists of three "Mut" proteins, MutS, MutL, and MutH. While MutS binds to mismatches, MutL integrates mismatch detection with downstream processing, and MutH cleaves the newly synthesized DNA strand for subsequent exonuclease activity [14–18]. In *S. cerevisiae*, multiple homologs of the bacterial "Mut" proteins are involved in mitotic and meiotic mutation avoidance (Fig. 5.1). While six MutS homologs (MSH1 to MSH6) and four MutL homologs (MLH1 to MLH3 and PMS1) have been identified, no homolog of MutH is known [18–21]. Among the MSH proteins, MSH1 maintains mitochondrial genomic stability and other MSH proteins function as heterodimers to maintain nuclear genomic stability. The MSH2-MSH6 heterodimer is primarily involved in repairing base-base and

single insertion/deletion mismatches, the MSH2-MSH3 heterodimer primarily repairs longer insertion/deletion loop mismatches, and the MSH4-MSH5 heterodimer facilitates crossing over during meiosis. The MLH heterodimers, MLH1-PMS1, MLH1-MLH2, and MLH1-MLH3 direct downstream events in mitotic mutation avoidance and meiotic recombination [18,22].

Non-synonymous mutations in one or more MMR genes can increase the mutation rate of the fungal strain, conferring a hypermutator phenotype. Considerable variation in the mutation rate of hypermutators have been observed in natural fungal populations [25-29]. The mutation rate is determined by three factors: a) the MMR gene that harbours the non-synonymous mutation; b) the amino acid position affected by the non-synonymous mutation and; c) the strain's genetic background.

Since MMR genes differ in their functions, the mutation rate of a hypermutator would depend on the defective MMR gene it harbours. Mutations in MSH2 and MLH1 genes are more disruptive for the organism than mutations in other MMR genes, as these mutations could disrupt the function of all the heterodimers involved in the MMR pathway [23,24]. Additionally, individual non-synonymous mutations can exhibit a wild-type mutation rate but can significantly increase the mutation rate when present together. For example, an incompatible combination (or negative epistatic interaction) of certain MLH1 and PMS1 alleles (cMLH1-kPMS1) can increase the mutation rate of *S. cerevisiae* up to 340-fold [25,26].

Different non-synonymous mutations in the same MMR gene can vary in the mutation rate they confer [4,11–13,24,27,28]. The position of the mutation would determine which motif it affects and to what degree it disrupts the protein's 3-D structure

[29,30]. For example, among 54 non-synonymous mutations in the MSH2 gene of *S. cerevisiae,* the increase in mutation rate varied from 1 to 282-fold. About 55% of the mutations conferred high mutation rates, 8% mutations conferred an intermediate increase in mutation rate, and 38% mutations showed wild-type mutation rate [29]. Interestingly, the same non-synonymous mutation can render different mutation rates in different strain backgrounds owing to the presence of genomic suppressors or enhancers of mutation rate [26,31–35]. For example, the incompatible cMLH1-kPMS1 combination showed 196-fold higher mutation rate in the S288c strain background but showed wild-type mutation rate in the YJM523 strain background [35].

Mutation spectra and their impact on evolutionary investigations

A defect in the MMR genes can increase the rate of all types of mutations: single nucleotide polymorphisms (SNPs), insertions/deletions (indels), structural variants, and aneuploidy [10,30,36]. While SNPs are more likely to occur in coding regions with a bias towards higher G-to-A transitions [24,30,36], indels are more likely to occur in non-coding regions [30]. Mutations in repetitive sequences is the hallmark of MMR defects. Studies in *S. cerevisiae, Candida glabrata, Cryptococcus deuterogattii,* and *Cryptococcus neoformans* show that a defective MMR leads to mutations in long homopolymeric nucleotide tracts [10,24,27,30,36–38] and microsatellites [30,36,39]. This can be attributed to the inefficacy of DNA polymerase proofreading activity to rectify errors in homopolymer runs of >7 nucleotides long, rendering MMR as the sole machinery repairing such defects [37,40]. Indels in repetitive sequences are more prominent than elsewhere in the genome [30]. The mutability of the repetitive sequence

increases with its length. A 51,000 fold-increase in mutability was observed in indels in 14 bp long homopolymer sequences as compared to 4 bp long homopolymer runs [37].

Owing to extensive mutations and rapidly changing mutation profiles, determining evolutionary relationships with hypermutator strains using traditional models may lead to erratic conclusions [9]. In phylogenetic studies, distantly related hypermutator strains may form a pseudo-phylogenetic cluster owing to the increased indels in homopolymer runs. This phenomenon is called Long Branch Attraction (LBA). Parsimony methods are more prone to LBA than likelihood methods. For example, a phylogenetic study of *Cryptococcus deuterogattii* strains in the VGIIa-like sublineage that have the same MSH2 mutation was performed. The analysis included a clinical strain isolated in Brazil in 1981 (ICB107), an environmental strain isolated in California in 1990 (CBS7750), a clinical strain isolated in Seattle, WA in 1975 (NIH444), and a copy of the clinical strain from Seattle that was maintained in a different laboratory [NIH444(v)] [27]. Phylogenetic relationships showed NIH444(v)) was more closely related to CBS7750 and ICB107 than to the parent strain, NIH444, from which the strain originated. This observation suggests that the MMR defect in NIH444 allowed rapid divergence of the isolates from each other during subculturing and storage, such that they were more closely related to geographically distinct isolates than to each other.

Authors of some studies of *Candida glabrata* concluded that different MSH2 defective alleles can be genotype specific [11,12,28]. These studies used microsatellites and/or multi locus sequence typing (MLST) for genotyping. All strains (n = 63) belonging to one microsatellite genotype had the V239L mutation in the MSH2 gene [12]. However, two different microsatellite genotypes (Gt22 and Gt36) consisted of both

the wild-type MSH2 allele and P208S/N890I mutations [11]. Results from microsatellite genotyping are questionable since MMR defects lead to microsatellite instability. When *Candida glabrata* strains were genotyped using MLST, all the strains (n = 10) in the ST10 genotype had the same P208S/N890I mutation in two different studies [12,28]. In contrast, the V239L mutation was found to be associated with ST7 genotype in one study (n = 104) [12] and with ST8 genotype in another study (n = 2) [10]. Since homopolymeric runs can occur in several genes [27] used in MLST and mutations can also occur in coding sequences devoid of homopolymer runs, MLST genotyping may be affected by MMR defects.

Although extensive genomic mutations can be deleterious for the fitness of a hypermutator over time, an MMR defect can hitchhike with a beneficial allele and get indirectly selected for short-term adaptation. A balance between fitness-cost and mutation-benefit determines the prevalence (or frequency) of hypermutators in a population. This balance is further governed by species and population specific factors.

Hypermutator dynamics in fungal populations

Experimental evolution studies in *S. cerevisiae* populations have evaluated the mutation-benefit and fitness-cost of hypermutators and found that results vary with ploidy, mode of reproduction, and population size [8,41,42]. Populations with a fixed ratio of msh2Δ strains and wild-type strains were propagated for 100–400 generations for mutation accumulation. The final frequency of msh2Δ strains indicated if mutation-benefit or fitness-cost was higher.

The frequency of hypermutators is expected to decline in sexual populations due to a lack of association between the mutator and beneficial alleles owing to recombination. However, a beneficial allele generated by a hypermutator can still propagate in a sexual population and aid in adaptation. In sexual populations of *S. cerevisiae*, the frequency of hypermutators declined [41]. In addition to outcrossing, the decline could have been due to reduced spore viability due to deletion of one MMR gene. Although MMR deletion mutants have reduced spore viability [22,25,43,44], naturally occurring non-synonymous mutations in MMR genes do not show such defect [31].

In asexual populations, mutator alleles can hitchhike with beneficial alleles and increase in frequency. However, the outcome can be affected by ploidy. An increase in ploidy can mask deleterious alleles and be advantageous for adaptation [45,46]. Consistent with this hypothesis, an increased fitness and frequency of hypermutators was observed in diploid asexual populations of *S. cerevisiae* [8,41]. Hypermutators in haploid asexual populations would be expected to yield more deleterious mutations and lead to a decline in the frequency of the hypermutator strains, but varying results have been observed in different population sizes of *S. cerevisiae* [42]. If a beneficial allele emerges earlier in a hypermutator strain, hypermutators would increase in their frequency within the population [47]. In small populations (~10^5 cells) of *S. cerevisiae*, mutator allele hitchhiked with the beneficial allele to fixation in 100 generations. With an increase in population size, the mutator allele took longer to hitchhike with the beneficial allele. This delay could have been due to clonal interference, which is a competition between clonal lineages with different beneficial mutations. In large (10^6–10^7 cells) to very large populations (~10^8 cells), there is an increased probability of wild-type to generate

beneficial alleles early on, which decreases the relative benefit of the MMR defect and hypermutators decrease in frequency [8,41,42]. These experiments suggest that a complex interplay among ploidy, mode of reproduction, and population size may determine the prevalence of hypermutators in a population. It should be noted that these evolutionary trajectories are determined for deletion strains that represent extreme cases. However, mutation rates of hypermutators in natural populations show considerable variation, which may affect their evolutionary trajectories.

Prevalence of non-synonymous MMR mutations in natural populations varies among and within species. About 13% isolates of *A. fumigatus* had a non-synonymous mutation in the MSH2 gene [48], 44–72% isolates of *Candida glabrata* had a non-synonymous mutation in the MSH2 gene [4,11–13], and 2% of the isolates had the incompatible MLH1 and PMS1 alleles in *S. cerevisiae* [35]. Such variation in prevalence of non-synonymous MMR mutations can be explained by the differences in the mode of reproduction of the species. In sexually reproducing *A. fumigatus* and *S. cerevisiae*, outcrossing between hypermutators and wild-type strains could have broken the association of mutator and beneficial alleles. *Saccharomyces cerevisiae* showed less prevalence of MMR defects than *A. fumigatus* because the probability of three alleles occurring together (one beneficial allele and two incompatible MMR alleles) is lower than two alleles occurring together. Additionally, the differences can be attributed to the dynamics of nuclear cooperation and competition in the multinucleate *A. fumigatus*. Since only asexual reproduction has been documented in *Candida glabrata*, a higher prevalence of non-synonymous mutations shows that a hypermutator phenotype can be

an important mechanism to increase genetic diversity and the mutation-benefit can be higher than the fitness-cost in asexual haploid populations.

In a given population, there can be alternating periods of high and low prevalence of hypermutators [49]. Even in the absence of recombination, the mutation rate of a population may change over time [50,51]. Fungal pathogens encounter a number of stressors when adapting to the host like high temperature, hypoxia, unfavorable pH, nutrient deprivation, and reactive oxidative and nitrosative species [52]. After successful colonization of the host, pathogens can be exposed to antifungal stress. Under these changing stress conditions, hypermutators can rescue the population to adaptation. Mutator alleles can frequently emerge in a population, get selected by hitchhiking with beneficial alleles and help the population to survive a particular stress condition. Over time, hypermutators can decrease in frequency due to negative selection owing to reduced fitness or by emergence of antimutator (or suppressor) alleles. The frequency of hypermutators in a population not only depends on species and population biology but may also depend on the population's recent history of stress exposure [50].

Role of hypermutators in adaptation of human fungal pathogens

The role of hypermutators in antifungal resistance development and/or within-host adaptation has been investigated in several human pathogens: *Aspergillus fumigatus* [48], *Candida albicans* [53], *Candida glabrata* [4,10–13,28], *Cryptococcus deuterogattii* [27], and *Cryptococcus neoformans* [9,24]. Pathogens with non-synonymous MMR mutations were isolated from patients and MMR genes were deleted from some strains to determine their effect on antifungal resistance and virulence. In *Candida glabrata, in*

vitro transfers on antifungal amended media led to an increased resistance of msh2Δ strains by ~82-, 18- and 9-fold for caspofungin, fluconazole and amphotericin B as compared to the wild-type strains. An increased resistance rate to caspofungin was also observed in mouse models. However, when mice were co-infected with both the wild-type and msh2Δ strains in a ratio of 1:1, wild-type strains were able to colonize the mouse gut better than the mutants [4]. In *Cryptococcus neoformans*, msh2Δ, mlh1Δ, and pms1Δ mutants rapidly developed resistance to fluconazole and amphotericin-B than the wild-type strains in the presence of the drug. Although pms1Δ mutants showed reduced virulence, msh2Δ and mlh1Δ mutants did not reduce virulence [24]. Wild-type strains have a fitness advantage in favorable conditions or once adaptation has been achieved [8,27,35,54] because an accumulation of deleterious mutations can reduce their virulence [4,27,48].

Direct evidence of non-synonymous MMR mutations mediating stress adaptation has been shown by isolating paired samples from patients, before and after stress exposure. Non-synonymous mutations in MSH2 and MSH5 genes led to the microevolution of *Cryptococcus neoformans* in an HIV-positive patient causing a recurrent infection [9]. Microevolution to antifungal drug resistance has also been observed. One pair of *Candida glabrata* strains with a non-synonymous mutation in the MSH2 gene was isolated before and after 50 days of fluconazole therapy from an HIV-positive patient [10]. Owing to the high selection pressure, the sequential isolate developed azole resistance. Thus, hypermutators are beneficial for stress adaptation in human fungal pathogens.

MMR defects have been found in both antifungal resistant and susceptible clinical strains of *Candida glabrata*. Non-synonymous MSH2 polymorphisms were observed in 42.9% of fluconazole resistant isolates, 80.6% fluconazole sensitive isolates, and 100% echinocandin-resistant isolates [12]. Because of a high prevalence of MMR defective strains and their lack of association with antifungal resistance, the role of hypermutators in antifungal drug resistance has been questioned [11–13]. However, this observation can be explained by the variation in selection pressures on MMR defective strains. Hypermutators can only confer antifungal resistance if they had an antifungal drug exposure. In clinical strains of *Candida glabrata* isolated from France, MSH2 non-synonymous polymorphisms were observed in 48% of the isolates with high fluconazole MICs and 42.8% of isolates with low fluconazole MICs [11]. When the treatment history for each patient was taken into account, exposure to antifungal drugs was found to be associated with resistance occurrence. Clinical strains of *Candida glabrata* isolated from India had 69% prevalence of MMR defective strains, but no echinocandin or azole resistant strains were found [13]. Such an observation may have resulted from a relatively weak selection pressure on the population, as echinocandin treatment was only given to 1% of the patients in the study and strains were isolated from patients within 2 weeks of azole therapy. Additionally, despite a high prevalence of non-synonymous MMR mutations, the presence of antimutator alleles could have mitigated the increase in mutation rate.

High prevalence of MMR defective strains in the asexual *Candida glabrata* populations may reflect the importance of this phenotype to adapt to changing stress conditions in the human body. Since hypermutators can expedite stress adaptation in

human fungal pathogens, it is likely that hypermutators may hasten adaptation of fungal pathogens present in other stressful environments like agriculture. Currently, no study has evaluated the role of hypermutators in the evolution of fungal plant pathogens. The following are some implications and considerations for pursuing research on hypermutators in this area.

Can hypermutators expedite evolution in fungal plant pathogens?

In agriculture, the practice of monoculture is prevalent, which means that genetically uniform plants are grown over large acreages. Monoculture exerts a strong selection pressure on pathogen populations for host adaptation. Host adaptation is especially important for obligate biotrophic pathogens as they can only survive on a living host and are under a high selection pressure to evolve virulence. Biotrophic plant pathogenic fungi secrete proteins, called effectors, to combat plant defences and mediate virulence. Effector genes are often located in rapidly evolving compartments of the fungal genome such as repeat rich regions [55] and many effector proteins themselves contain repetitive sequences like leucine rich repeats. Since MMR defects especially increase mutations in repetitive sequences, a hypermutator phenotype can be advantageous in evolving novel effectors.

Fungicide applications also exert a strong selection pressure to develop resistant plant pathogens. Extensive fungicide use has resulted in rapid evolution of resistance in some pathogens. Resistance was reported as early as two years after the launch of some fungicides [56]. Interestingly, resistance comes at a cost of virulence in some isolates of different plant pathogenic species [57,58,59,60]. In *Cercospora beticola*, 50% of

competition experiments between isolates that were sensitive and resistant to demethylation inhibitor fungicides showed that resistance was associated with reduced spore production and virulence [59]. Although a genetic linkage between virulence and resistance genes is possible, an increased resistance and reduced virulence can also be a characteristic of a hypermutator.

Experimental and epidemiological studies are required to assess the role of hypermutators in stress adaptation of plant pathogens. Currently, MMR genes have not been experimentally validated in plant pathogenic fungi, but genome sequencing and transcriptomic projects in several pathogens including *Fusarium verticillioides* [61] have identified putative genes involved in the MMR pathway. Mutation accumulation experiments can be conducted for validating the putative MMR genes. However, mutation accumulation studies in plant pathogens will be different from those conducted in *S. cerevisiae* as most of the plant pathogenic fungi are strictly filamentous. In filamentous fungi, cells are not discrete entities but are connected to each other to form hyphae. This may combine mutations from different nuclei and cause rapid accumulation of mutations [62], decreasing the likelihood of emergence of a hypermutator phenotype. However, a recent study in the filamentous human fungal pathogen, *A. fumigatus*, suggests that hypermutators can confer an adaptive advantage under stress [48]. Thus, filamentous growth of plant pathogenic fungi may still permit the emergence of hypermutators.

Conclusion and future directions

Hypermutators can expedite antifungal resistance and host adaptation in human fungal pathogens, thus rescuing populations from stress. However, such a phenotype may not be beneficial in long-term adaptation. The frequency of hypermutators in a population is determined by an interaction of ploidy, mode of reproduction, population size, and its recent population history. Although hypermutators facilitate evolution, their rapidly changing mutation profiles may render them unreliable in determining their evolutionary relationships with other strains. Knowledge gained from *S. cerevisiae* and human fungal pathogens can be applied in plant pathogens to enhance our understanding about the role of hypermutators in fungicide resistance development and host adaptation.

A limitation of the majority of studies on hypermutators is that they mainly focus on the MSH2 gene. Although it is one of the major genes involved in the MMR pathway, further research is required to understand the role of other MMR genes in evolution of hypermutators. Additionally, identification of biochemical targets of antimutator alleles is required. These alleles have been found to modulate the phenotype of MMR defects [26,31–35]. The YJM523 strain of *S. cerevisiae* was homozygous for cMLH1-kPMS1 incompatibility but still conferred a wild-type phenotype, owing to antimutator alleles present in the genome [35]. Knowledge of biochemical pathways used by antimutator alleles to suppress the hypermutator phenotype can be used to design novel drugs to mitigate the evolution of fungal hypermutators in medicine and agriculture.

References

1. Manhart CM, Alani E. DNA replication and mismatch repair safeguard against metabolic imbalances. Proc Natl Acad Sci U S A. 2017. pp. 5561–5563.
2. Iyer RR, Pluciennik A, Burdett V, Modrich PL. DNA mismatch repair: Functions and mechanisms. Chem Rev. 2006. pp. 302–323. doi:10.1002/chin.200620268.
3. Oliver A, Mena A. Bacterial hypermutation in cystic fibrosis, not only for antibiotic resistance. Clin Microbiol Infect. 2010. pp. 798–808. doi:10.1111/j.1469-0691.2010.03250.x
4. Healey KR, Zhao Y, Perez WB, Lockhart SR, Sobel JD, Farmakiotis D, et al. Prevalent mutator genotype identified in fungal pathogen *Candida glabrata* promotes multi-drug resistance. Nat Commun. 2016;7: 11128.
5. Peltomäki P. Role of DNA mismatch repair defects in the pathogenesis of human cancer. J Clin Oncol. 2003. pp. 1174–1179. doi:10.1200/jco.2003.04.060
6. Denamur E, Matic I. Evolution of mutation rates in bacteria. Mol Microbio. 2006. pp. 820–827. doi:10.1111/j.1365-2958.2006.05150.x
7. Chopra I, O'Neill AJ, Miller K. The role of mutators in the emergence of antibiotic-resistant bacteria. Drug Resist Updat. 2003;6: 137–145.
8. Thompson DA, Desai MM, Murray AW. Ploidy controls the success of mutators and nature of mutations during budding yeast evolution. Curr Biol. 2006;16: 1581–1590.
9. Rhodes J, Beale MA, Vanhove M, Jarvis JN, Kannambath S, Simpson JA, et al. A population genomics approach to assessing the genetic basis of within-host microevolution underlying recurrent cryptococcal meningitis infection. G3. 2017;7: 1165–1176.
10. Vale-Silva L, Beaudoing E, Tran VDT, Sanglard D. Comparative genomics of two sequential clinical isolates. G3. 2017;7: 2413–2426.
11. Dellière S, Healey K, Gits-Muselli M, Carrara B, Barbaro A, Guigue N, et al. Fluconazole and echinocandin resistance of *Candida glabrata* correlates better with antifungal drug exposure rather than with msh2 mutator genotype in a french cohort of patients harboring low rates of resistance. Front Microbiol. 2016. doi:10.3389/fmicb.2016.02038
12. Hou X, Xiao M, Wang H, Yu S-Y, Zhang G, Zhao Y, et al. Profiling of PDR1 and MSH2 in *Candida glabrata* bloodstream isolates from a multicenter study in China. Antimicrob Agents Chemother. 2018. doi:10.1128/aac.00153-18
13. Singh A, Healey KR, Yadav P, Upadhyaya G, Sachdeva N, Sarma S, et al. Absence of azole or echinocandin resistance in *Candida glabrata* isolates in India despite background prevalence of strains with defects in the DNA mismatch repair pathway. Antimicrob Agents Chemother. 2018. doi:10.1128/aac.00195-18
14. Su SS, Modrich P. *Escherichia coli* mutS-encoded protein binds to mismatched DNA base pairs. Proc Natl Acad Sci U S A. 1986;83: 5057–5061.

15. Grilley M, Welsh KM, Su SS, Modrich P. Isolation and characterization of the *Escherichia coli* mutL gene product. J Biol Chem. 1989;264: 1000–1004.

16. Au KG, Welsh K, Modrich P. Initiation of methyl-directed mismatch repair. J Biol Chem. 1992;267: 12142–12148.

17. Modrich P, Lahue R. Mismatch repair in replication fidelity, genetic recombination, and cancer biology. Annu Rev Biochem. 1996;65: 101–133.

18. Boiteux S, Jinks-Robertson S. DNA repair mechanisms and the bypass of DNA damage in *Saccharomyces cerevisiae*. Genetics. 2013;193: 1025–1064.

19. Reenan RA, Kolodner RD. Isolation and characterization of two *Saccharomyces cerevisiae genes* encoding homologs of the bacterial HexA and MutS mismatch repair proteins. Genetics. 1992;132: 963–973.

20. New L, Liu K, Crouse GF. The yeast gene MSH3 defines a new class of eukaryotic MutS homologues. Mol Gen Genet. 1993;239: 97–108.

21. Marsischky GT, Filosi N, Kane MF, Kolodner R. Redundancy of *Saccharomyces cerevisiae* MSH3 and MSH6 in MSH2-dependent mismatch repair. Genes Dev. 1996;10: 407–420.

22. Prolla TA, Christie DM, Liskay RM. Dual requirement in yeast DNA mismatch repair for MLH1 and PMS1, two homologs of the bacterial mutL gene. Mol Cell Biol. 1994;14: 407–415.

23. Fishel R. The selection for mismatch repair defects in hereditary nonpolyposis colorectal cancer: revising the mutator hypothesis. Cancer Res. 2001;61: 7369–7374.

24. Boyce KJ, Wang Y, Verma S, Shakya VPS, Xue C, Idnurm A. Mismatch repair of DNA replication errors contributes to microevolution in the pathogenic fungus *Cryptococcus neoformans*. mBio. 2017. doi:10.1128/mbio.00595-17

25. Heck JA, Argueso JL, Gemici Z, Reeves RG, Bernard A, Aquadro CF, et al. Negative epistasis between natural variants of the *Saccharomyces cerevisiae* MLH1 and PMS1 genes results in a defect in mismatch repair. Proc Natl Acad Sci U S A. 2006. pp. 3256–3261. doi:10.1073/pnas.0510998103

26. Raghavan V, Bui DT, Al-Sweel N, Friedrich A, Schacherer J, Aquadro CF, et al. Incompatibilities in mismatch repair genes MLH1-PMS1 contribute to a wide range of mutation rates in human isolates of baker's yeast. Genetics. 2018. pp. 1253–1266. doi:10.1534/genetics.118.301550

27. Billmyre RB, Blake Billmyre R, Clancey SA, Heitman J. Natural mismatch repair mutations mediate phenotypic diversity and drug resistance in *Cryptococcus deuterogattii*. eLife. 2017. doi:10.7554/elife.28802

28. Healey KR, Ortigosa CJ, Shor E, Perlin DS. Genetic drivers of multidrug resistance in *Candida glabrata*. Front Microbiol. 2016. doi:10.3389/fmicb.2016.01995

29. Gammie AE, Erdeniz N, Beaver J, Devlin B, Nanji A, Rose MD. Functional characterization of pathogenic human MSH2 missense mutations in *Saccharomyces cerevisiae*. Genetics. 2007;177: 707–721.

30. Lang GI, Parsons L, Gammie AE. Mutation rates, spectra, and genome-wide distribution of spontaneous mutations in mismatch repair deficient yeast. G3. 2013. pp. 1453–1465. doi:10.1534/g3.113.006429

31. Argueso JL, Kijas AW, Sarin S, Heck J, Waase M, Alani E. Systematic mutagenesis of the *Saccharomyces cerevisiae* MLH1 gene reveals distinct roles for Mlh1p in meiotic crossing over and in vegetative and meiotic mismatch repair. Mol Cell Biol. 2003;23: 873–886.

32. Demogines A, Wong A, Aquadro C, Alani E. Incompatibilities involving yeast mismatch repair genes: a role for genetic modifiers and implications for disease penetrance and variation in genomic mutation rates. PLoS Genet. 2008;4: e1000103.

33. Skelly DA, Magwene PM, Meeks B, Murphy HA. Known mutator alleles do not markedly increase mutation rate in clinical *Saccharomyces cerevisiae* strains. Proc Biol Sci. 2017. p. 20162672. doi:10.1098/rspb.2016.2672

34. Drotschmann K, Shcherbakova PV, Kunkel TA. Mutator phenotype due to loss of heterozygosity in diploid yeast strains with mutations in MSH2 and MLH1. Toxicol Lett. 2000;112-113: 239–244.

35. Bui DT, Friedrich A, Al-Sweel N, Liti G, Schacherer J, Aquadro CF, et al. Mismatch repair incompatibilities in diverse yeast populations. Genetics. 2017;205: 1459–1471.

36. Serero A, Jubin C, Loeillet S, Legoix-Né P, Nicolas AG. Mutational landscape of yeast mutator strains. Proc Natl Acad Sci U S A. 2014;111: 1897–1902.

37. Tran HT, Keen JD, Kricker M, Resnick MA, Gordenin DA. Hypermutability of homonucleotide runs in mismatch repair and DNA polymerase proofreading yeast mutants. Mol Cell Biol. 1997;17: 2859–2865.

38. Greene CN, Jinks-Robertson S. Frameshift intermediates in homopolymer runs are removed efficiently by yeast mismatch repair proteins. Mol Cell Biol. 1997;17: 2844–2850.

39. Wierdl M, Dominska M, Petes TD. Microsatellite instability in yeast: dependence on the length of the microsatellite. Genetics. 1997;146: 769–779.

40. Kroutil LC, Register K, Bebenek K, Kunkel TA. Exonucleolytic proofreading during replication of repetitive DNA. Biochemistry. 1996;35: 1046–1053.

41. Raynes Y, Gazzara MR, Sniegowski PD. Mutator dynamics in sexual and asexual experimental populations of yeast. BMC Evol Biol. 2011;11: 158.

42. Raynes Y, Gazzara MR, Sniegowski PD. Contrasting dynamics of a mutator allele in asexual populations of differing size. Evolution. 2012. p. no–no. doi:10.1111/j.1558-5646.2012.01577.x

43. Reenan RA, Kolodner RD. Characterization of insertion mutations in the *Saccharomyces cerevisiae* MSH1 and MSH2 genes: evidence for separate mitochondrial and nuclear functions. Genetics. 1992;132: 975–985.

44. Williamson MS, Game JC, Fogel S. Meiotic gene conversion mutants in *Saccharomyces cerevisiae*. I. Isolation and characterization of pms1-1 and pms1-2. Genetics. 1985;110: 609–646.

45. Selmecki AM, Maruvka YE, Richmond PA, Guillet M, Shoresh N, Sorenson AL, et al. Polyploidy can drive rapid adaptation in yeast. Nature. 2015;519: 349–352.

46. Sliwa P, Kluz J, Korona R. Mutational load and the transition between diploidy and haploidy in experimental populations of the yeast *Saccharomyces cerevisiae*. Genetica. 2004;121: 285–293.

47. Tanaka MM, Bergstrom CT, Levin BR. The evolution of mutator genes in bacterial populations: the roles of environmental change and timing. Genetics. 2003;164: 843–854.

48. Reis TF dos, dos Reis TF, Silva LP, de Castro PA, do Carmo RA, Marini MM, et al. The *Aspergillus fumigatus* mismatch repair MSH2 homolog is important for virulence and azole resistance. mSphere. 2019. doi:10.1128/msphere.00416-19

49. Giraud A, Radman M, Matic I, Taddei F. The rise and fall of mutator bacteria. Curr Opin Microbiol. 2001;4: 582–585.

50. Desai MM, Fisher DS. The balance between mutators and nonmutators in asexual populations. Genetics. 2011;188: 997–1014.

51. McDonald MJ, Hsieh Y-Y, Yu Y-H, Chang S-L, Leu J-Y. The evolution of low mutation rates in experimental mutator populations of *Saccharomyces cerevisiae*. Curr Biol. 2012;22: 1235–1240.

52. Brown SM, Campbell LT, Lodge JK. *Cryptococcus neoformans*, a fungus under stress. Curr Opin Microbiol. 2007. pp. 320–325. doi:10.1016/j.mib.2007.05.014

53. Legrand M, Chan CL, Jauert PA, Kirkpatrick DT. Role of DNA mismatch repair and double-strand break repair in genome stability and antifungal drug resistance in *Candida albicans*. Eukaryot Cell. 2007;6: 2194–2205.

54. Giraud A, Matic I, Tenaillon O, Clara A, Radman M, Fons M, et al. Costs and benefits of high mutation rates: adaptive evolution of bacteria in the mouse gut. Science. 2001;291: 2606–2608.

55. Dong S, Raffaele S, Kamoun S. The two-speed genomes of filamentous pathogens: waltz with plants. Curr Opin Genet Dev. 2015;35: 57-65.

56. Brent KJ, Hollomon DW. Fungicide resistance in crop pathogens: how can it be managed? FRAC Monograph 1. 2007. Vol. 2. BrusselsCropLife International

57. Chen Y, Zhou M-G. Characterization of *Fusarium graminearum* isolates resistant to both carbendazim and a new fungicide JS399-19. Phytopathology. 2009. pp. 441–446. doi:10.1094/phyto-99-4-0441

58. Ritchie DF. Mycelial growth, peach fruit-rotting capability, and sporulation of strains of *Monilinia fructicola* resistant to dichloran, iprodione, procymidone, and vinclozolin. Phytopathology. 1983. p. 44. doi:10.1094/phyto-73-44

59. Karaoglanidis GS, Thanassoulopoulos CC, Ioannidis PM. Fitness of *Cercospora beticola* field isolates–resistant and–sensitive to demethylation inhibitor fungicides. Eur J Plant Pathol. 2001 Mar 1;107(3):337-47.

60. Beever RE, Laracy EP, Pak HA. Strains of *Botrytis cinerea* resistant to dicarboximide and benzimidazole fungicides in New Zealand vineyards. Plant Pathol. 1989 Sep;38(3):427-37.

61. Ma L-J, van der Does HC, Borkovich KA, Coleman JJ, Daboussi M-J, Di Pietro A, et al. Comparative genomics reveals mobile pathogenicity chromosomes in *Fusarium*. Nature. 2010;464: 367–373.

62. Jeon J, Choi J, Lee G-W, Dean RA, Lee Y-H. Experimental evolution reveals genome-wide spectrum and dynamics of mutations in the rice blast fungus, *Magnaporthe oryzae*. PLoS One. 2013;8: e65416.

Figure

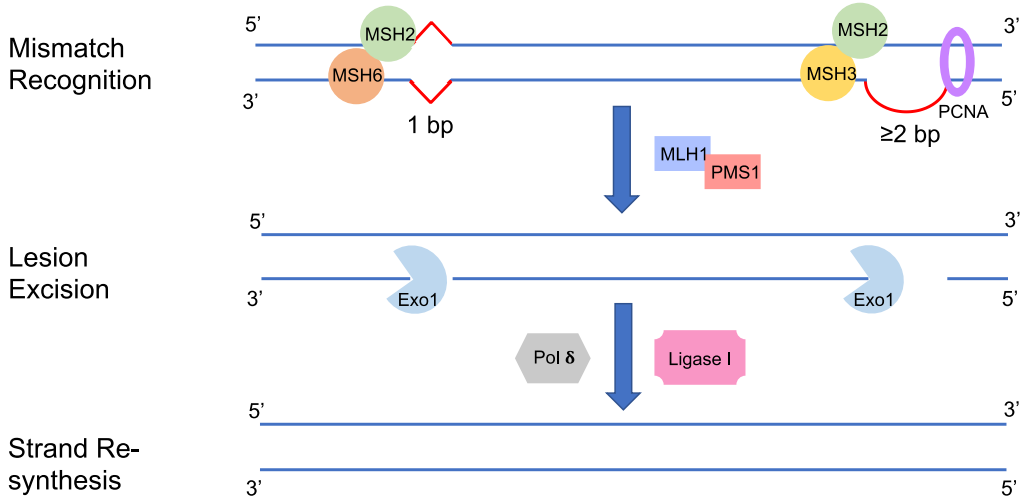

Adapted from Tosti E, et al. Genome Med. 2014; 6:68 and Reilly N.M., et al. Molecular Oncol. 2019; 13: 681-700.

Fig. 5.1. Concise diagram of the MisMatch Repair (MMR) pathway in *Saccharomyces cerevisiae*. Mismatches are recognized by the MSH heterodimers. The MSH2-MSH6 heterodimer primarily identifies base-base and single insertion/deletion mismatches, the MSH2-MSH3 heterodimer primarily identifies longer insertion/deletion loop mismatches, and the MLH1-PMS1 heterodimer directs downstream events [18,22]. Lesions in the newly synthesized strand are then excised by Exo1. DNA Polymerase, Pol δ, synthesizes the new strand and Ligase I ligates the fragments of the new strand.

CHAPTER-6

CONCLUSIONS

Fungicide-resistant pathogens are an increasing threat to fungicide efficacy and plant health. The goal of this dissertation was to advance the foundational knowledge required to prevent and detect fungicide resistance development in the seedling disease pathogen, *Rhizoctonia zeae* and the white mold pathogen, *Sclerotinia sclerotiorum.*

In Chapter 2, fungicide sensitivity of *R. zeae* isolates from corn and soybean fields in Nebraska was determined. Most of the *R. zeae* isolates were extremely sensitive to fludioxonil, prothioconazole, and sedaxane. However, this pathogen could not be controlled by azoxystrobin. This is an important finding because azoxystrobin seed treatment is generally used for control of *Rhizoctonia* spp. in corn and soybean (Ajayi-Oyetunde and Bradley 2018; Specht et al. 2017). This was the first study to evaluate sensitivity of *R. zeae* from corn and soybean fields. In previous studies, *R. zeae* from turfgrasses has been reported to be both sensitive (Amaradasa et al. 2014) and insensitive to QoI fungicides (Kerns et al. 2017). This information will help to guide strategies for chemical control of *R. zeae*. The sensitivity of *R. zeae* to different fungicides varied among years, host crops, and within and among counties. The discriminatory concentrations identified in this study can be used to monitor shifts in fungicide sensitivity in the future. Using single discriminatory concentrations would be a time- and cost-effective way to determine fungicide sensitivity shifts rather than using the serial dilution method with more than (or equal to) four concentrations. Additionally, *R. zeae* isolates reduced the biomass of the soybean plant. This is an important finding since the

amount of biomass can partly determine the crop yield (Long et al. 2006). This finding indicates that *R. zeae* can potentially negatively impact yield and further research is needed to quantify the economic impact of this understudied pathogen.

To prevent fungicide resistance, it is important to understand the intrinsic risk of resistance development in a pathogen population. The risk of resistance development in *R. zeae* can be estimated by characterizing its population structure. In Chapter 3, six microsatellite markers were designed and used to genotype 200 *R. zeae* isolates obtained mostly from corn and soybean fields in the North Central and Southern United States. It was inferred that *R. zeae* populations had high genotypic diversity and mixed reproductive mode, which are characteristics of populations with high evolutionary potential (McDonald and Linde 2002). This finding suggests that *R. zeae* populations may be at high risk of developing fungicide resistance. Thus, using Integrated Pest Management (IPM) strategies rather than heavily relying on a single management strategy can circumvent management failure. Additionally, the high genotypic diversity found in the U.S. complements previous speculations that Americas might be the origin of *R. zeae* (Aydin et al. 2013; Gürkanli et al. 2016). With rise in global temperatures, the prominence of *R. zeae* might increase owing to its ability to be virulent at 30–33°C, a temperature range higher than that optimum for *R. solani* (Elliott 1999; Erper et al. 2006; Li et al. 1998; Martin and Lucas 1984; Sumner and Bell 1982; Voorhees 1934). This study provides the foundational understanding of the distribution and evolutionary potential of *R. zeae* in the U.S. and information obtained from this study can be used to design effective disease management strategies against this pathogen.

For possible intervention in the evolution of fungicide resistance, it is important to understand the factors that accelerate it. In Chapter 4, sublethal fungicide exposure was found to increase the genome-wide mutation frequency in certain genomic backgrounds of *S. sclerotiorum*. Higher mutation frequency can potentially accelerate the emergence of alleles conferring fungicide resistance. Previous studies on fungal plant pathogens gave an unclear picture of the role of sublethal fungicide dose in increasing mutation rate (Ajouz et al. 2010; Amaradasa and Everhart 2016; Chen et al. 2015; Dowling et al. 2016; Schnabel et al. 2014; Troncoso-Rojas et al. 2013). Additionally, these studies relied on genetic markers to determine the effect of fungicide exposure on mutational frequencies, which could only assess the impact of fungicide stress on a small fraction of the genome. Whole genome sequencing conducted in Chapter 4 showed that sublethal fungicide stresses can increase point mutations and suppress Transposable Element (TE) insertions. The relationship between TE insertion and stress has not been examined in *S. sclerotiorum* before. In other organisms, TEs are known to be activated or suppressed under stress and the consequences varied with genomic background (Horváth et al. 2017).

Irrespective of fungicide exposure, extensive Copy Number Variants (CNVs), specifically aneuploidy and large duplications on chromosome 7 were observed in the *S. sclerotiorum* genome. Interestingly, this chromosome harbored regions with high density of repetitive sequences and Repeat Induced Point mutations (RIP), which were associated with clusters of secreted and effector-like proteins (Derbyshire et al. 2017). Rapid gain and loss of the extra copy of this chromosome suggests that this strategy might be frequently used by *S. sclerotiorum* and may be helpful for host stress adaptation. Extensive CNVs were also observed during the vegetative growth of the haploid fungus

Zymoseptoria tritici (Möller et al. 2018), suggesting that chromosomal rearrangements might be a common mechanism of generating genetic variation in at least some plant pathogens. Additionally, a pronounced effect of the genomic background was observed on genome instability. This suggests that strains with a highly mutable genomic background can hasten adaptation by generating a bigger allele-pool. This study provided a better understanding of the factors that accelerate resistance emergence, which is important for devising disease management strategies that delay resistance evolution and prolong the life of currently used fungicides.

Similar to the results of Chapter 4, a study conducted in *Candida albicans* found that the genomic background influences genomic stability and evolution (Gerstein and Berman 2020). Environmental and clinical fungal strains with an increased mutation rate due to faulty DNA repair machinery, called hypermutators, have been shown to adapt more rapidly to antifungal therapy and host stress (Boyce et al. 2017; Healey et al. 2016; dos Reis et al. 2019). Understanding the factors that accelerate resistance emergence is important to devise disease management strategies that delay resistance evolution and prolong the life of currently used fungicides. In Chapter 5, literature was reviewed to examine the evolutionary role of hypermutators in fungal pathogen populations and project implications of hypermutators in the evolution of fungal plant pathogen populations. Studies in human fungal pathogens suggested that hypermutators can expedite antifungal resistance and host adaptation, thus rescuing populations from stress (Boyce et al. 2017; Healey et al. 2016). However, such a phenotype may not be beneficial in long-term adaptation. The frequency of hypermutators in a population has been found to be determined by an interaction of ploidy, mode of reproduction, population size, and

its recent population history (Thompson and Murray 2006; Raynes et al. 2011; Desai and Fisher 2011). Although hypermutators facilitate evolution, their rapidly changing mutation profiles may render them unreliable in determining their evolutionary relationships with other strains. This review provided an insight into how knowledge gained from *S. cerevisiae* and human fungal pathogens can be applied in plant pathogens to enhance our understanding about the role of hypermutators in fungicide resistance development and host adaptation.

Overall, this dissertation established the status quo of fungicide resistance in *R. zeae* and advanced the knowledge about the risk of resistance development in *R. zeae*, which can inform fungicide resistance management, specifically for *R. zeae* on soybean and corn. It also provided new information about the effects of sublethal fungicide stress on the genomes of *S. sclerotiorum* and how information on hypermutators may be a new factor to consider in development of fungicide resistance.

References

Ajayi-Oyetunde, O.O., and Bradley, C.A. 2018. *Rhizoctonia solani*: Taxonomy, population biology, and management of rhizoctonia seedling disease of soybean. Plant Pathol. 67:3-17.

Ajouz, S., Decognet, V., Nicot, P.C., and Bardin, M. 2010. Microsatellite stability in the plant pathogen *Botrytis cinerea* after exposure to different selective pressures. Fungal Biol. 114:949-954.

Amaradasa, B.S., and Everhart, S.E**.** 2016. Effects of sublethal fungicides on mutation rates and genomic variation in fungal plant pathogen, *Sclerotinia sclerotiorum*. PLoS One 11:e0168079.

Amaradasa, B.S., Lakshman, D., McCall, D.S., and Horvath, B.J. 2014. *In vitro* fungicide sensitivity of *Rhizoctonia* and *Waitea* isolates collected from turfgrasses. J. Environ. Hortic. 32:126-132.

Aydin, E.B., Gurkanli, C.T., Ozkoc, I., Demirci, E., Erper, I., Karaca, G., Hsieh, T.F., Vajna, L. and Poltronieri, L.S. 2013. rDNA-ITS diversity of *Waitea circinata* var. *zeae* (anamorph: *Rhizoctonia zeae*). J. Plant Pathol. 95:587-595.

Boyce, K.J., Wang, Y., Verma, S., Shakya, V.P., Xue, C., and Idnurm, A. 2017. Mismatch repair of DNA replication errors contributes to microevolution in the pathogenic fungus *Cryptococcus neoformans*. mBio 8:e00595-17.

Chen, F., Everhart, S.E., Bryson, P.K., Luo, C., Song, X., Liu, X., and Schnabel, G. 2015. Fungicide-induced transposon movement in *Monilinia fructicola*. Fungal Genet. Biol. 85:38-44.

Derbyshire, M., Denton-Giles, M., Hegedus, D., Seifbarghi, S., Rollins, J., Kan van, J., Seidl, M.F., Faino, L., Mbengue, M., Navaud, O., Raffaele, S., Hammond-Kosack, K., Heard, S., and Oliver, R. 2017. The complete genome sequence of the phytopathogenic fungus *Sclerotinia sclerotiorum* reveals insights into the genome architecture of broad host range pathogens. Genome Biol. Evol. 9:593-618.

Desai, M.M., and Fisher, D.S. The balance between mutators and nonmutators in asexual populations. 2011. Genetics. 188:997-1014.

dos Reis T.F., Silva, L.P., de Castro, P.A., do Carmo, R.A., Marini, M.M., da Silveira, J.F., Ferreira, B.H., Rodrigues, F., Lind, A.L., Rokas, A., and Goldman, G.H. 2019. The *Aspergillus fumigatus* mismatch repair MSH2 homolog is important for virulence and azole resistance. mSphere. 4:e00416–19.

Dowling, M.E., Bryson, P.K., Boatwright, H.G., Wilson, J.R., Fan, Z., Everhart, S.E., Brannen, P.M., and Schnabel, G. 2016. Effect of fungicide applications on *Monilinia fructicola* population diversity and transposon movement. Phytopathology 106:1504-1512.

Elliott, M.L. 1999. Comparison of *Rhizoctonia zeae* isolates from Florida and Ohio turfgrasses. HortScience 34:298-300.

Erper, I., Karaca, G.H., Turkkan, M. and Ozkoc, I., 2006. Characterization and pathogenicity of *Rhizoctonia* spp. from onion in Amasya, Turkey. J. Phytopathol. 154:75-79.

Gerstein, A.C., and Berman, J. 2020. *Candida albicans* genetic background influences mean and heterogeneity of drug responses and genome stability during evolution to fluconazole. bioRxiv, 360347.

Gürkanli, C.T., Aydin, E.B., Demirci, E., Erper, I., Karaca, G., Hsieh, T.F., Poltronieri, L.S. and Özkoç, I. 2016. 18S rDNA and β-tubulin diversity in *Rhizoctonia zeae* Voorhees. Pak. J. Bot. 48:645-651.

Healey, K.R., Zhao, Y., Perez, W.B., Lockhart, S.R., Sobel, J.D., Farmakiotis, D., Kontoyiannis, D.P., Sanglard, D., Taj-Aldeen, S.J., Alexander, B.D., and Jimenez-Ortigosa, C. 2016. Prevalent mutator genotype identified in fungal pathogen *Candida glabrata* promotes multi-drug resistance. Nat. Commun. 7:11128.

Horváth, V., Merenciano, M., and González, J. 2017. Revisiting the relationship between transposable elements and the eukaryotic stress response. Trends Genet. 33:832-841.

Kerns, J., Yan, Y., and Butler, E. 2017. Characterization, pathogenicity, and *in vitro* sensitivity of *Rhizoctonia* spp. associated with leaf and sheath spot of bermudagrass putting greens in North Carolina and Alabama. Int. Turfgrass Soc. Res. J. 13:203-212.

Li, H.R., Wu, B.C., and Yan, S.Q., 1998. Aetiology of *Rhizoctonia* in sheath blight of maize in Sichuan. Plant Pathol. 47:16-21.

Long, S.P., Zhu, X.G., Naidu, S.L., and Ort, D.R. 2006. Can improvement in photosynthesis increase crop yields? Plant Cell Environ. 29:315-330.

Martin, S.B. and Lucas, L.T. 1984. Characterization and pathogenicity of *Rhizoctonia* spp. and binucleate *Rhizoctonia*-like fungi from turfgrasses in North Carolina. Phytopathology 74:170-175.

McDonald, B.A., and Linde, C. 2002. Pathogen population genetics, evolutionary potential, and durable resistance. Annu. Rev. Phytopathol. 40:349-379.

Möller, M., Habig, M., Freitag, M., and Stukenbrock, E.H. 2018. Extraordinary genome instability and widespread chromosome rearrangements during vegetative growth. Genetics 210:517-529.

Raynes, Y., Gazzara, M.R., and Sniegowski, P.D. 2011. Mutator dynamics in sexual and asexual experimental populations of yeast. BMC Evol. Biol. 11:158.

Schnabel, G., Chen, F., Everhart, S.E., Bridges, W.C., and Liu, X. 2014. Studies on sensitivity reduction in solo and mixture treatments and fungicide-induced mutagenesis in *Monilinia fructicola*. Modern fungicides and antifungal compounds VII: proceedings of the 17th International Reinhardsbrunn Symposium, April 21-25, 2013, Friedrichroda, Germany.

Specht, J., Hoegemeyer, T., Graef, G., Ruff, L., Torrion, J., Grassini, P., Edreira, J., Tenorio, F., Farmaha, B., Miller, J., Shaver, T., Wortman, C., Shapiro, C., Krienke, B., Knezevic, S., Jhala, A., Krueger, G., Werle, R., Procter, C., Blanco, H., Elmore, R., Irmak, S., Wright, R., Hunt, T., Giesler, L., Ziems, T., Shulski, M., Dutcher, A., Cooper, S., Glewen, K., Mueller, N., Rees J., and Thompson, L. 2017. Nebraska soybean and corn pocket field guide. University of Nebraska-Extension.

Sumner, D.R. and Bell, D.K. 1982. Root diseases induced in corn by *Rhizoctonia solani* and *Rhizoctonia zeae*. Phytopathology 72:86-91.

Thompson, D.A., Desai, M.M., and Murray, A.W. 2006. Ploidy controls the success of mutators and nature of mutations during budding yeast evolution. Curr. Biol. 16:1581-1590.

Troncoso-Rojas, R., Báez-Flores, M.E., Pryor, B., García, H.S., and Tiznado-Hernández, M.E. 2013. Inter simple sequence repeat polymorphism in *Alternaria* genomic DNA exposed to lethal concentrations of isothiocyanates. Afr. J. Microbiol. Res. 7:838-852.

Voorhees, R.K. 1934. Sclerotial rot of corn caused by *Rhizoctonia zeae*, n. sp. Phytopathology 24:1290-1303.